AN OBSERVATIONAL STUDY OF THE SURFACE-BASED RADIATION TEMPERATURE INVERSION

IN FAIRBANKS, ALASKA

A

THESIS

Presented to the Faculty

Of the University of Alaska Fairbanks

In Partial Fulfillment of the Requirements

For the Degree of

MASTER OF SCIENCE

By

Julie A. Malingowski, B.S.

Fairbanks, Alaska

August 2010

Abstract

Steep, surface-based inversions are a common occurrence in the valleys of interior Alaska due to the frequent occurrence of thermodynamically stable air masses caused in large part by the large negative net surface radiation balance present in high-latitude regions during wintertime. The inversion typically does not exceed heights of several hundred meters and can exhibit temperature ranges of up to 30˚C from valley bottoms up to the top of the inversion. The main objective of this project was to improve the understanding of the surface-based inversion's temporal evolution by analyzing a suite of extra upper-air balloon launches released during clear and calm nights in Fairbanks. A series of radiosonde launches at high temporal frequency were conducted over seven case-study days spanning spring 2009 and fall/winter 2010. These case studies each present a unique story due to variability with respect to the effects of incoming solar radiation, snow cover, and winds on the development of the surface-based inversion. Several generalizations emerged which provided insight into the development of the surface-based inversion with respect to these variables. In general, the surface temperature decreased most rapidly just after sunset. After this initial cooling pulse at the surface the profile begins to cool vertically. Another feature that appeared on several launches was when surface cooling appeared to cease, suggesting that some sort of temperature minimum had been attained. Cases without snow on the ground had larger surface temperature changes than those with snow cover. The presence of snow cover limits the diurnal surface temperature drop due to reflectivity of radiation which would heat up the surface during the day. This unique data set of two to three hour radiosonde launches could be the basis of future projects in air quality studies, modeling studies, and micrometeorological studies.

Table of Contents

Page

List of Figures

List of Tables

Chapter 1: Background and Justification

1.1 Earth-Atmosphere Energy Balance

The basic surface energy balance for the Earth can be represented as the algebraic sum of the short- and long-wave radiative components incident upon and emitted by the surface. The most essential form of this relationship may be considered for a planet devoid of an atmosphere on a surface that is a perfect absorber and emitter of radiation. In this case, the surface can be treated as a *blackbody*, defined to be a medium that absorbs all radiation incident upon it. One property of a blackbody is the total quantity of emitted energy is a function of the temperature of the surface of the blackbody (i.e. and not its core temperature). This is expressed by the Planck function and is explained by the Stefan-Boltzmann law that represents blackbody emission as,

$$E=\sigma T^4 \qquad (1)$$

where σ is the Stefan-Boltzmann constant (5.67 x 10-8 $Wm^{-2}K^{-4}$) and T is the temperature of the emitting surface in Kelvin. This is termed “outgoing longwave radiation” or OLR. For most practical purposes, the Earth functions almost like a blackbody. Thus, incorporating this idea and taking the first step towards a more realistic Earth surface, that is, one that reflects away some sunlight, the total incoming radiation from the sun must be balanced by the outgoing radiation from earth, therefore,

$$K\,(1-\alpha) = \alpha T^4 \qquad (2)$$

K being the radiation flux from the sun, α is albedo, or "the ratio of reflected flux density, referenced to some surface" (Glossary of Meteorology, 2000), and T is the temperature of the Earth's surface.

The real Earth of course possesses an atmosphere which further complicates the radiation pathway to and from the surface. The radiative contributions of the dominant gases in the atmosphere, nitrogen and oxygen, contribute very little to this balance and may be neglected. Several of the minor constituents, however, are very radiatively active in the longer, thermal wavelengths. These include water vapor, which comprises on average about 1% of the atmosphere (Bohren and Clothiaux, 2006), carbon dioxide, accounting for 380 ppm, methane, accounting for 1.75 ppm, and other more scarce species (Wallace and Hobbs, 2006). These species radiatively insulate the surface of the earth by inhibiting the escape to space of longwave radiation emitted from the surface of the Earth (Salby, 1996), creating a higher temperature at the surface than that which would be expected of a system in which no atmosphere is present. These gases function as absorption bands in the atmosphere. This represents the essence of the atmospheric "greenhouse effect", defined to be the "heating effect exerted by the atmosphere upon the earth because certain trace gases in the atmosphere (water vapor, carbon dioxide, etc.) absorb and reemit infrared radiation" (Glossary of Meteorology, 2000). Water vapor exerts a further influence because water can take the form of a cloud. Clouds are strong longwave radiation absorbers/emitters and, unlike any other gas, clouds directly block shortwave radiation and prevent it from reaching the surface. While the proportion of water vapor in the atmosphere has remained relatively constant over the years, carbon dioxide, methane, and the other radiatively active species have been increasing since the

Industrial Revolution. This increase, with the accompanying increase in the thermal state of the atmosphere that this must in turn necessitate, underlies current concerns about climate change.

At the Earth's surface an imbalance in the system of ground-atmosphere fluxes results in an initial response in the form of a surface temperature change – temperature increase if the balance exceeds zero, decrease if it is less than zero – which is then transmitted into the atmospheric layers nearest the ground. Temperature changes are then transmitted vertically upward into the atmosphere.

1.2 The Surface-based Inversion

1.21 The Basics

Assuming clear sky conditions during the solar day, incoming shortwave radiation passes relatively unobstructed through the atmosphere and that which is not reflected away is absorbed into the ground. The ground responds by warming, which heats the overlying layers of the atmosphere via radiation and conduction, and convection if the surface warms enough. Moving vertically upward into the atmosphere a decrease in temperature is typically observed in the troposphere as distance from the atmospheric heating source, the surface, increases. In the absence of solar radiation, the mechanism which heats the surface is turned off. The surface cools in response as heat is removed through longwave emission. The lowest levels of the atmosphere in turn cool relative to the layers above and a surface-based inversion (SBI) of temperature is established.

An inversion therefore may be defined simply as *an increase in temperature with height*, which is opposite to, or an "inversion" of, the more typically observed, average terrestrial atmosphere

in which temperature decreases with height. SBIs are not uncommon nor particular to northern regions: given clear and calm conditions at a given location, as the sun sets and the surface radiation balance adjusts to favor excess longwave emission from the surface (i.e. a negative balance), the surface will begin cooling and, along with it, the bottom-most layer of the atmosphere. Once the sun returns during daytime and shortwave input again exceeds longwave output, the ground will heat back up and the surface-based inversion will disappear, or "break". Thus for many areas a shallow nighttime SBI is a common feature.

During the winter in high-latitudes, many days can pass during which incident shortwave radiation never exceeds emitted longwave. This allows the negative net radiation balance at the surface to persist which allows cooling to proceed unchecked. If the prevailing synoptic conditions dictate low wind then what happens near the surface is unaffected by, or "decoupled" from, higher levels in the troposphere. Under these conditions – negative surface radiation balance and low winds – a strong SBI will form. The top of the inversion is defined as the point at which cooling ceases, which often coincides with levels where winds are strong enough to mix the air.

It is apparent given these formative criteria, that for northern regions the autumn, winter and spring seasons bring favorable conditions for the formation of strong SBIs. They are a common occurrence in the valleys of interior Alaska due to extremely stable air masses located over the region and little to nil incoming solar radiation. Inversion tops typically may reach heights of several hundred meters. The difference in temperature between the ground surface and the top of the inversion can be large – a temperature difference of up to 30K within the inversion is not uncommon in the subarctic region (Bradley et al., 1992).

1.2.2 Mechanics and Formation of the Surface-based Radiation Temperature Inversion

The formation of a surface inversion is in fact more complex than indicated above. The steepness, or strength, and height of an inversion can be altered by many different factors, including clouds and moisture, cloud properties, winds at the surface and upper-levels, heat flux from snowpack, radiation strength, sun angle, chemical constituents in the atmosphere, the nearby presence of open water, radiative properties of ice crystals, and topography. Clouds and moisture play a large role in the radiation budget of the atmosphere, working as a medium between short wave radiation of the sun and longwave radiation released from the ground. Cloud cover - including the type of cloud, opacity of cloud, thickness of cloud, and height of cloud - all play a role in the amount of heating which will be released or gained at the surface. Specifically in Fairbanks, ice fog, which forms in the deep cold of the winter when homogenous nucleation occurs at ~-40K, influences the surface-based temperature inversion as well. Surface winds will weaken or destroy any form of purely radiative inversion at the surface. If strong, winds can cause horizontal advection of warmer air masses from the south. Winds aloft, even relatively weak, can also affect the surface temperature inversion by the downward mixing (Andre and Mahrt, 1981; Ball, 1956; Wexler, 1936; Bowling, Ohtake, Benson, 1968; Hartmann, Wendler, 2005; Hogan and Ferrick, 1997; Kahl, Serreze, Schnell, 1992; Wendler and Jayaweera, 1972, Wendler and Nicpon, 1974) of warmer air aloft into the inversion zone. Simulations done by a one-dimensional nocturnal boundary layer (NBL) model by Estournel and Guedalia suggest that, even in the presence of weak winds, the stable layer will thicken all night long due to the strong vertical radiative cooling (Estournel and Guedalia, 1985).

These variables which play a role in the formation and dissipation of the surface-based temperature inversion are part of a very complex ground-atmosphere balance at the Earth's surface. This array of variables, combined with the small spatial scales at which many of these are manifested and a lack of detailed understanding of inversion life-cycle (see below), means that capturing the full potential extent of temperature inversions has been a major challenge for computer models and weather forecasters. Computer forecasting models can be incorrect by 15K or more at the surface during the event of a SBI in interior Alaska (Morton, 2009).

1.2.3 Previous research on high-latitude inversions

Previous work on surface-based inversions in Interior Alaska and the broader sub-Arctic/Arctic region has focused largely on the classification of inversion patterns (e.g. Tilley and Weatherby, 2001; Hartman and Wendler, 2005). These efforts have utilized the only observational data set available for this type of work: profiles of temperature, humidity, pressure, wind speed and wind direction taken by radiosondes mounted on a balloon launched twice a day from six-hundred stations around the world at standard times: 0000 UTC and 1200 UTC. In Fairbanks, Alaska, the upper-air weather station is located at the International Airport.

By analyzing these data, the diurnal trend of inversion formation and dissipation during the shoulder seasons may be observed and general conclusions about the inversion lifecycle may be arrived at. However, since the standard observations are only taken every twelve hours, questions concerning details about the formation and dissipation of the inversion between the hours of 0000 UTC and 1200 UTC remain. The twice daily radiosonde soundings yield little more than the knowledge that inversions have a strong diurnal variation (Kadygrov et al, 1999). A more detailed understanding of the temporal evolution of an inversion is important not only for

temperature forecasts but also for dispersion forecasting of pollutants which create health concerns. Previous work has shown that pollutants and aerosols concentrate at the top of the inversion (Bridgman et al., 1989). Thus, it is of interest to know in greater detail how the inversion temporally evolves. This information would be of use to computer modeling efforts as well.

Very little work has been done to investigate in greater detail inversion life-cycle evolution. In a recent article about the surface-based temperature inversion in Finland (Pepin et al., 2009) the authors discuss the settling of cold air in valleys as a major feature of high-latitude climates of the Arctic and report on their study in which temperature sensors were placed in a vertical transect to study the temporal and spatial evolution of the surface-based temperature inversion in Kevo Valley, Finland. This work focused in particular on the annual climatology of the SBI and the possible mechanisms behind their formation and destruction in the local area. There is a strong negative net radiation balance in the study area, and therefore the only way that the surface-based temperature inversion will break past a certain date in the winter would be through a change in synoptic conditions (Pepin et al., 2009). The SBI in the Kevo Valley, had two steep inversion anomalies during March and November, rather than in the deep of winter – an interesting and counter-intuitive result. Pepin et al. (2009) did not find a seasonal forcing of these shallow, steep inversions, but these anomalies indicate a time period where solar input is differing, and a significant inversion developed.

Research on surface-based temperature inversions in Fairbanks has been done in recent years in the Department of Atmospheric Sciences at the University of Alaska Fairbanks. A study was done in 2007 by Kankanala using a Doppler SODAR to depict drainage winds, low-level jets, the

development of the inversion, and estimation of the mixing layer height. Though this study encompasses a similar topic to the presented research, the instrumentation during the 2007 study had some limitations and was used only from December to April. Kankanala's measurements showed that the temperature inversions were strongest, deepest and most frequent during the deep winter months of December and January (Kankanala, 2007). Bourne in 2008 studied the climatological variability in the surface-based inversion. Bourne's work indicates when surface temperatures are warm, inversion depths are shallow, and vice versa (Bourne, 2008).

1.2.4 Surface-based Temperature Inversions in Fairbanks, AK

Fairbanks, Alaska, located at 64.84 N, is situated at the north end of the broad Tanana River Valley and is surrounded on three sides (north, east and west) by hills of approximately 1000 meter elevation. When radiation and synoptic conditions are suitable – that is, clear and calm – cold air pools within the valley and a SBI forms. Such is the frequency of these conditions that a SBI is present in Fairbanks approximately 77% of the time climatologically during the months of December through February (Hartmann and Wendler, 2005). When the SBI is strong, the particulate matter coming from combustion processes is trapped, resulting in a significant increase in pollutants such that Fairbanks often exceeds EPA standards for particulate concentrations in the wintertime (Fig. 1.1). These particulate concentrations can pose health risks to its residents. With the increasing population and rising fuel prices forcing an increase in the use of woodstoves in the Fairbanks region, air quality forecasts are becoming more important to the residents of the area. Currently, weather models have a difficult time

modeling the surface-based temperature inversion because of their inability to accurately predict wind speeds in the lower ABL (Molders and Kramm, 2010).

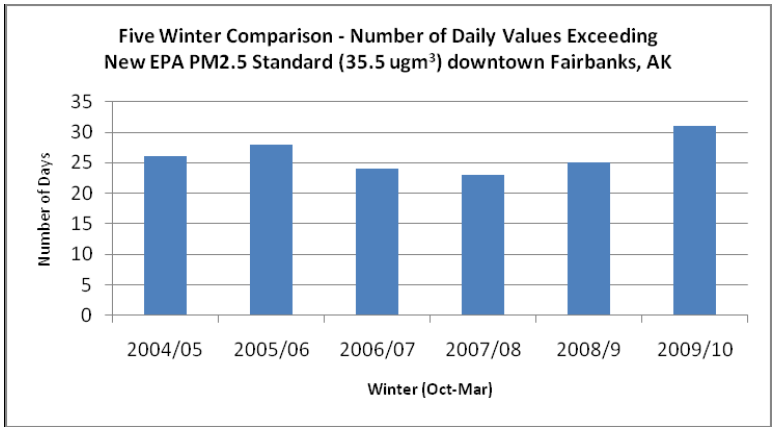

Figure 1.1: Number of Days Fairbanks Alaska's air quality exceeds EPA standards. Courtesy of Fairbanks Department of Environmental Conservation (DEC).

By analyzing surface temperature readings at different elevations in the Middle Tanana Valley, we know that when it is clear and calm out, the valleys are substantially colder than the hills. The disconnect between model estimates, which are relatively spatially coarse, and the fine spatial scale at which these features are manifested is apparent using satellite thermal infrared imagery. Figure 1.2 shows a topographic image of the Fairbanks area, and figure 1.3 shows an infrared satellite image of the Fairbanks area on a clear night. One can see the cold bowl of Fairbanks and the Tanana Valley with warmer temperatures up in the hills surrounding the city. This is also strongly evident in the Yukon Flats, northeast of Fairbanks. The strength of the surface cold is not reproduced by weather forecast models currently in use by the National Weather Service.

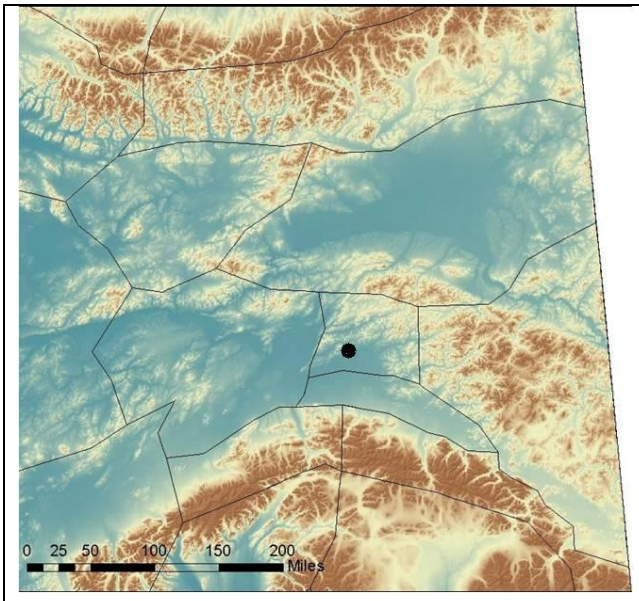

Figure 1.2 – Topography of the central Alaska Interior. Higher elevations are designated by brown and lower elevations are designated by green. Fairbanks is designated by the black dot. The lowland areas of the Tanana Valley (south of Fairbanks), Minto Flats (west of Fairbanks), and the Yukon Flats (northeast of Fairbanks) are visible (National Elevation Dataset for Alaska (USGS), National Weather Service Fairbanks).

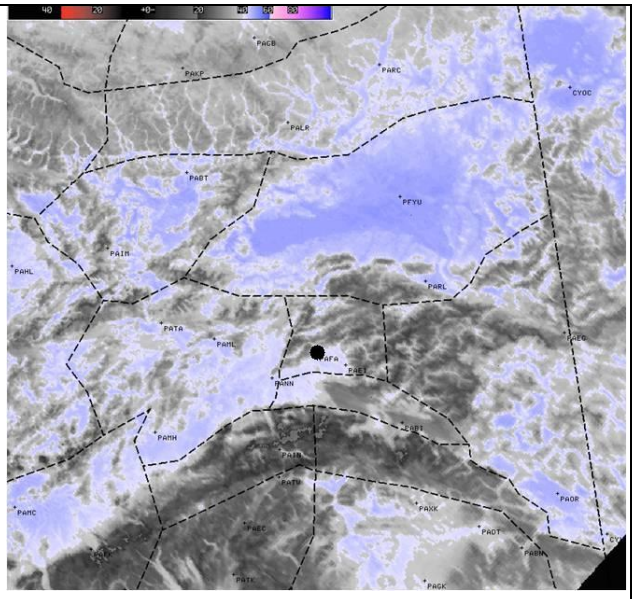

Figure 1.3 – Infrared satellite image of Fairbanks area during a clear night. Fairbanks is designated by the black dot. Gray designates areas of warmer temperatures and blue designates colder air (Polar Operational Environmental Satellite infrared image, February 2003, National Weather Service Fairbanks).

1.2.5 The Surface-based Temperature Inversion and Snowpack

During the spring/autumn shoulder seasons, a significant shift in the patterns of high and low temperature occurs as the snowpack disappears/forms (Stevens, 2009). For this study, this time of year has been defined as the "shoulder season", to signify a time of year when the amount of radiation changes rapidly (i.e. the daylight increases or decreases a significant amount), up to 7 minutes per day. For example, the day length increases from 13.5 hours on April 1 to 17 hours by April 30. The presence of a snowpack can modify the radiation balance through changes in conductive and latent heat fluxes at the surface, the reflection of incoming solar radiation, and the emissivity of the surface (Walsh et. al, 1985). The snowpack has a higher albedo than bare

ground, therefore reflecting a greater proportion of incoming shortwave radiation. In these cases the main effect of snow on the strengthening of the SBI is that the emittance of the ground depends on the fluxes between the ground and the atmosphere above it.

During the spring shoulder season the winter snowpack still exists in Fairbanks but, despite its presence, the elevation to which the sun is rising, combined with the solar duration, creates incoming radiation values that are high enough to cause large diurnal fluctuations. This typically breaks the inversion in the day, thus confining the SBI to the night.

1.3 Goals of this Research

In light of the gaps evident in the research conducted to date on SBIs, it is the objective of this project to improve understanding of the SBI temporal evolution by analyzing a suite of extra upper-air balloon launches, taken in addition to the regular 0000 and 1200 UTC launches by:

a) Analyzing the potential effects on the atmospheric temperature profile due to mechanical mixing by horizontal wind;

b) Evaluating the relationship between snow cover versus no snow cover on the development of the inversion throughout the nighttime between sunset and sunrise; in particular one would expect to see a smaller amount of heat transfer between the ground and the atmosphere just above it due to the insulating properties of the snow layer, as well as the incoming solar radiation which get reflected by the snow surface.

c) Qualitatively see how atmospheric cooling progresses vertically with height after the surface air reaches a near minimum temperature at night, assuming a balance could be reached between the IR fluxes between the ground and the atmosphere just above the surface.

Chapter 2: Data and Methods

2.1 Methods

In order to capture details of the temporal evolution of SBI formation, a series of seven detailed case studies were conducted. A case study represents one afternoon-night-morning time-cycle during which a series of radiosondes were launched every two to three hours from the Upper Air Facility near Fairbanks International Airport (FAI) between sunset and sunrise.

Two broad time frames were chosen for this study – spring 2009, between the months of February and May, and fall 2009, between the months of September and November. January and February – the coldest part of the winter – were not selected because during this time, the only factor which will break the inversion is a change in synoptic conditions. These dates were selected to examine how the inversion development differs under varying conditions of radiation strength, night duration, and snow cover. Within these broader time frames specific case study days were selected on fairly short notice based on weather forecasts which called for favorable conditions (see section 2.2).

2.1.1 Instrumentation

Vaisala RS-80 radiosondes were used for the spring 2009 set of launches. In summer 2009 the National Weather Service upgraded its equipment to the new Sippican MKII GPS radiosondes. These instruments have a much greater vertical resolution than the RS-80s and were used for the fall 2009 set of launches. The Vaisala RS-80s recorded data every 6 seconds, or approximately every 30 meters vertically in the spring cases, depending on the balloon's rate of ascent. The Sippican MKIIs recorded data several times per second, or approximately every 4 to

5 meters. Although of coarser vertical resolution, the February soundings are still able to capture the basic inversion development, although they are not sufficient to capture the most subtle changes in the vertical temperature profile.

This project also had access to data from a Remtech PA-2 Phased Array Doppler SODAR. This device emits an acoustic pulse in the audio band and then processes the phase shift of the return signal. It is able to provide time-evolving temperature, wind speed and direction, and turbulence parameter signals up to ~1100m ASL at a vertical resolution of 40m. This instrument was co-located at the upper-air launch facility during the autumn radiosonde launches. The plots seen from the SODAR are of CT^2 and wind speed. CT^2 indicates the heights of the inversion indicated by the level of acoustic reflectivity. The inversion is located at the levels where the signal goes from high reflectivities to low reflectivities or no reflectivity- black or white points. The increase in acoustic reflectivity is due to turbulence induced by temperature or wind speed.

2.1.2 Error, Bias, and Precision of Vaisala RS-80 and Sippican MKII Radiosondes

The change in instrumentation during this field study should be noted in order to show that the change did not affect the overall results of this project. The Vaisala RS-80 and Sippican MKII radiosondes have very similar specifications, including 0.1 hPa pressure resolution, 0.5 hPa pressure accuracy, a temperature measuring range of -90˚C to +60˚C and a 1% humidity resolution. The temperature resolution differs slightly, – 0.1K on the Vaisala RS-80 radiosondes versus ±0.2K for the Sippican MKII radiosondes. The humidity measuring range also varies slightly, 0 to 100% for the Vaisala RS-80s and 5 to 100% for the Sippican MKIIs.

An intercomparision study was done in Brazil in 1999 to compare the performance of the Vaisala RS-80 and Sippican MKII radiosondes (Fisch et. al, 1999). Results of the study show that the statistical mean temperature difference between radiosondes (RS-80 minus MKII) is only -0.1K to -0.2K. The two types of radiosondes have a negative bias for relative humidity of 5-7%, and a negative bias for pressure of about 0.2-0.3 hPa. With these differences on such a subtle scale, these biases are not impactful to this study.

The Vaisala RS-80 radiosonde's wind measurements used a radio-theodolite which is a term for a small tracking radar system, which interpolates winds by measuring the position of the radiosonde relative to the earth's surface as the balloon rises. This system can cause problems operationally since the wind speed and direction must be calculated using the tracking radar, and if the radar does not "lock on" to the radio signal, then wind measurements may be missing. This is particularly difficult during no wind conditions because the tracking antenna located at the site of weather balloon launches has problems receiving signal from a high elevation angle, as seen in this study. The Sippican MKIIs in practice have a much higher return rate of wind data, since the winds are depending on GPS tracking, which is initiated before launch and not reliable on a radio-theodolite.

2.2 Synoptic Conditions

Case studies were run on nights for which the weather forecast suggested the likelihood of strong SBI development: clear nights under synoptically quiescent conditions. The specific weather conditions required were mostly clear skies ($2/8^{th}$ or less sky) to minimize longwave-down radiation, and surface winds less than 4 kts, to minimize mechanical mixing. In practice,

the typical launch evening saw a synoptic condition that had a dominant ridge sitting over Interior Alaska, resulting in very little dynamic forcing.

Chapter 3: Results

3.1 Spring 2009 weather balloon launches

Of the seven case studies four took place in spring and three in autumn (Table 1). Spring launch dates included one in late February, two in mid April and one in early May. The solar conditions encompassed by these spring launches, for maximum sun angle, ranged from about 16 degrees above the horizon (Feb) to just over 40 degrees (May) (Fig. 3.1). The maximum incoming solar radiation ranged from about 150Wm-2 to nearly 700Wm-2; thus the dataset enables a comparison of the surface-based temperature inversion throughout the transition season. Autumn launches included two in mid-October and one in mid-November; solar angles ranged from 5˚ to 17˚ above the horizon (Fig. 3.1) and maximum incoming solar radiation went from 22 Wm^{-2} to 255 Wm^{-2}.

Snow cover was present for 4 of the 7 case studies. Each case is considered separately below. For all descriptions “surface” indicates surface mean sea level pressure plots with a basic level of analysis applied (NOAA Marine Facsimile charts), and the three aloft levels (in Appendix A) portray patterns of geopotential height, temperature, and winds at the 850, 700, and 500hPa levels, as derived from NOAA Global Forecast System model initialization, and are labeled “850”, “700”, and “500”, respectively.

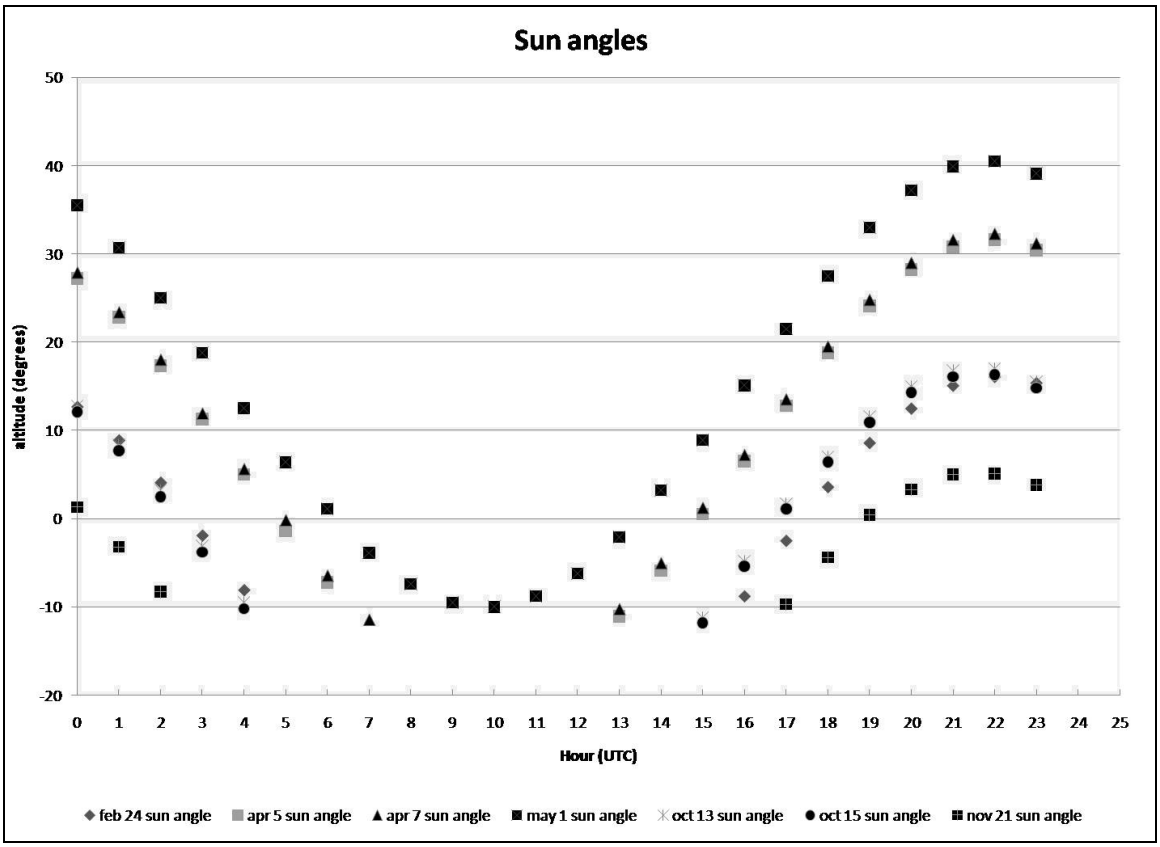

Figure 3.1: Range of sun angles for case studies in Fairbanks, AK. UTC/GMT is -9 hours standard time and -8 hours daylight time. Values courtesy of U.S. Naval Observatory.

Table 3.1: Timings and details of radiosonde launches

Date, time (UTC/AST) and # launches	Strongest surface wind during observation window	Ceiling development? (SCT or more)	Minimum temperature reached at PAFA (˚C)	Snow depth (in)	Hours after sunset when min temp was reached	Hours before sunrise when min temp was reached	Max incoming radiation	Max solar angle
2/24/2009 (0100-1900 /4pm-10am) 7 launches	4kts (0700-0800 UTC)	Y (BKN 1900 UTC)	-22	21	11	3	255 W/m2	16
4/5/2009 (0400-1800 /7pm-9am) 7 launches	4kts (0400-0500, 1200, 1900 UTC)	Y (BKN 0400 UTC)	-21	25	9	1	548 W/m2	31
4/7/2009 (0400-1800/7pm-9am) 7 launches	5 kts (1300 UTC)	N	-16	25	10	0	568 W/m2	32
5/1/2009 (0400-1700/7pm-8am) 7 launches	4 kts (0500-0600, 0900-1000 UTC)	Y (BKN 0400-0500 UTC)	3	0	7	2	750 W/m2	41
10/13/2009 (0200-1900/5pm-10am) 7 launches	4 kts (0900 UTC)	N	-3	0	10	4	257 W/m2	17
10/15/2009 (0200-1900/5pm-10am) 7 launches	3 kts (0900, 1600-1700 UTC)	N	-8	0	14	0	251 W/m2	16
11/21/2009 (0200-2000/5pm-11am) 7 launches	3 kts (0200-0300, 0500-0700 UTC)	N	-36	7	13	5	23 W/m2	5

3.1.1 February 24, 2009

During the February 24th case study, the sunset at 0250 UTC and rose the next day at 1718 UTC. The weather balloon launches were released at 0100, 0400, 0700, 1100, 1530, 1700, and 1900 UTC. During this time of year, there was snow cover on the ground.

Synoptic overview: At the surface, a ridge of high pressure extended from the Yukon Territory west into eastern Alaska (Figs 3.2 a and b). This acted to generally suppress cloud formation; however by 1400 UTC a few high clouds had developed in the northern horizon. These clouds were possibly a result of turbulence associated with the strong shear zone formed by the wind speed gradient between the jet axis lying over the northwest corner of Alaska and the center of the ridge. The clouds were not close enough to the study site, however, to drastically alter the radiation flow. Aloft a ridge was present, oriented north-northeastward from the central Gulf of Alaska, and increasingly well identified with elevation up into the atmosphere. These patterns persisted through the case study period. Thus the combination of a surface high pressure region, resulting from a thermal density maxima, and a general dynamic situation aloft also favoring high pressure (the ridge feature associated with the strong trough to the west), served to suppress cloud formation and set the stage for rapid radiative loss at the surface.

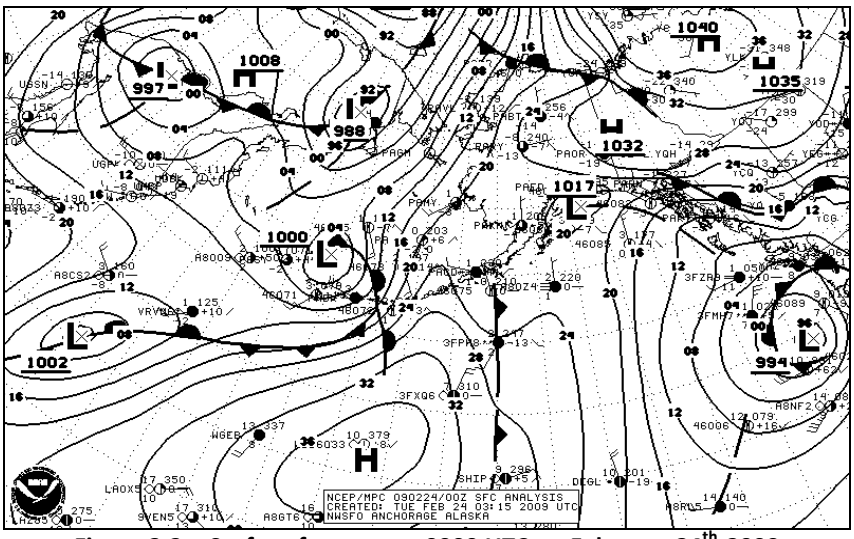

Figure 3.2a: Surface features at 0000 UTC on February 24th, 2009

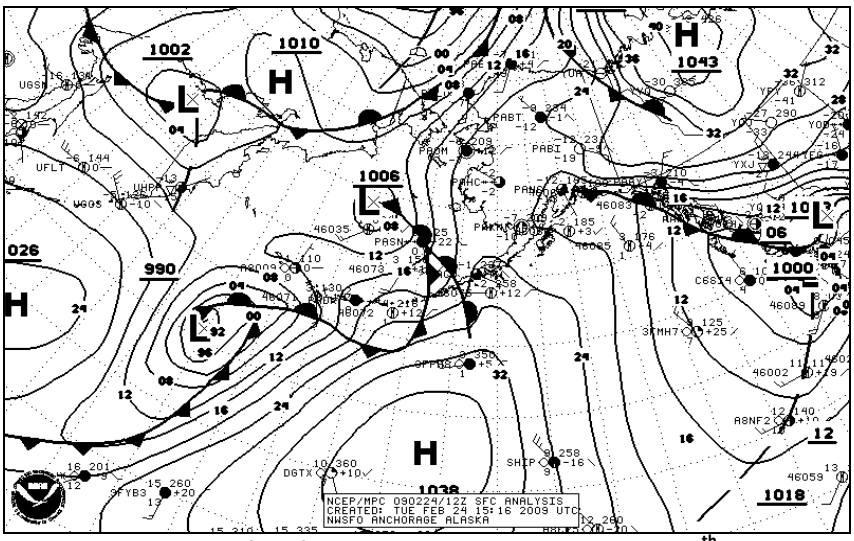

Figure 3.2b: Surface features at 1200 UTC on February 24th, 2009

General observations during launches

At 0100 UTC during the beginning of the period of study, the vertical temperature profile was near isothermal at ~ -6˚C up to 800m ASL. Above this level an inversion feature was in place, extending to 1200-1300m. At this time the first hint of a surface inversion process was already underway. Calm winds were observed, which persisted until about 0500 UTC.

At 0400UTC some mid-level clouds were observed on the horizon at about 3600m altitude, but by 0400 UTC the skies had cleared. The surface temperature continued to drop rapidly, approximately 6K since 0100 UTC as surface radiation emission proceeded after the sunset at 0250 UTC. By 0400 the first inversion maximum height was established at ~300m ASL at -6˚C to -7˚C. It fluctuates around this height for the next three launches.

At 0700 UTC, the low-layer temperature dropped by ~3K since 0400 UTC. From 05 UTC to 0700 UTC surface winds picked up slightly to 2-4 kts from the northeast. After 0700 UTC surface winds died off and remained calm through the rest of the night.

By 1100 UTC, the surface temperature had dropped another 4K over four hours and established itself at its apparent minimum surface temperature of -20˚C, remaining there for the next few hours.

By 1530 UTC a few mid-level scud clouds had formed on the north horizon, too far away to affect the radiation balance. Winds remained calm and the inversion did not mix out. While the low-level temperature remained steady, the temperature aloft began to drop and the inversion height to rise. Although a little indistinct, arguably the inversion height has reached ~600m ASL by this time.

At 1700 UTC the surface temperature remained at -20˚C, however higher up the inversion continued to deepen (dz) with height throughout the evening before sunrise. By this time the inversion height, although growing indistinct due to the action of winds aloft (see later case study discussion), was arguably around 800m ASL.

At 1900 UTC about two hours post-sunrise (Fig. 3.4), the inversion began to break from the surface, but continues deepening with height. The surface inversion pulse is merged with the signals aloft, resulting in an overall inversion height of 1600m ASL.

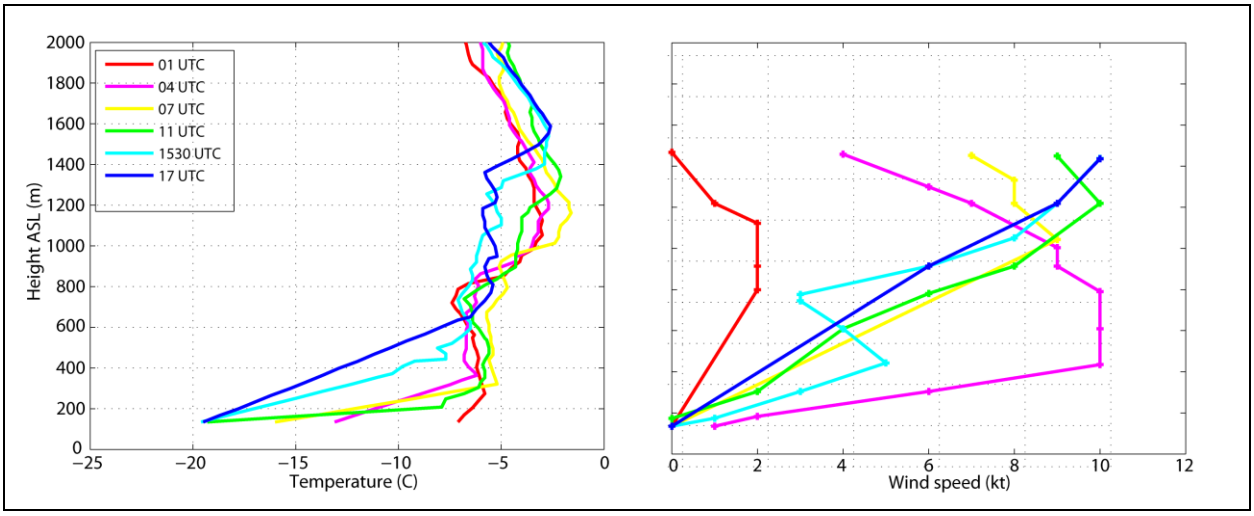

Figure 3.3: Vertical structure of the SBI development post-sunset February 24, 2009. Sunset – 0250 UTC. The surface temperature decreases with time until a minimum temperature is reached. The atmosphere cools vertically after as is seen in the 1530 and 17 UTC data.

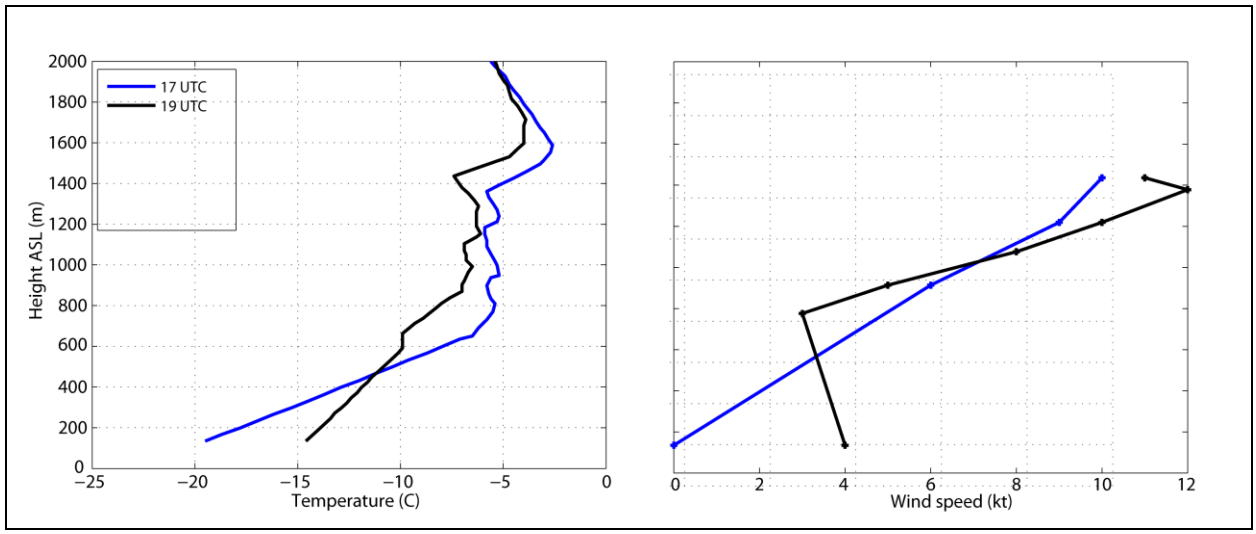

Figure 3.4: Vertical structure of the SBI dissipation post-sunrise on February 24, 2009. Sunrise – 1718 UTC

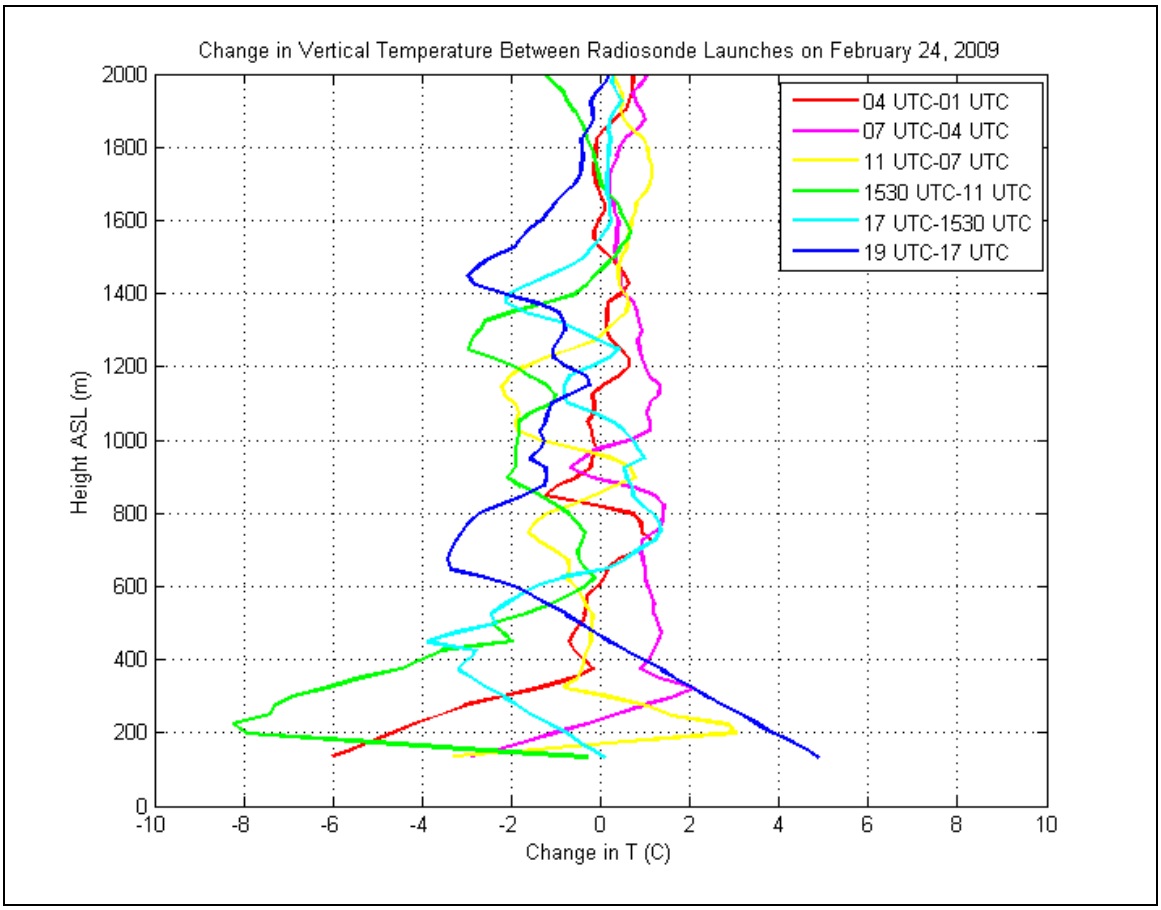

Figure 3.5: Change in Temperature between Radiosonde Launches on February 24, 2009 at Fairbanks, AK. Note that these are changes between launch times, so are not standardized to a common time-step.

Case summary:

In looking at the temporal evolution of temperature on February 24th (Fig 5) a zone of temperature cooling is apparent above 800m ASL, possibly indicative of advective processes aloft. To best isolate radiative cooling effects, there would be no advection at higher elevations affecting the surface balance, but in reality, some advection was likely occurring. In general, these launches support the idea that the temperature inversion cools with height as the ground and atmosphere reach a minimum temperature. There is cooling just above the surface, maximizing near 200m ASL between the 1100 and 1530 UTC launches. This first series gives a

good idea of the height of the PBL – diurnal pulse to ~800m ASL with extension up to ~1200m ASL.

This case study has provided insight into the influence of winds and their capacity to alter the vertical profile. For example, the Feb 24th launch exhibited two main wind episodes, each of which produced a discernible effect on the profile. The first, short lived event occurred at the 0400 launch – a pronounced wind speed maxima between ~300 and ~700m ASL (Fig. 3.4). Although of short duration, the 0400 profile shows a warming layer above ~600m ASL of ~200m thickness and a cooling below that of ~200m thickness. The likely explanation for these patterns is wind redistribution of warm air aloft down the column and cool air developing at the surface up into the column. The second wind episode occurs higher up in the profile and is of longer duration, although the case could be made that the wind maxima core is moving up throughout the evening. That is, the maximum at 0400 is ~700m ASL; at 0700, ~1000m ASL; at 1100, ~1200m ASL; and at 1530, 1700 and 1900, more or less stabilized at ~1400m ASL. As well, after the initial maxima at 0400, there was a weak tendency towards a gradual increase in wind speed throughout the evening. The second wind episode occurred at the end of the case study period, and cannot be separated from the variable of incoming solar radiation breaking the inversion.

3.1.2. April 5, 2009

During the April 5th case study, the sunset at 0455 UTC and rose the next day at 1451 UTC. The weather balloon launches were released at 0400, 0600, 0800, 1100, 1400, 1600, and 1800 UTC. During this time of year, there was snow cover on the ground.

Synoptic overview: A surface ridge of 1030 hPa high pressure extended northeastward from west coast Alaska into northern Nunavut, Canada. A 999 hPa low in the Gulf of Alaska weakened gradually to a 1010 hPa low throughout the day on April 4th. This feature was likely responsible for the cloud cover seen in interior Alaska on the previous day until just before balloon launches began. Once this low weakened, and the ridge continued to build into the region, cloud formation was suppressed and clear skies persisted through and beyond the period of study. Upper air dynamics were minimal (Figs. A.4-A.6), with a general pattern of weak high pressure.

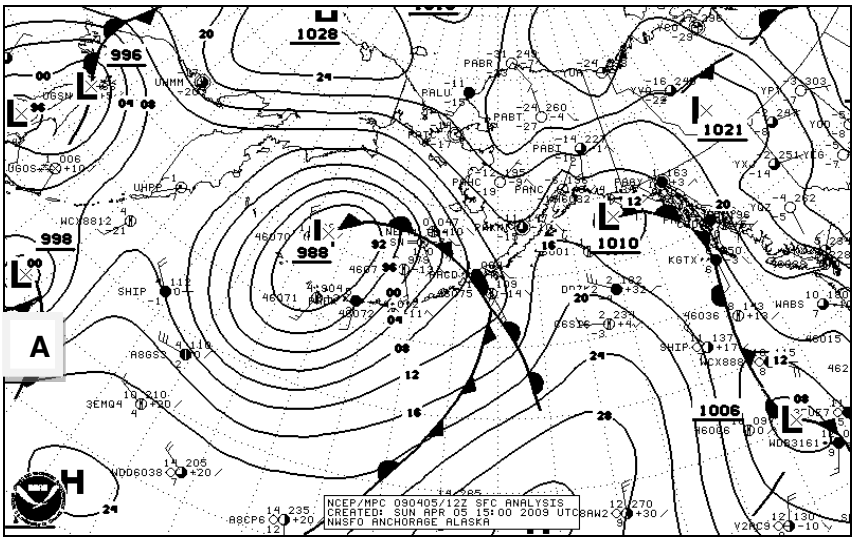

Figure 3.6a: Surface features at 0000 UTC on April 5, 2009

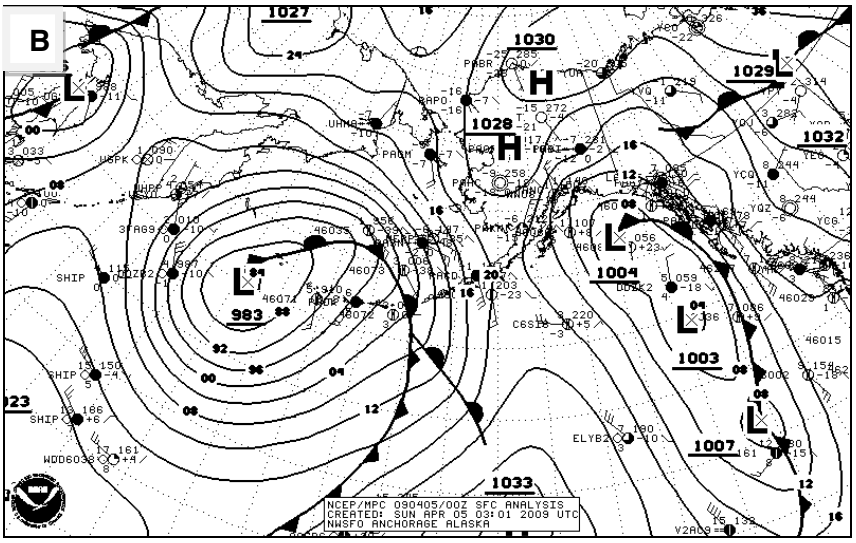

Figure 3.6b: Surface features at 1200 UTC on April 5, 2009

General observations during launches

On the evening of April 4th (April 5 UTC), partly cloudy skies dissipated to clear conditions by around 0400 UTC (8pm local) for the first radiosonde launch of the case study. The few remaining clouds were located on the north horizon and did not block any shortwave radiation from reaching the surface or any longwave radiation to release into space. From the beginning of the launch period until about 0600 UTC light winds of 2-4 kts were recorded at PAFA. At this time the sun was low in the horizon about 5˚ above the horizon and the surface temperature was beginning to gradually fall.

At 0600 UTC winds became calm after 0600 UTC, about an hour and fifteen minutes after sunset. The surface temperature decreased by 2K since the 0400 UTC launch. The top of the inversion was defined to be ~200m ASL.

At 0800 UTC, a strong surface temperature decrease of 6K in was observed since 06.

At 1100 UTC, the surface-based inversion seemed to stabilize at a minimum value for the evening of approximately -19˚C. Surface winds of 2-4 kts were recorded for two hours from 1100 to 1200 UTC. These winds may have delayed the surface temperature inversion from strengthening as much as it would have with completely calm winds, but did not seem to affect the development of the inversion, since the top of the SBI was at its lowest altitude for the night, sitting at ~180m ASL, only 45m above the ground level.

At 1400 UTC, the surface temperature reached the case study minimum (-20˚C) after two hours of calm winds. During the next few hours, the surface temperature remained near -20˚C but became deeper as the top of the inversion moved upward slightly to ~220m ASL.

By the 1600 UTC launch, slightly over an hour post-sunrise (Fig. 3.8), a slight increase (1K) in the surface temperature is observed as shortwave radiation warms the surface.

At 1800 UTC, the surface-based temperature inversion is still continuing to break, but interestingly temperatures between 250 and 800 m ASL have remained unchanged during the last 4 hours. Between the surface and 250m ASL the temperature profile warms and the inversion, while still present, has lost a lot of its steepness as the atmosphere mixes via convection.

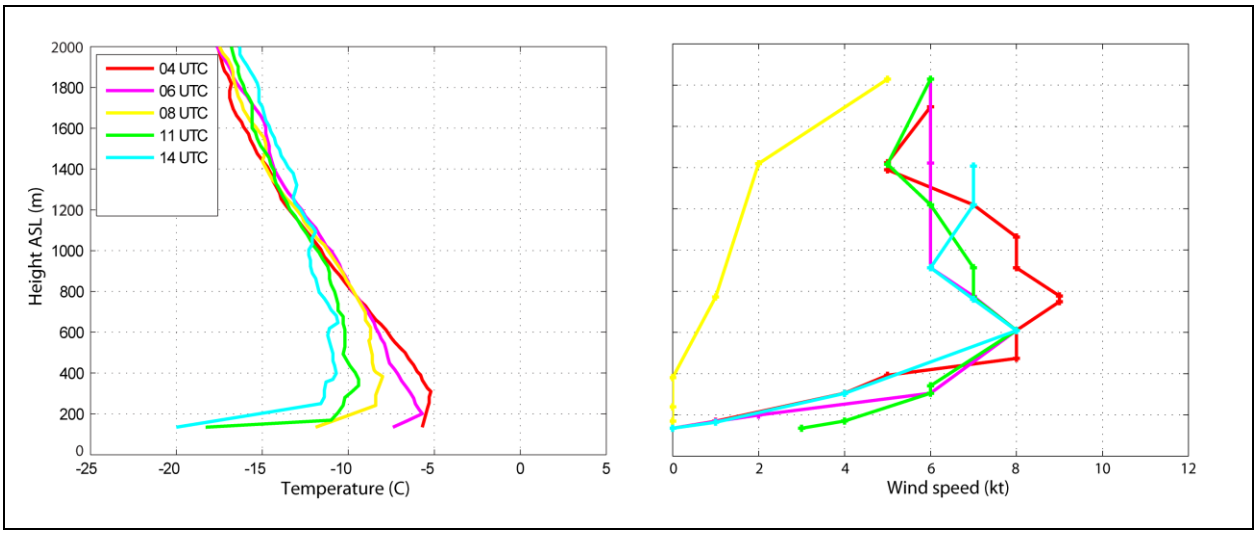

Figure 3.7: Vertical structure of the SBI development post-sunset on April 5, 2009. Sunset – 0455 UTC

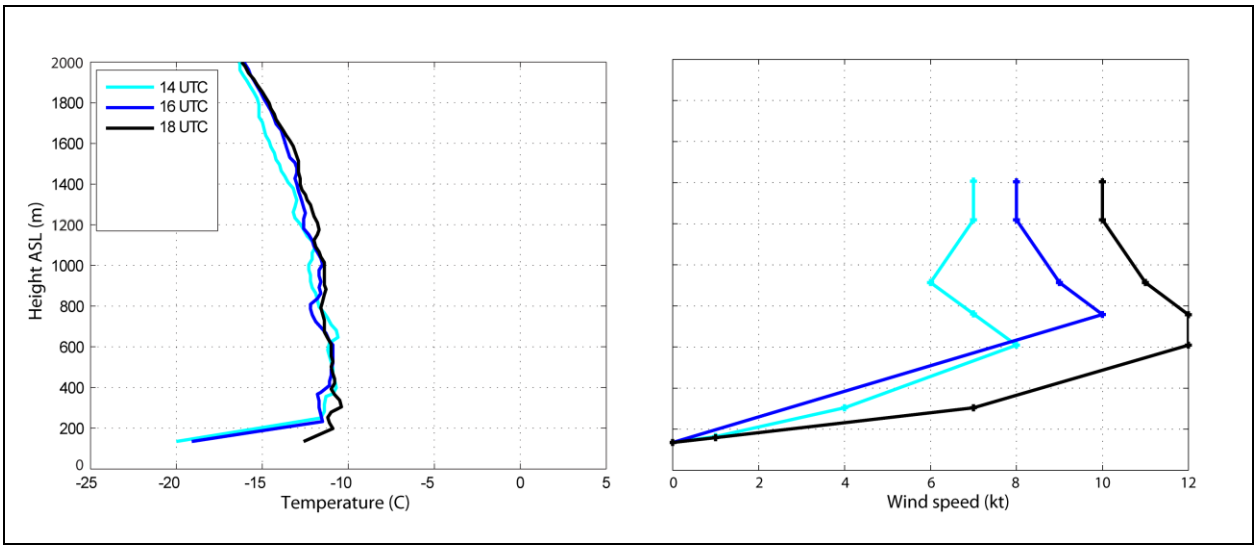

Figure 3.8: Vertical structure of the SBI dissipation post-sunrise on April 5, 2009. Sunrise – 1451 UTC

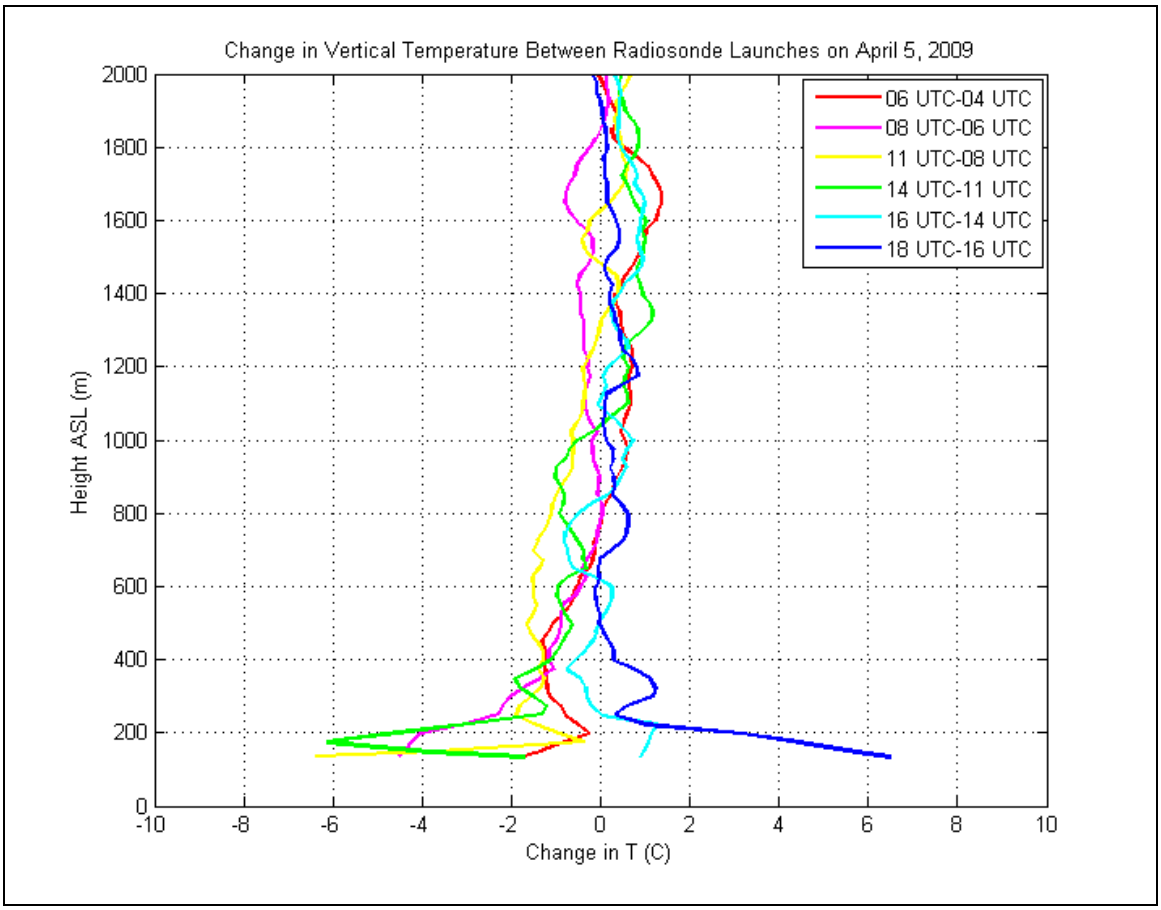

Figure 3.9: Change in Vertical Temperature between Radiosonde Launches on April 5, 2009 at Fairbanks, AK

Case summary:

The April 5th launches exhibited an instance in which the synoptic conditions hindered cloud development due to a lack of moisture and dynamic forcing – an ideal case for this type of study. A wind speed maximum is indicated around 600m ASL, which shows an increase between the 1400, 1600, and 1800 UTC launches. The surface temperature dropped 6C in two hours at of 0800 UTC. This is one of the largest 2-hour drops observed in the project. As seen in the previous case on February 24th, the maximum cooling of the inversion just above the surface happens between 1100 and 1400 UTC.

3.1.3. April 7, 2009

During the April 7th case study, the sunset at 0501 UTC and rose the next day at 1444 UTC. The weather balloon launches were released at 0400, 0600, 0800, 1100, 1400, 1600, and 1800 UTC. During this time of year, there was snow cover on the ground.

Synoptic overview: This case study was conducted the day after the previous case study. Mostly clear skies and calm to light winds persisted through the previous case study into the next several days. Though a ridge of high pressure was not a prominent feature at any level between the surface and 500 hPa (Figs. A.7-A.9), there no major synoptic features were present to create clouds. Another set of balloons were launched on the evening of April 6th (April 7th UTC). There was no cloud development during the entire span of balloon releases.

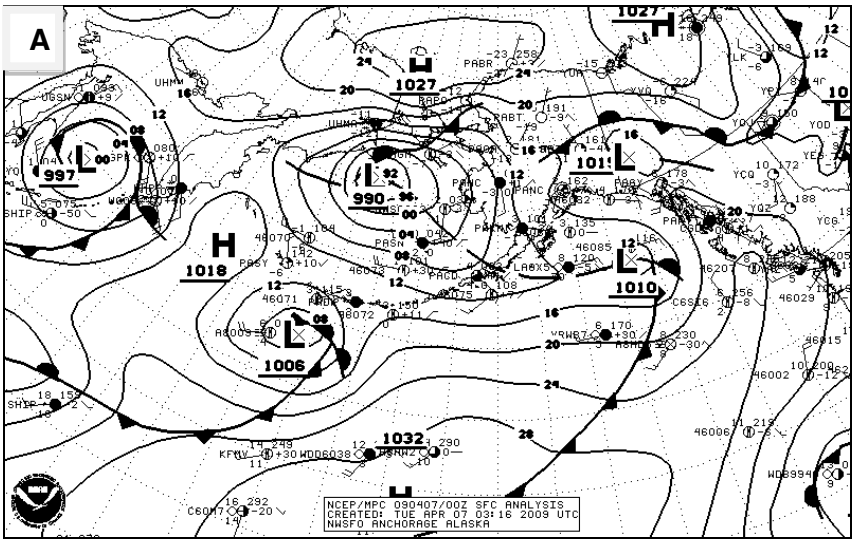

Figure 3.10a: Surface features at 00 UTC on April 7, 2009

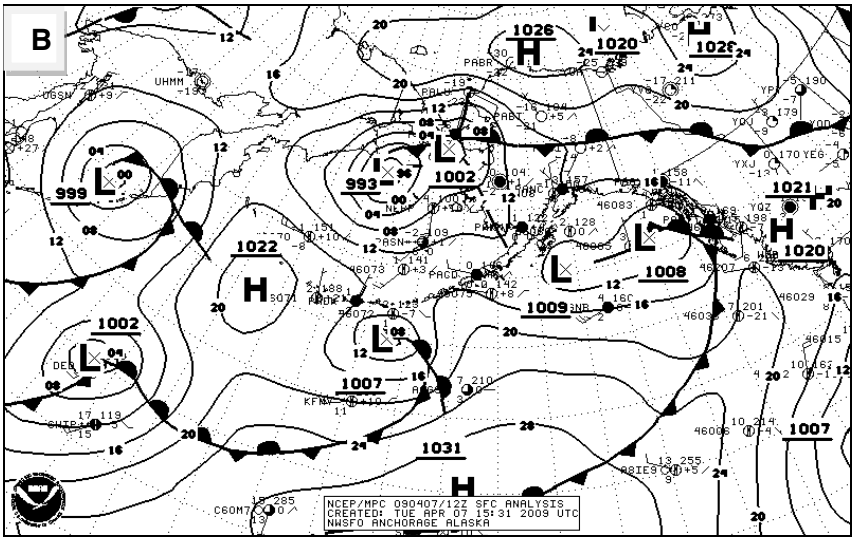

Figure 3.10b: Surface features at 1200 UTC on April 7, 2009

General observations during launches

At 0400 UTC, just before sunset the atmosphere has a very similar profile to the April 5th 0400 UTC sounding (i.e. previous case study start launch), but with a slightly lower inversion top (260m versus ~320m ASL) The inversion development was already underway during this first launch, before the sun had fully set.

Between 0400 and 0600 UTC, the surface temperature dropped 5.6K – a sign of radiative cooling at the surface. 3 kts of winds were measured from 0500 to 0600 UTC and the inversion height rose to near 380m ASL.

At 0800 UTC, the surface temperature dropped 3.4K in two hours. Winds became calm during this time, and the inversion height dropped to near 260m ASL.

At 1100 UTC, surface temperature dropped another 2.9K in 3 hours, a slower cooling rate than earlier in the evening. A light 3 kt wind occurred around 1000 UTC, and the inversion height dropped to near 220m ASL.

At 1400 UTC there were no winds above 4 kts during the launch period until 1300 UTC when the hourly observation recorded 5 kt at the airport. With these winds not persisting and conditions becoming calm, a similar pattern to the April 5th launches revealed itself. A few high clouds on the north horizon formed around 1400 UTC, but did not hinder the escape or penetration of radiation. Temperature at the surface dropped 3.2K since 1100 UTC despite the 5 kt wind spike. Inversion height stayed fairly constant at about 210m ASL.

At 1600 UTC, at the time of launch the winds were calm at the upper air station, but a 3 kt wind was recorded at the Fairbanks ASOS near launch time. The sun had risen about an hour and fifteen minutes before this launch, and the surface inversion was just beginning to break. The temperature rose 1.6K in the two hours since the previous launch and the inversion height rose slightly to about 220m ASL.

At 1800 UTC the inversion quickly began to break from the surface upward as seen in the 1800 UTC launch. The temperature rose 5.6K at the surface and began to warm vertically up to about 400m ASL, a level at which the profile indicates cooling above 400m ASL. The surface inversion height rose to about 300m ASL, but contained either isothermal layers or slight inversions all the way up to 800m ASL.

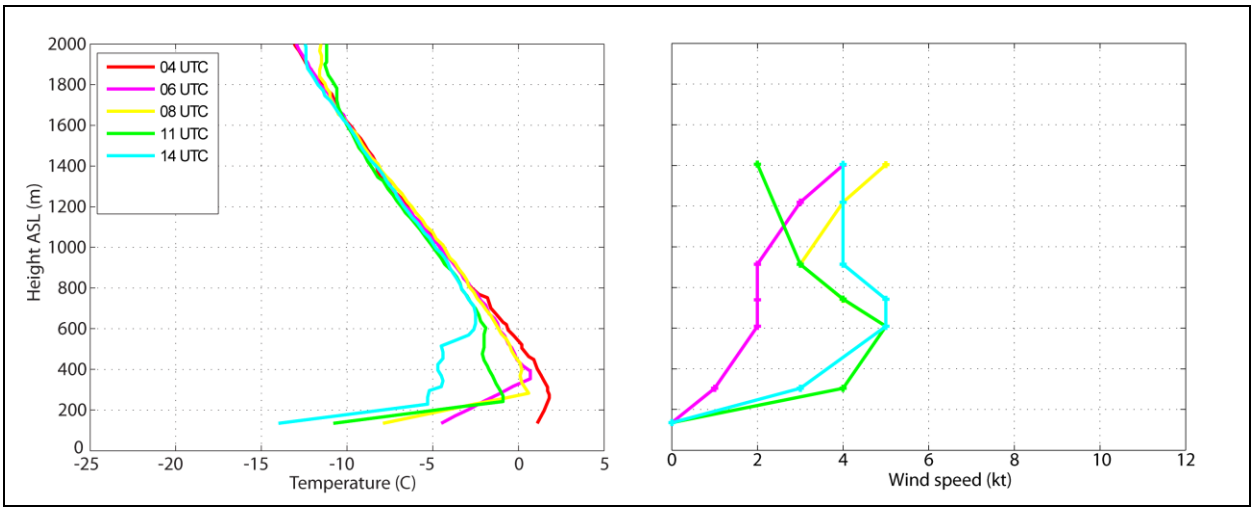

Figure 3.11: Vertical structure of the SBI development post-sunset on April 7, 2009. Sunset – 0501 UTC

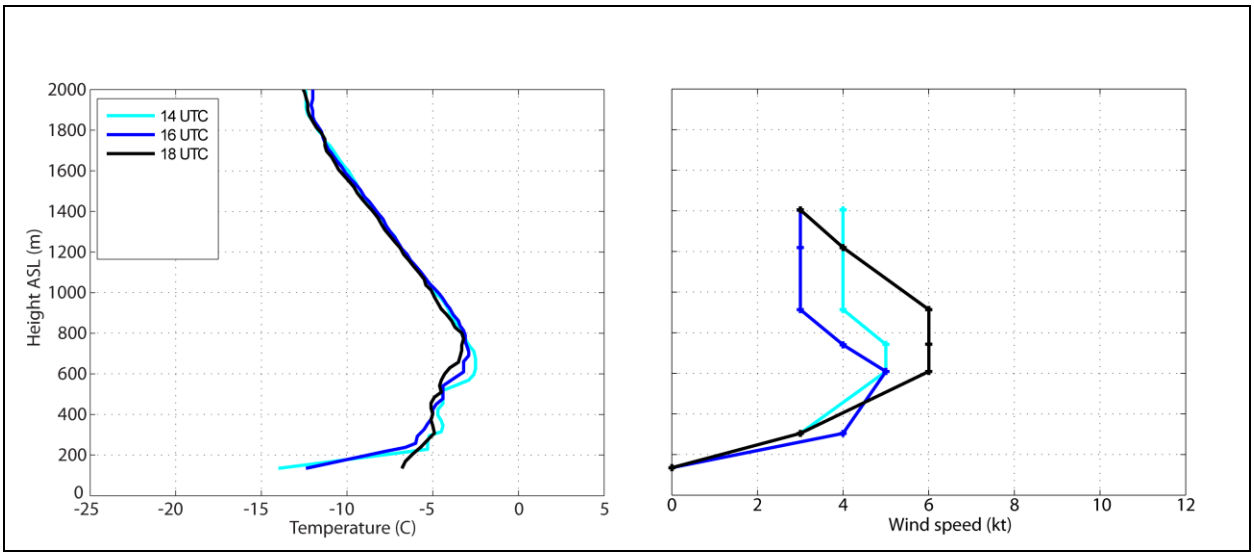

Figure 3.12: Vertical structure of the SBI dissipation post-sunrise on April 7, 2009. Sunrise – 1444 UTC

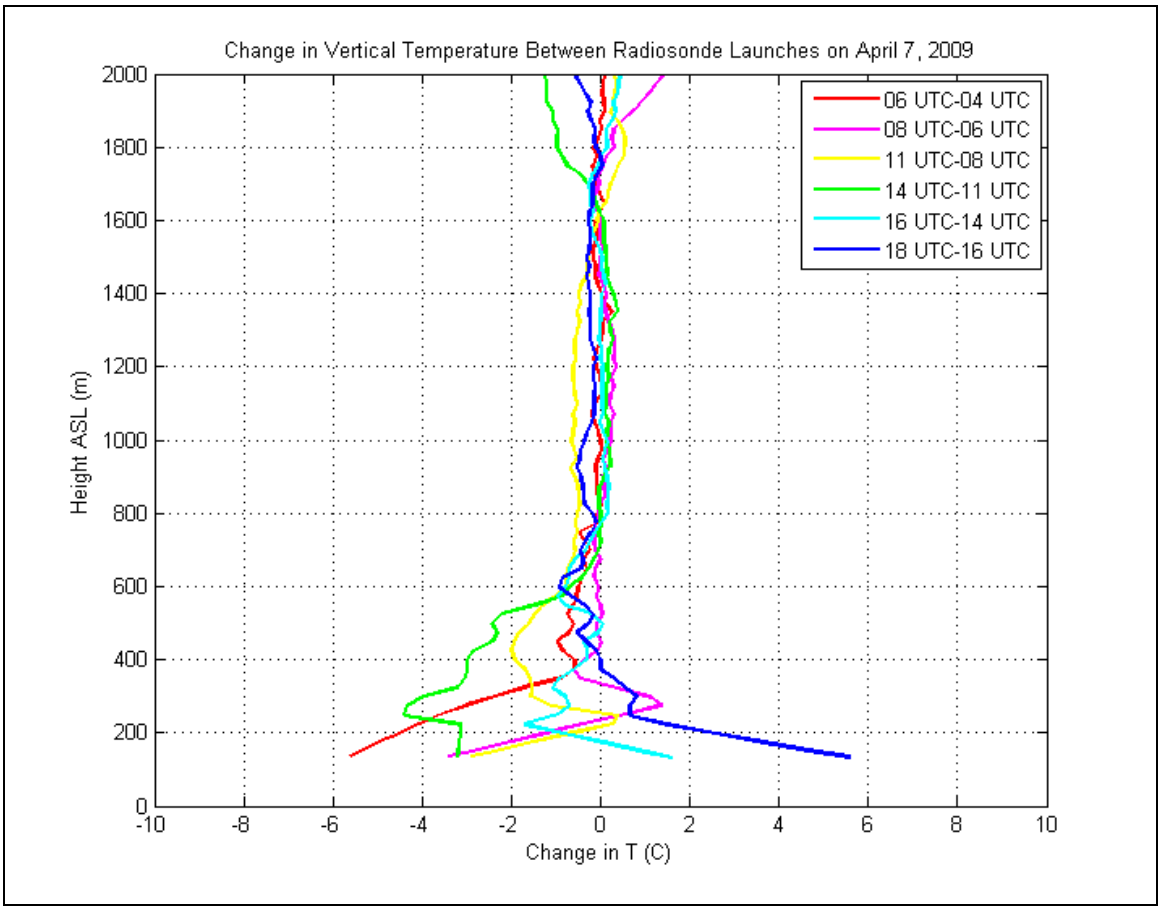

Figure 3.13: Change in Vertical Temperature between Radiosonde Launches on April 7, 2009 at Fairbanks, AK

Case summary: During this set of balloon launches, it should be noted that similar to the April 5th launches, the inversion did not "bottom out" as seen in the February 24th launches. The surface did reach its lowest temperature during the 1400 UTC launch as seen in the April 5th launches, which makes logical sense since the radiative input during the daylight hours, and number of hours of darkness were very similar. Once again, the three launches which occurred near or after sunrise have very similar vertical profiles above the level of inversion. Winds above the surface level were much lower on April 7th than two days earlier during the April 5th launches. On April 7th, there is a very uniform temperature profile between launch times above 800m ASL,

very likely due to the low vertical wind profile (Fig. 3.11). Similar to February 24th and April 5th, there is cooling just above the surface between the 1400 and 1100 UTC launches– but in this case, the surface also has decreased a few degrees during that timeframe, unlike the other two dates. The influence of winds to propagate a surface cold pulse up into the atmosphere was noted at the 11 and 14 launches, both of which exhibited large temperature drops in the 200-600m elevation band – coincident with the zone of wind speed maxima observed at these times.

3.1.4 May 1, 2009

During the May 1st case study, the sunset at 0619 UTC and rose the next day at 1317 UTC. The weather balloon launches were released at 0400, 0600, 0800, 1100, 1300, 1500, and 1700 UTC. The winter snowpack had disappeared the day before this set of launches.

Synoptic overview: Surface map indicates a 1026 hPa high extending west to east cutting into northern Alaska from the northern Yukon Territory, disrupted by a horizontal thermal trough in the Yukon Flats, which is a frequent feature in interior Alaska summer. A closed 5670 hPa high at 500 hPa (Fig. A.12) indicates a system which will hinder any type of cloud formation.

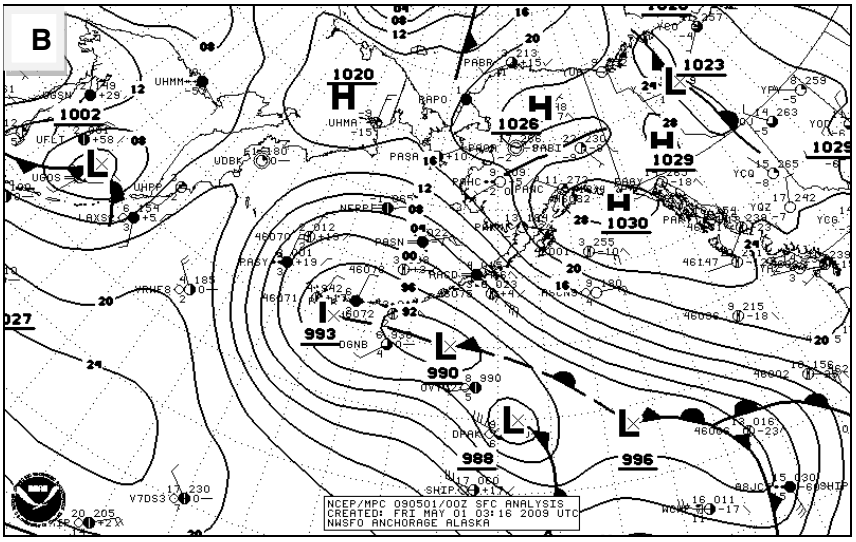

Figure 3.14a: Surface features at 0000 UTC on May 1, 2009

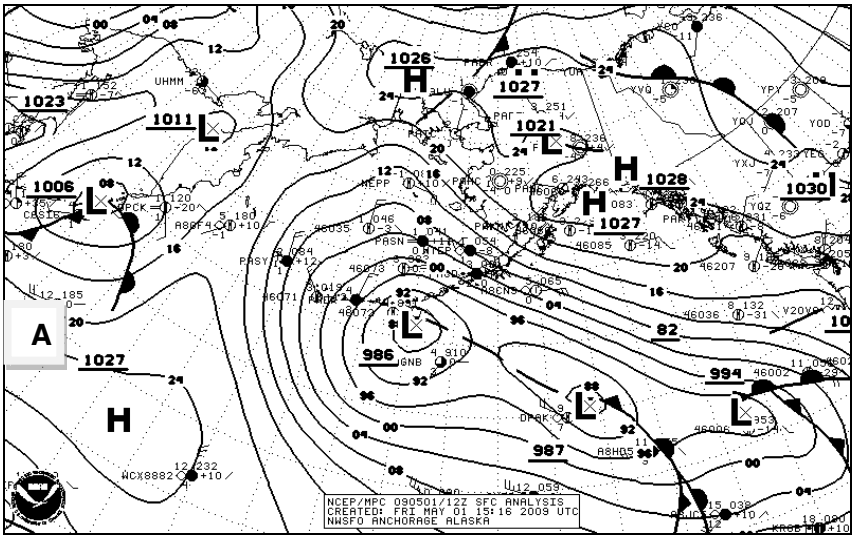

Figure 3.14b: Surface features at 1200 UTC on May 1, 2009

General observations during launches

For the beginning of the observing period at 0400 UTC, the sky was 7/8ths covered by very high cirrus. These high clouds did not seem to affect radiation input since a record high temperature of 24˚C was reached this day. No inversion had developed yet during this launch. A 3 kt wind

was recorded at the airport weather station beginning at 04 UTC and continued through 0700 UTC.

By the second launch at 0600 UTC, very high cirrus decreased in coverage to about 3 octas of the sky. Clouds present in the sky were mainly on the northern horizon therefore should not have hindered radiation input or output during the observation period. Hourly observations were not representative of the sky – which reported broken skies at 6100 m. Clouds in the northern sky looked to visually be scattered at 6100 m. Surface temperature began to drop quickly (6K) as the inversion began to form, establishing itself with an initial height of 240m AGL.

By 0800 UTC clouds had almost completely dissipated and the inversion height fell slightly to 220m ASL. About 1/16 of high cirrus was left in the northern sky. A slight southwest breeze continued from the time of the previous launch but no more than 4 kt of wind was recorded. At time of launch, winds had died down to zero at the upper air facility and the surface temperature dropped another 5.7K in two hours.

Winds of 3-4 kts were present between the hours of 0900 and 1100 UTC. The inversion height rose slightly to 310m ASL at the 1100 UTC launch as the surface temperature continued its rapid decrease by another 4.6K.

The temperature bottomed out at -0.1˚C at the upper air site at 1340 UTC. At 1300 UTC, the surface inversion height is at 210m ASL, but in this launch, a complex vertical profile that included a triple inversion is indicated, with isothermal layers in between, ranging vertical to 500m ASL. At 1300 UTC launch, the base of the inversion fell another 5.7K in two hours.

At 1500 UTC, the ASOS was reporting winds from the NE at 3 kt, but according to the upper air weather station, winds are calm. The sun had risen about two hours before this launch, and warming of the surface of 2.3K since the previous launch is observed. The inversion height was recorded near the top of the 1300 UTC triple layer inversion near 520m ASL.

For the 1700 UTC launch, a few clouds moved in at about 6100 m which covered about 1/8 of sky. By this time, shortwave radiation from the sun was warming up the ground surface to break the surface based inversion, warming the ground temperature up another 5.4K. The top of the surface Inversion was 310m ASL, but with another inversion between 580 and 750m ASL.

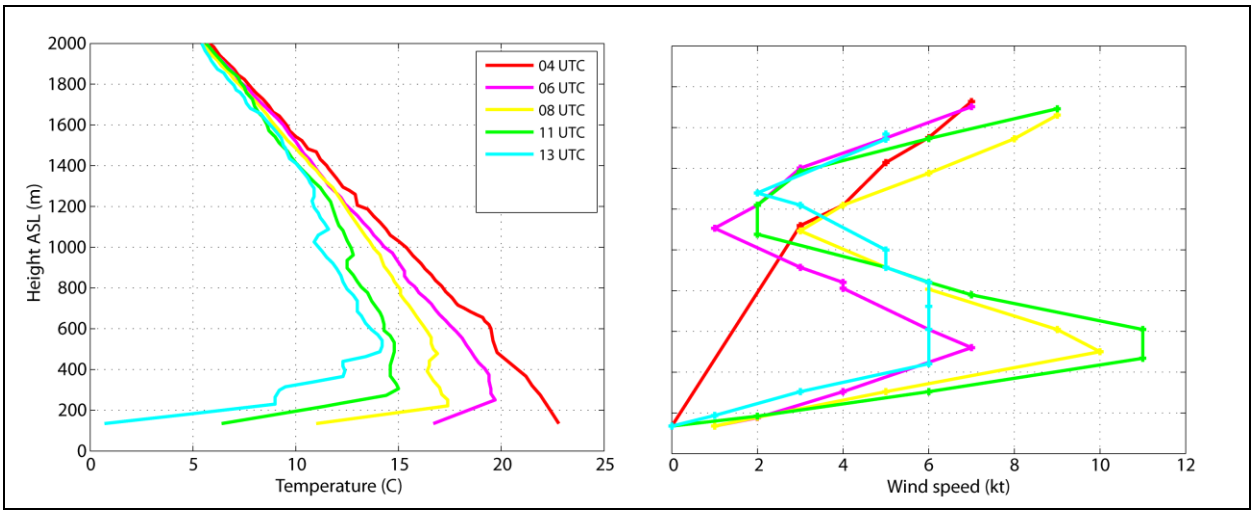

Figure 3.15: Vertical structure of the SBI development post-sunset on May 1, 2009. Sunset – 0619 UTC

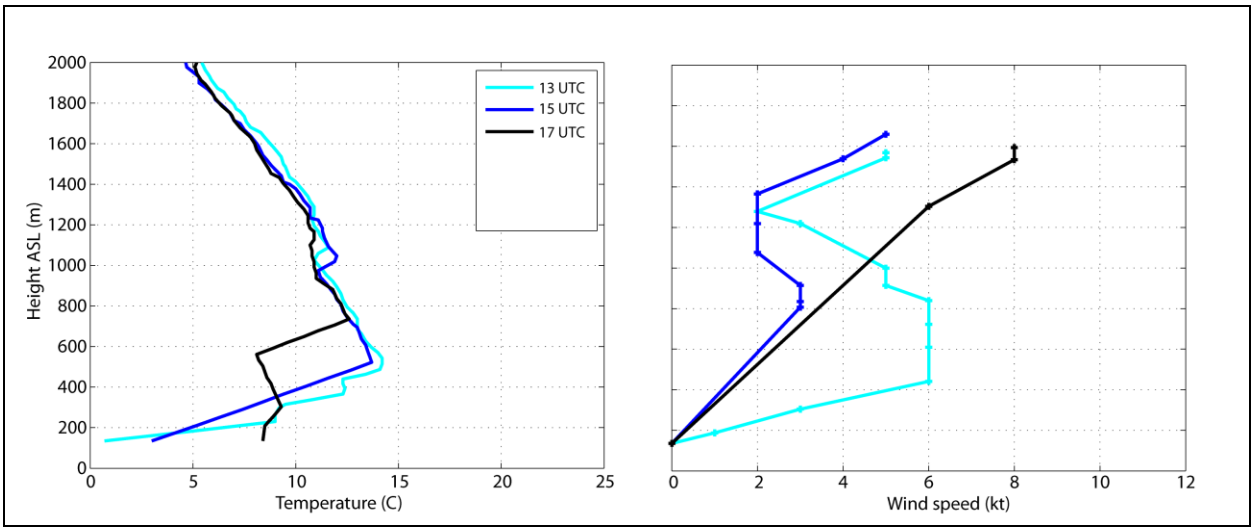

Figure 3.16: Vertical structure of the SBI development post-sunrise on May 1, 2009. Sunrise – 1317 UTC

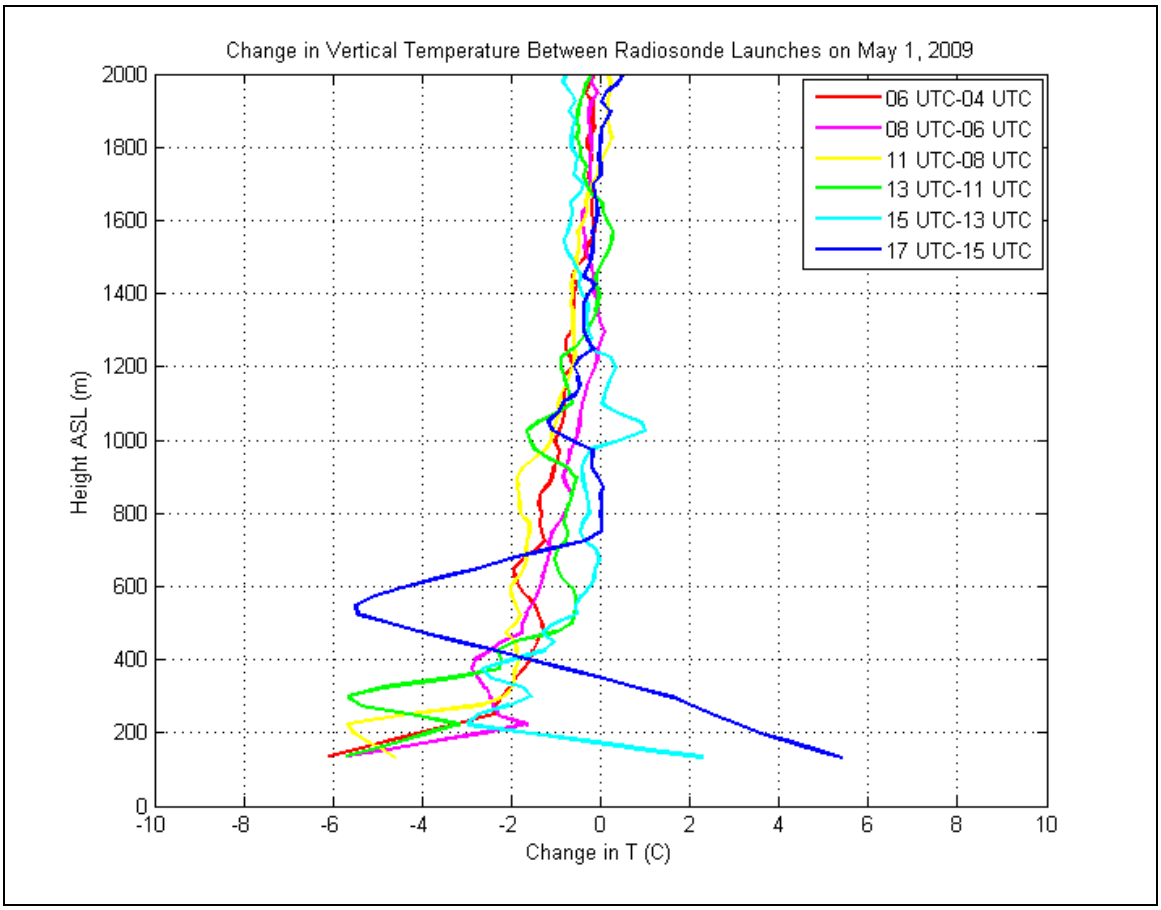

Figure 3.17: Change in Vertical Temperature between Radiosonde Launches on May 1, 2009 at Fairbanks, AK

Case summary:

A characteristic of the May 1 launch was the striking consistency in vertical cooling between the surface and 1000m ASL over almost the entire period of record. This is most likely attributable to the 750 W/m2 of incoming radiation warming up the surface, creating more energy to release radiationally once the sun sets.

The making and breaking of the inversion during this case study is particularly unique from the earlier studies because there is no specific pattern that was found from sunset to sunrise except for the similarity of temperature profiles above the inversion layer for the 1300, 1500, and 1700

UTC launches. In the 1700 UTC launch it should be noted that, as the incoming radiation warms up the surface, a very noticeable elevated inversion still exists.

3.2 Fall 2009 weather balloon launches

3.2.1 October 13, 2009

During the October 13th case study, the sunset at 0238 UTC and rose the next day at 1638 UTC. The weather balloon launches were released at 0200, 0400, 0600, 1100, 1500, 1700, and 1900 UTC. During this time of year, there was not snow cover on the ground.

Synoptic overview: A stable pattern is indicated by upper air plots, particularly at 500 hPa where a 5650m high is elongated from north to south centered over the eastern interior of Alaska and western interior of Yukon Territory (Fig. A.15). Ideal weather conditions were in place for October 13th, as skies were visually clear the entire night, other than a wispy cloud on the north horizon which appeared on the hourly observations as "FEW200", and wind was very sparse.

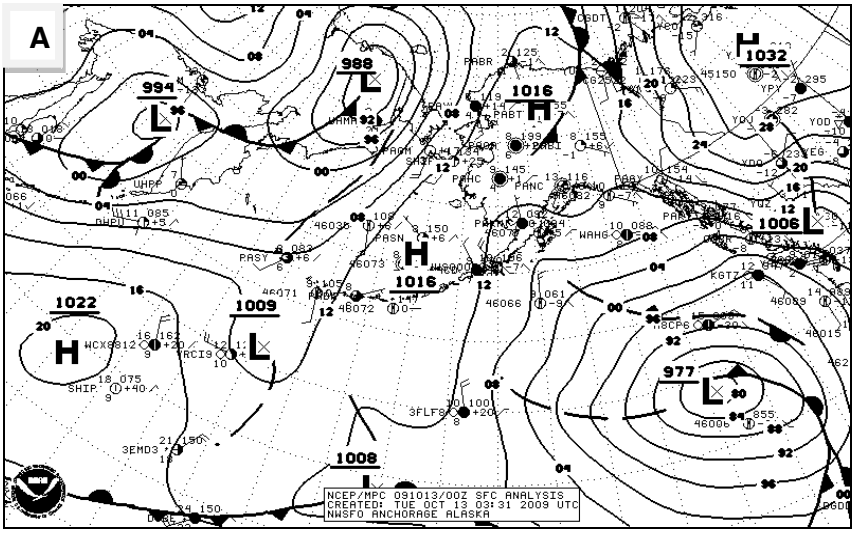

3.18a. Surface features at 0000 UTC on October 13, 2009

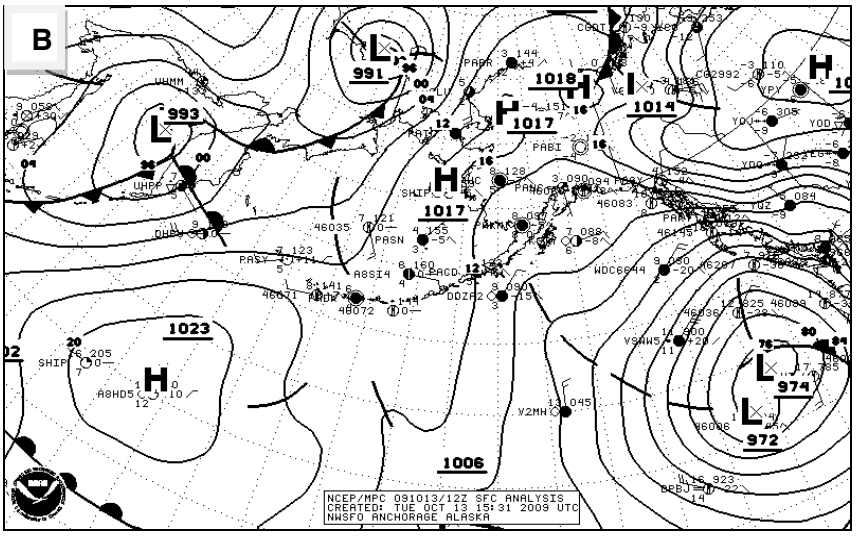

3.18b. Surface features at 1200 UTC on October 13, 2009

General observations during launches

A slight surface wind of 3 kts was recorded between 0200 and 0300 UTC. At 0200 UTC, the inversion began to show signs of development with an initial height of 180m ASL.

At 0400 UTC, the surface temperature decreased 5K in 2 hours, steepening the inversion and increasing its height to 210m ASL.

At 0600 UTC, the surface temperature decreased another 2.5K in 2 hours as the inversion height remained constant near 210m ASL. The profile of the inversion cooled slightly overall, but remained a similar steepness.

At 1100 UTC, the surface temperature decreased another 1.7K in 5 hours, illustrating the slowdown of the inversion development. The inversion height remained near 210m ASL, as the atmospheric temperature upward to ~720m AGL cooled substantially.

At 1500 UTC, a 4 kt wind was recorded at 0900 UTC – the first observation of any dynamic forcing at the surface. The surface temperature fell another 1.3K in 4 hours as the inversion top fell to 190m ASL.

At 1700 UTC, the surface temperature continued to decrease, although barely, with a change of -0.1K in 2 hours as the sun rose just before 1700. The inversion height slightly increased back up to about 210m ASL.

At 1900 UTC, as the sun rose, temperatures rose 3.9K at the surface, maintaining a shallow inversion of about 170m ASL height. The atmospheric profile demonstrates that the atmosphere from the surface to 200m ASL warmed substantially over a couple of hours, whereas vertically above 200m ASL, the air temperature continued to either fall slightly or remain isothermal to the previous launch.

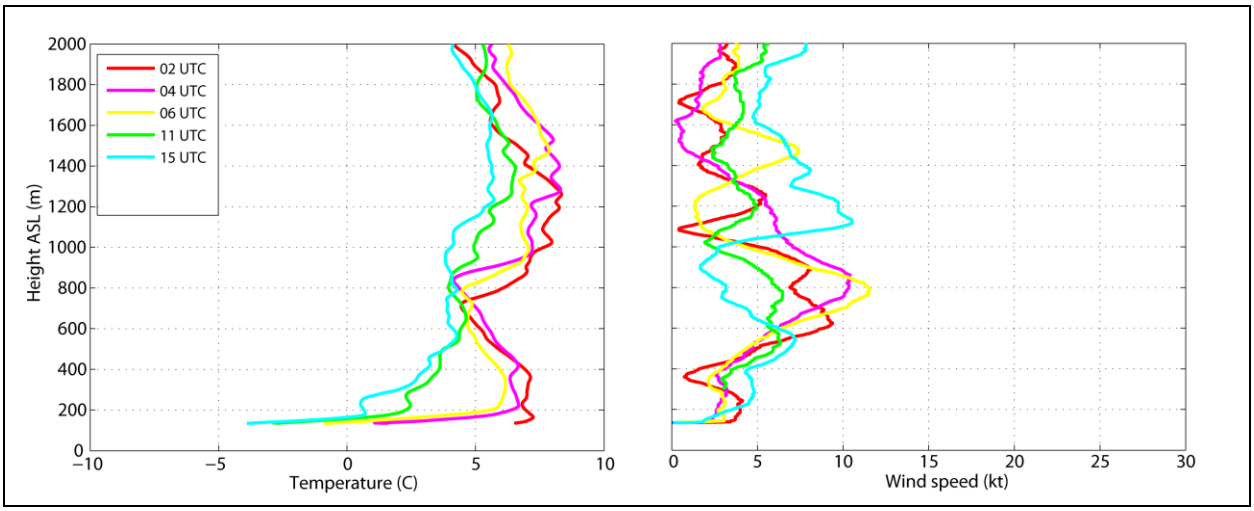

Figure 3.19: Vertical structure of the SBI development post-sunset on October 13, 2009. Sunset - 0238 UTC

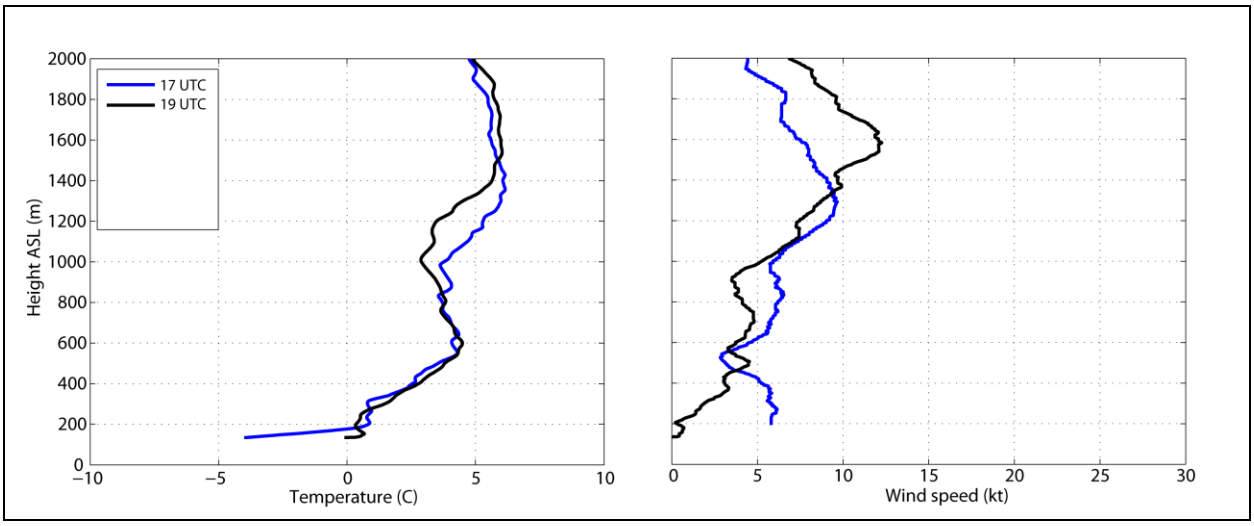

Figure 3.20: Vertical structure of the SBI dissipation post-sunrise on October 13, 2009. Sunrise - 1638 UTC. The 17 UTC data and the 15 UTC launch (shown in Fig. 3.19) indicate the surface temperature reaching a minimum for the night before the sun rises.

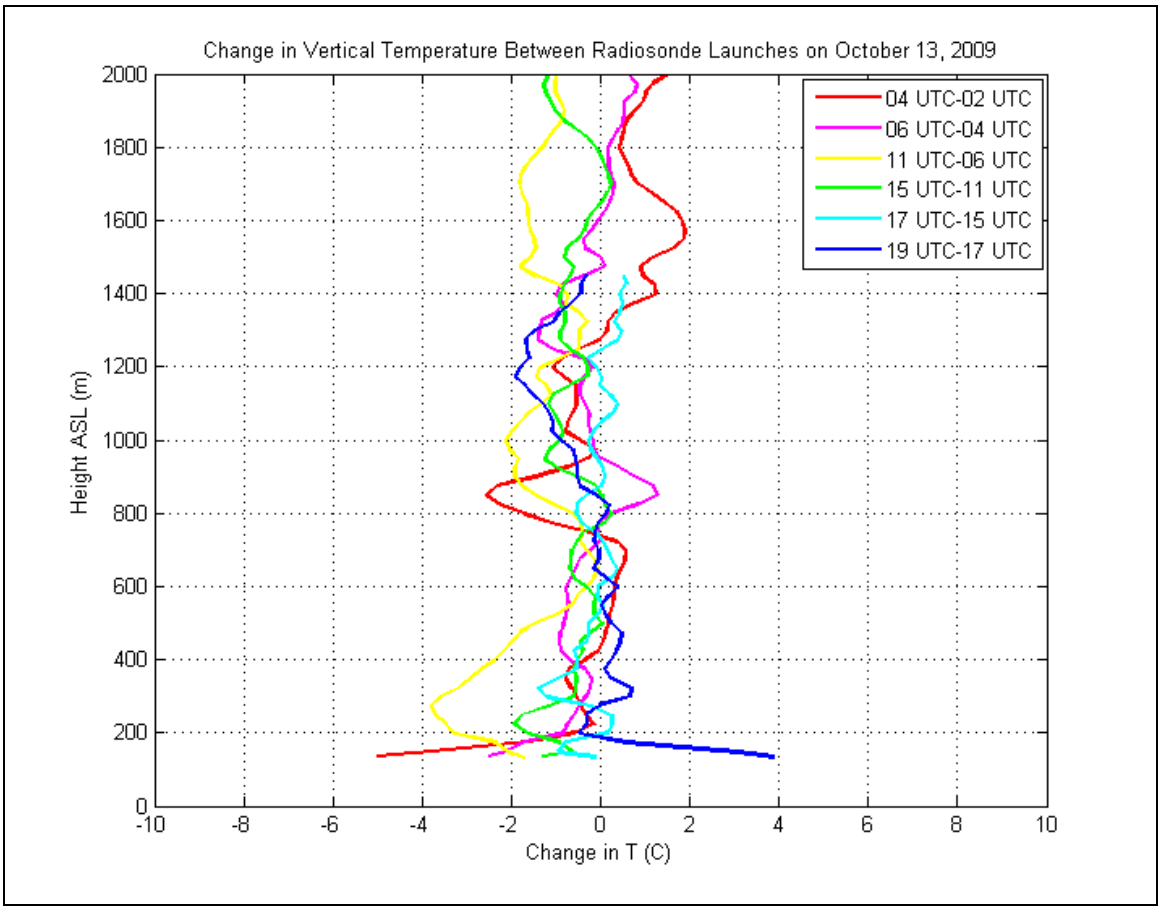

Figure 3.21: Change in Vertical Temperature between Radiosonde Launches on October 13, 2009 at Fairbanks, AK

Case summary: This case shows a similar pattern to the April case studies, where the temperature decreases rapidly just after sunset, and once the inversion cools to a near minimum, the inversion begins to deepen with height. While this is not extremely noticeable by looking at Figures 3.19 and 3.20, it is better seen in Fig. 3.21 in the change of temperatures between launches. It is important, though, to note that there is a five hour gap between the 06 and 11 UTC launches, unlike the mainly 2 hour time gap between launches.

3.2.2 October 15, 2009

During the October 15th case study, the sunset at 0227 UTC and rose the next day at 1645 UTC. The weather balloon launches were released at 0200, 0400, 0600, 1100, 1500, 1700, and 1900 UTC. During this time of year, there was not snow cover on the ground.

Synoptic overview: Clear and calm conditions persisted into the next set of launches on October 15th. A 5500m horizontal ridge defines the 500 hPa chart, while very little dynamics is indicated at levels below 500 hPa (Fig. A.18). The ground temperature during the night of this set of launches dropped lower than two days before, likely not only due to a colder air mass, but potentially also to the inversion repeatedly forming over a few days in a row.

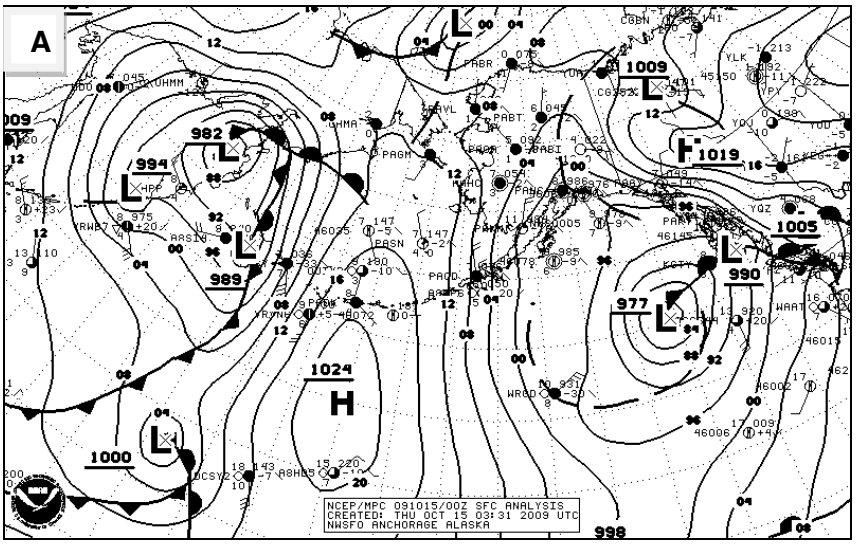

3.22a. Surface features at 0000 UTC on October 15, 2009

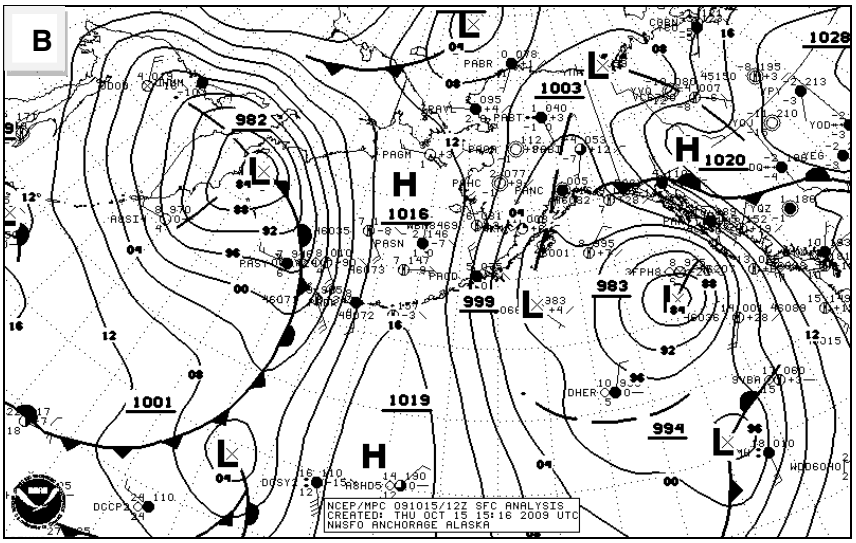

3.22b. Surface features at 1200 UTC on October 15, 2009

General observations during launches

A slight surface wind of 3 kts was observed before the study period at 0100 UTC. At 0200 UTC, the initial inversion height was 180m ASL, and notably steeper than first established at 0200 UTC two days earlier on October 13th. The atmosphere in general for this case study was much cooler, at least up to 2000m AGL, than the October 13th case.

During the period between 0200 and 0400 UTC, the surface temperature plummeted 5.9K while the inversion height rose slightly to 200m ASL. The surface inversion contains a defined lapse rate of 7.66 from ground level to 200m ASL.

At 0600 UTC, the surface temperature dropped only another 1.3K over two hours with a surface inversion height of 250m ASL. There is an isothermal layer between 250m and 310m ASL, and another inversion above that which tops out around 380m ASL.

At 1100 UTC, the surface dropped 2.8K in five hours. A slight surface wind of 3 kts was observed at 0900 UTC. The inversion height was 190m ASL with a thin isothermal layer at the top of the surface based inversion, and a second inversion upward to 380m ASL.

At 1500 UTC the surface temperature continued to drop slightly – another 2K over another 4 hours with a fairly constant inversion height of 205m ASL.

At 1700 UTC, as of fifteen minutes after official sunrise, the surface temperature dropped only 0.3K over three hours. A slight surface wind of 3 kts was observed between 1600 and 1700 UTC. The inversion height remained nearly unchanged at 200m ASL.

At 1900 UTC, although the ground air up to about 350m ASL warmed, with a 5.4K rise at the surface, the inversion height remained at 200m ASL.

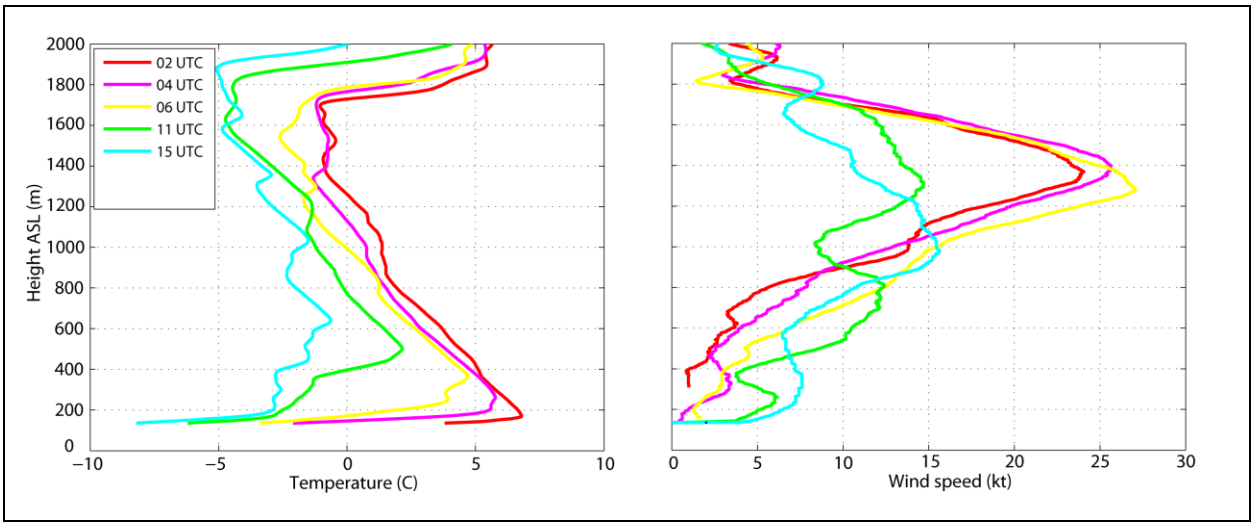

Figure 3.23: Vertical structure of the SBI development post-sunset on October 15, 2009. Sunset – 0227 UTC

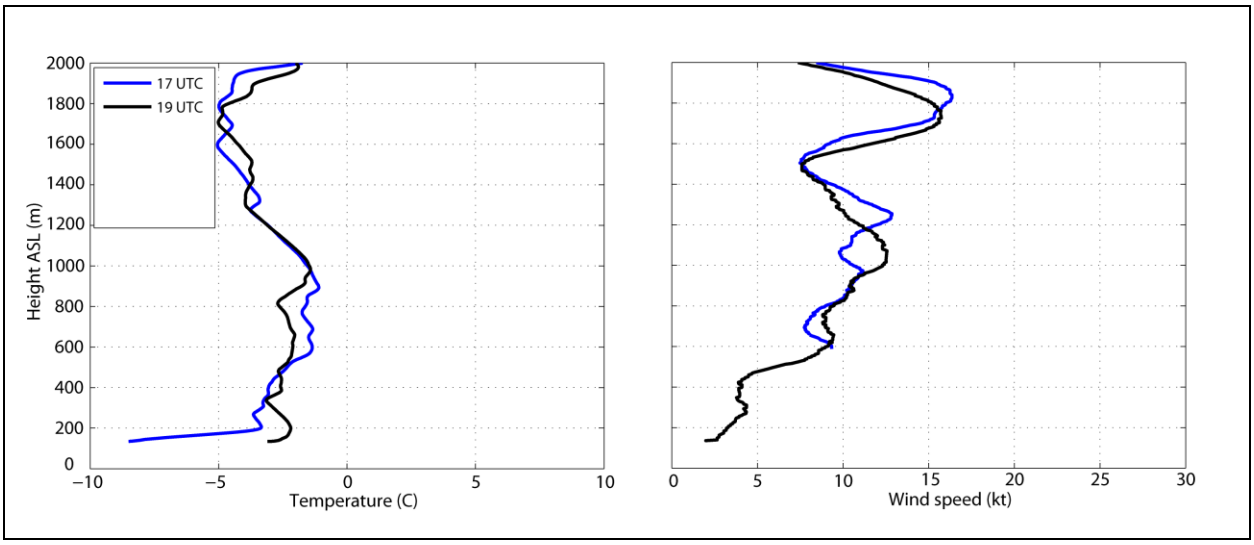

Figure 3.24: Vertical structure of the SBI dissipation post-sunrise on October 15, 2009. Sunrise – 1645 UTC. The 17 UTC data and the 15 UTC launch (shown in Fig. 3.19) indicate the surface temperature reaching a minimum for the night before the sun rises.

Case summary: This case shows a different profile than the Oct. 13th case study, with a much larger fluctuation between daily high and low temperatures. This is likely due to having three days in a row of clear and calm weather – which will maximize the incoming solar radiation during the day, and create a greater rate of energy loss at night. In the wind profile these results indicate a wind maximum around 1400m ASL during the 0400 UTC, 0600 UTC, and 0800 UTC. SODAR data (Fig. 3.26) also depicts a larger wind measurement during the beginning of the case study, with dwindling winds throughout the evening. By looking at the 850 hPa plot, it is evident that the GFS is not picking up on the wind maximum seen early in the data collection.

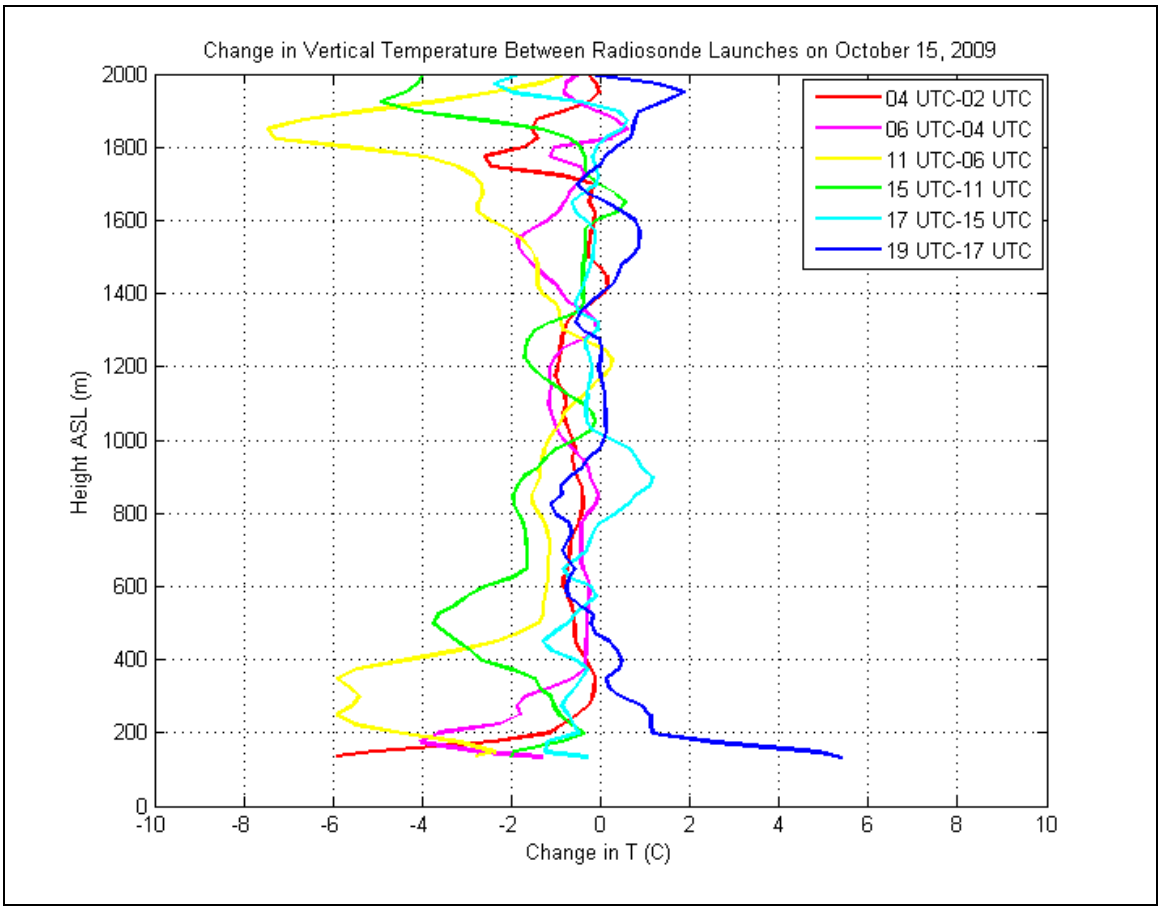

Figure 3.25: Change in Vertical Temperature between Radiosonde Launches on October 15, 2009

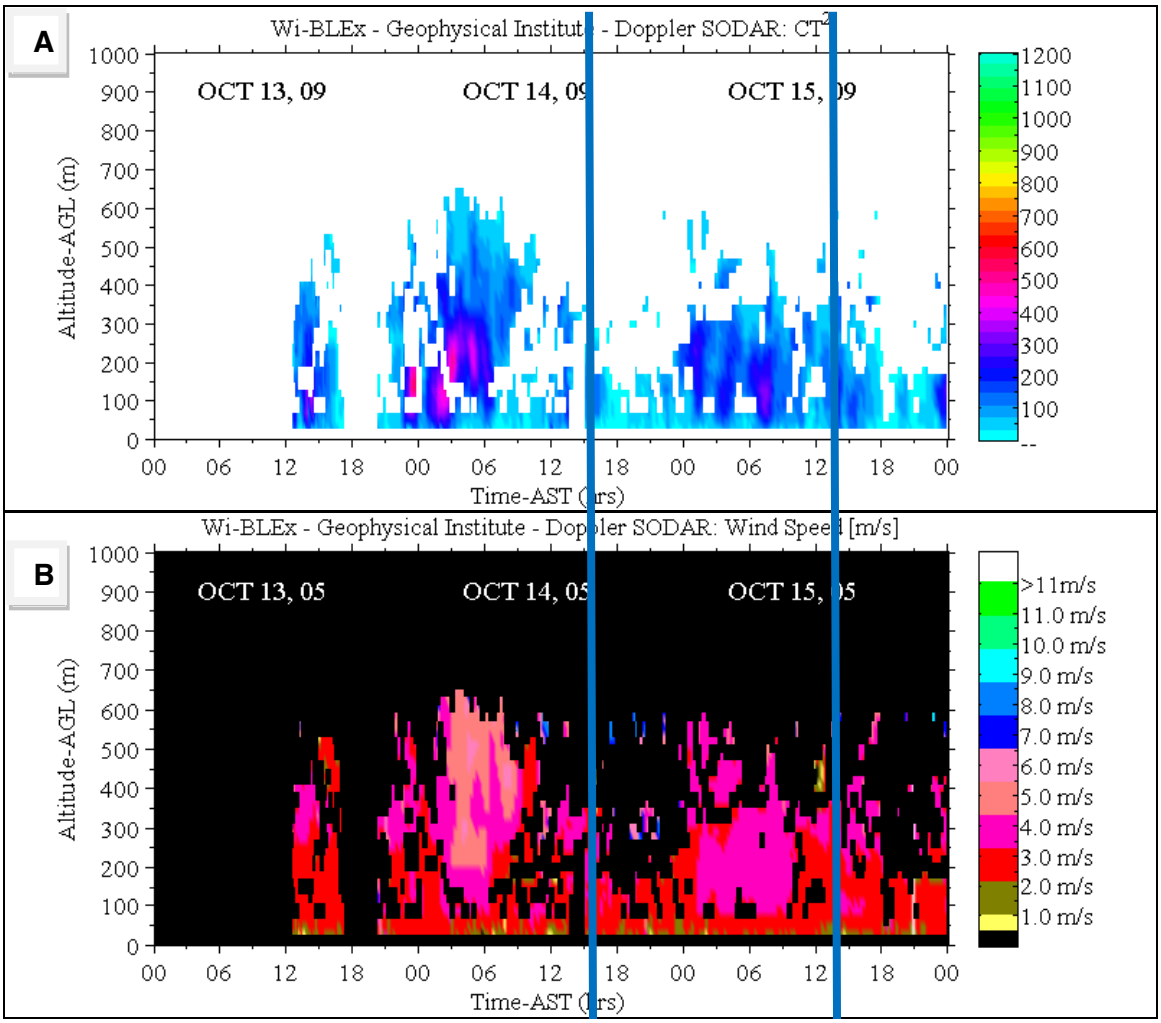

Figure 3.26: Plots from the Acoustic Phased Array Doppler Sodar – REMTECH PA-2. The first vertical blue line indicates the time at which the first radiosonde was released during the case study, and the second vertical line indicates the time at which the last radiosonde was released during the case study. CT^2 indicates the heights of the inversion indicated by the change from high reflectivity to low reflectivity. a. CT^2 plot from October 14th and 15th. b. Wind speed plot from October 14th and 15th.

3.2.3 November 21, 2009

During the November 21st case study, the sunset at 0028 UTC and rose the next day at 1848 UTC. The weather balloon launches were released at 0200, 0500, 0800, 1100, 1400, 1700, and 2000 UTC. During this time of year, there was snow cover on the ground.

Synoptic overview: A 1005 hPa surface ridge extended west to east across northern Alaska. At 500 hPa, a 4980dm low north of Barrow, Alaska pushed to the west throughout the day, but created increased winds aloft (Fig. A.21).

Past a certain date in the fall, incoming solar radiation is too insignificant to heat up the surface temperature. Up to November 21st, since the previous two case studies (Oct 13th and 15th), Fairbanks experienced a long stretch of cloudy days. By the time the next case study could be conducted on Nov 21st the incoming solar radiation was very small with a maximum sun angle on November 21st of five degrees above the horizon. The skies had a clearing trend during the afternoon in which the case study began.

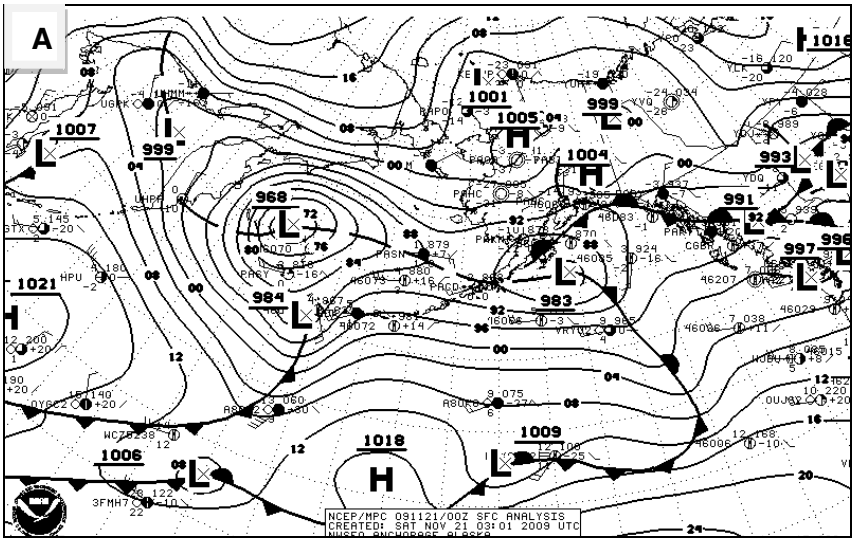

3.27a. Surface features at 0000 UTC on November 21, 2009

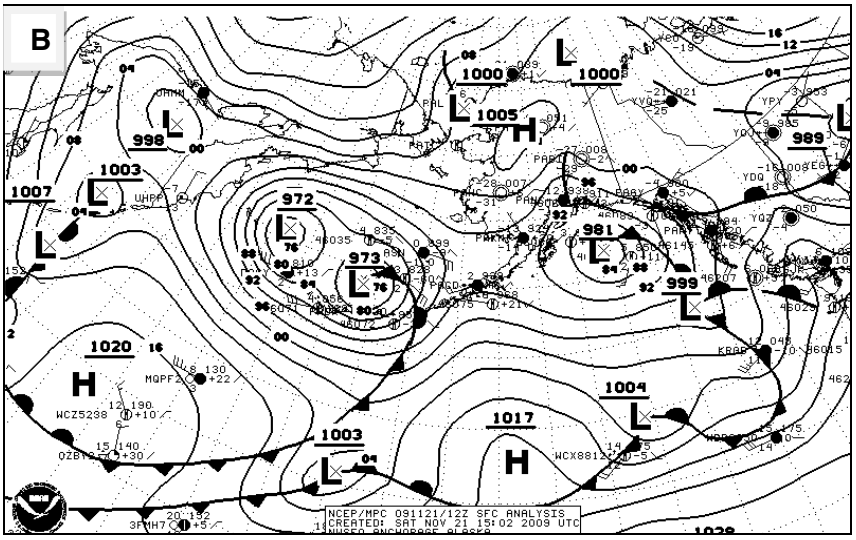

3.27b. Surface features at 1200 UTC on November 21, 2009

General observations during launches

At 0200 UTC, the initial radiosonde observation shows an inversion height of 220m ASL, with an already established surface based inversion, typical 24 hours a day during this time of year when the sun's influence is small.

At 0500 UTC after a three hour period, the surface temperature dropped 1.9K and the Inversion height remained nearly steady at 230m ASL. The vertical profile dropped linearly from the surface up to about 700m ASL. At 0800 UTC, the extent of cloud cover when the airport reported FEW060 from 0100 to 0900 UTC was a tiny scud cloud on the south horizon. The surface temperature dropped another 2.4K in three hours, and dropped consistently up to 335m AGL, with an inversion height of 240m ASL.

At 1100 UTC unlike the October launches, the most drastic surface temperature changed happened between 0800 and 1100 UTC, with a drop of 3.9K. The inversion height increased to 480m ASL, signifying a drastic overall cooling in the bottom layer of the atmosphere. At 1400

UTC, the surface temperature from 1100 to 1400 UTC actually increased 1.8K. Inversion height was 280m ASL, with a thin nearly isothermal layer and another inversion above the layer which tops out at 550m ASL.

At 1700 UTC, the skies became completely clear until a pollution cloud formed over the Fairbanks valley around 1700 UTC. The cloud layer was not visually above the upper air location, but was within the ASOS reporting sky surface. A layer of stratocumulus, separate from the pollution cloud, moved in from the south covering about 3/8ths of the sky, and quickly moved out by 1630 UTC, lasting only about a half hour. Though this small dose of cloud cover may have affected the strengthening of the temperature inversion, it seems insignificant according to the data. The surface temperature still dropped 0.4K in three hours, though slight, the inversion surface still did become slightly cooler. The inversion height hovered near 580m ASL.

At 2000 UTC, a little over an hour after sunrise, the surface temperature rose 1.2K. The layer between the surface and 300m ASL rose in temperature, the inversion height rose to 600m ASL, while the overall profile up to 2000m ASL remained relatively unchanged.

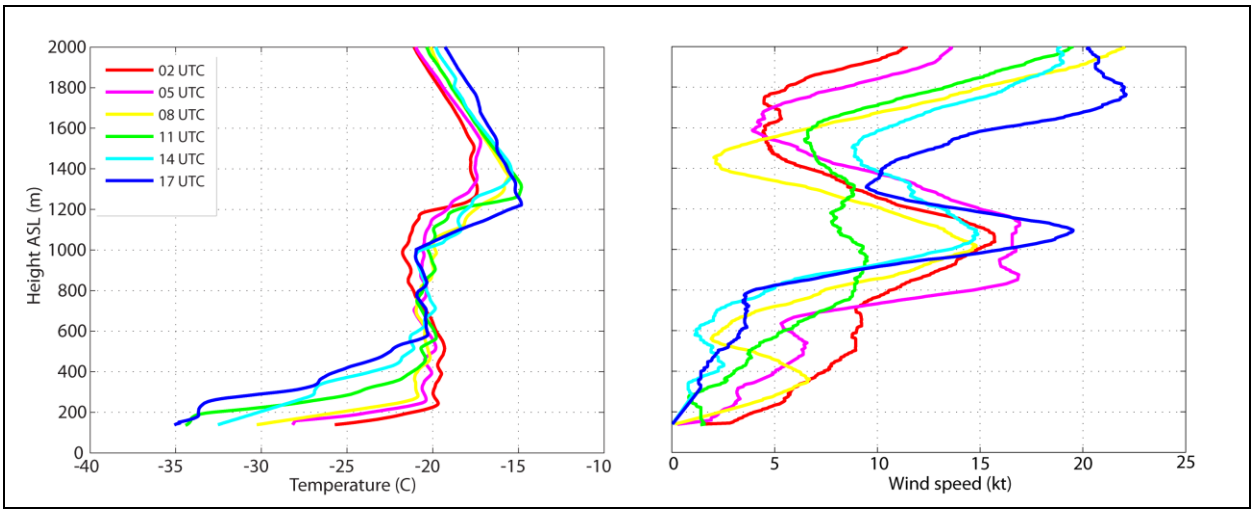

Figure 3.28: Vertical structure of the SBI development post-sunset on November 21, 2009. Sunset – 0028 UTC

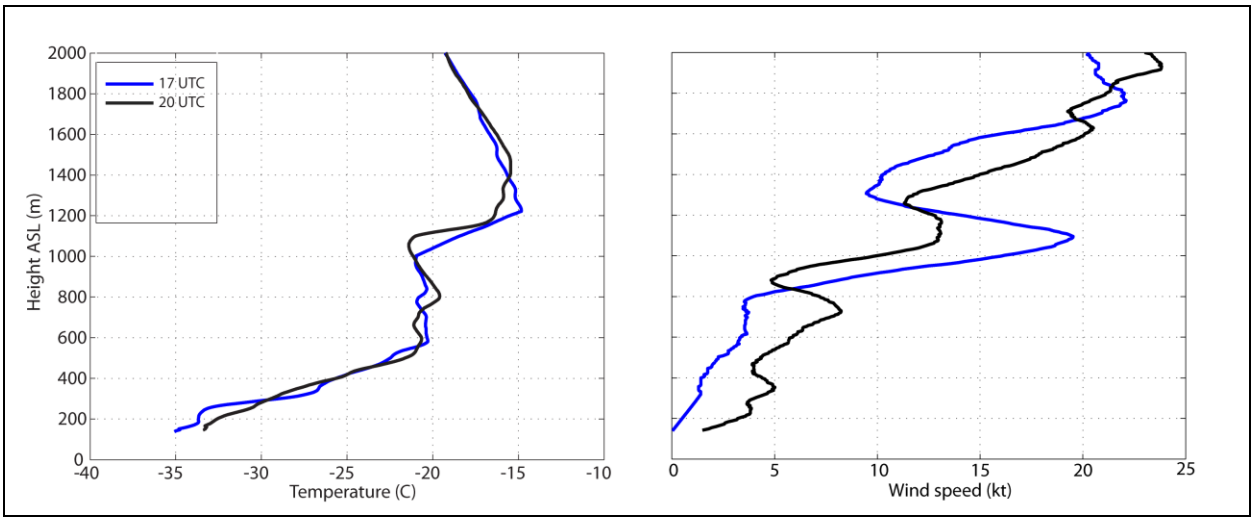

Figure 3.29: Vertical structure of the SBI dissipation post-sunrise on November 21, 2009. Sunrise – 1848 UTC

Case summary:

This last and final case study is different from the rest of the launches because of the very little incoming shortwave radiation that reached the ground in November in interior Alaska. Unfortunately, advective processes may be playing a role in this case, with the fairly strong winds near 1000m ASL. Even though these winds are high above the surface, vertical transport

could play a role in effecting the inversion from higher up. It appears that the surface temperature not only decreases after sunset, but the entire structure above the surface also decreases in a manner different to that observed in the other case studies. Comparing the radiosonde data collected with the SODAR data (Fig. 3.31a, 3.31b) from November 21st, the heights of the inversion over time agree with the deepening of the inversion seen in Fig. 3.28 and Fig. 3.29. Interestingly, the CT^2 plots shows that there is a pulsing in the inversion signal (Fig. 3.31a). The SODAR wind profile relatively agrees with raob profiles by showing initially higher winds (8-10kts) which dwindle throughout the night.

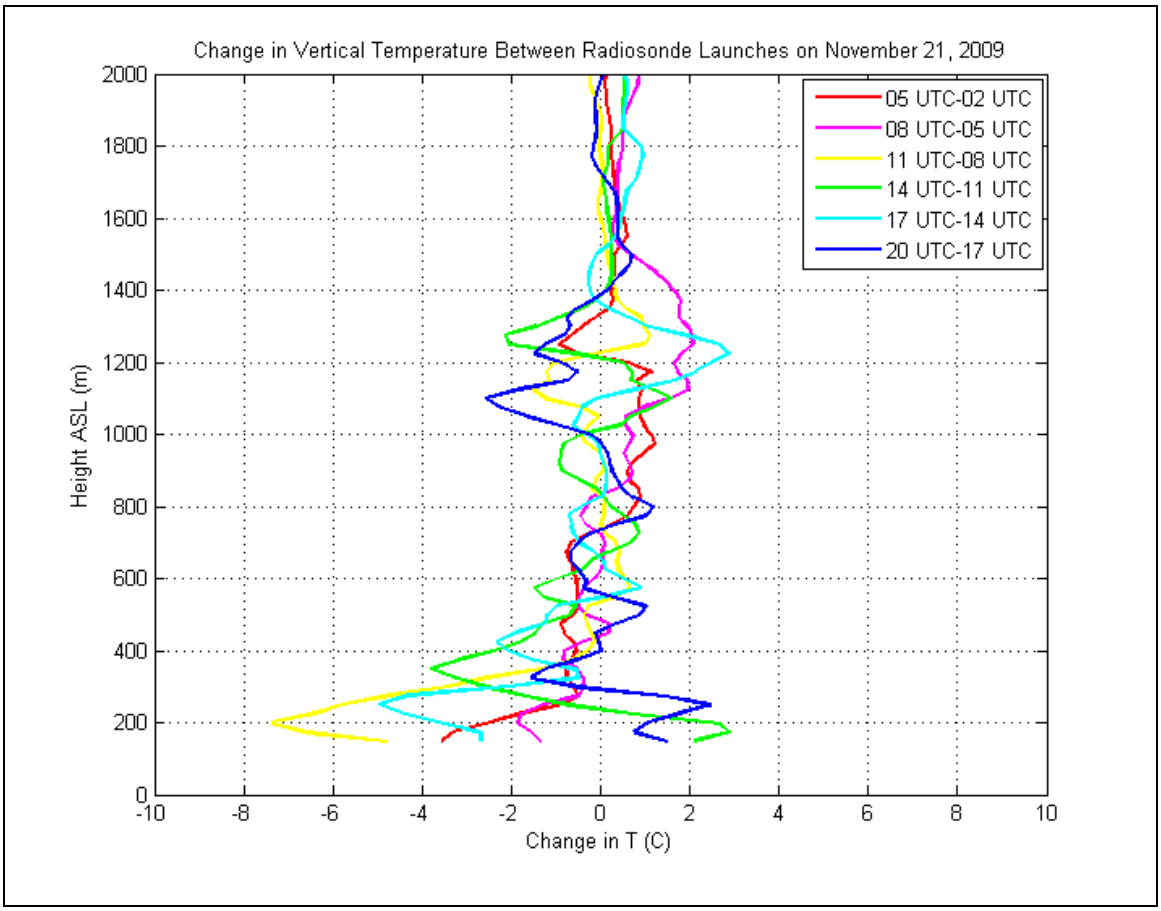

Figure 3.30: Change in Vertical Temperature between Radiosonde Launches on November 21, 2009 at Fairbanks, AK

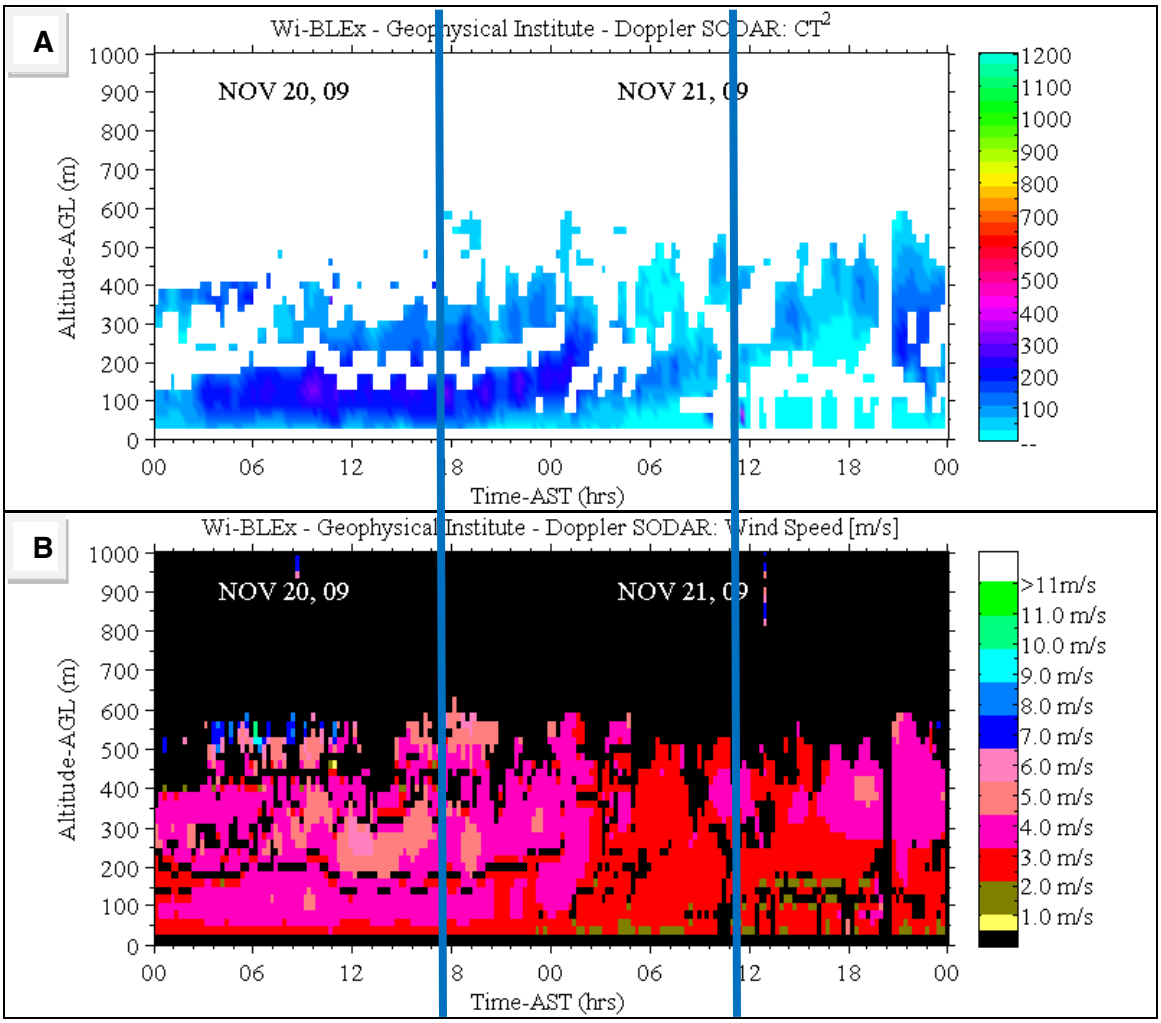

Figure 3.31: Plots from the Acoustic Phased Array Doppler Sodar – REMTECH PA-2. The first vertical blue line indicates the time at which the first radiosonde was released during the case study, and the second vertical line indicates the time at which the last radiosonde was released during the case study. CT^2 indicates the heights of the inversion indicated by the change from high reflectivity to low reflectivity.

a. CT^2 plot from November 20th and 21st. b. Wind speed plot from November 20th and 21st.

Chapter 4: Overall Discussion, Conclusions and Future Work

The results gathered during 42 individual radiosonde launches conducted during a series of seven case study days presented a suite of information about the structure, evolution, and dynamics of the cool and cold season surface-based inversion in the Alaska Interior. Although each case study presents a unique story due to variability with respect to incoming solar radiation and snow cover, several generalizations emerged which provided insight into the development of the SBI with respect to these variables. Overall, for each of the seven case studies, the minimum surface temperature was reached at sunrise, or just before sunrise. In general, the surface temperature decreased most rapidly just after sunset. After this initial cooling pulse at the surface the profile begins to cool vertically. Another feature that appeared on several launches were periods when cooling appeared to cease, suggesting that some sort of temperature minimum had been attained.

Incoming solar radiation and snow cover – near-surface temperature controls

The first control to consider is incoming solar radiation. As expected, May 1st shows that the greater the quantity of incoming solar radiation, the greater the surface heating will be during the day and the more possible cooling will occur after the incoming radiation no longer heats up the surface of the earth. This is reflective of the fact that solar heating in the transition seasons is confined to the lowest layers of the atmosphere because the atmosphere above is still fairly cool. In figure 4.1 below, The May 1st changes (red dots) indicates the fast and constant release of longwave solar radiation after sunset during a day when a substantial amount of incoming solar radiation is absorbed at the surface.

February 24th and October 13th and 15th show a slightly different story. All three cases have similar incoming solar radiation values of about 250Wm^{-2}, but differ with respect to snow cover (discussed in further detail below): for the February case there is snow on the ground while in October the ground is still bare. The inversion top heights on February 24th were much greater than the October cases, which coincides with the climatological asymmetry since between spring and fall inversions in Bourne et al. (2010). Considering that the major variable in these cases is the snow cover or lack thereof, comparison of these profiles suggests that the incoming solar radiation might not exert a strong influence on the final height of the inversion be a major factor above a certain value. The November 21st case study presents the effect of little incoming solar radiation on the general warming of the atmosphere when the sun angle was only 5˚ above the horizon. In this case, very little warming occurs in the atmospheric profile, and the surface inversion never completely breaks.

The expected response to the presence of a snow cover would be a smaller amount of heat transfer between the ground and the atmosphere above it due to the insulating properties of the snow layer. The high reflectivity will reduce the magnitude of cooling because the surface is unable to warm as much during the day. This should result in the observation of a less rapid temperature cooling at the surface, and vertical propagation would proceed more rapidly than for nights without snow cover.

The influence of snow cover can be examined by contrasting case studies with snow (February 24th, April 5th, April 7th, November 21st) and case studies without snow (May 1st, October 13th, October 15th), and in particular October and February since the solar input is approximately the

same amount of energy. As one can see in Fig. 4.1, the cases without snow on the ground had larger surface temperature changes throughout the case studies than those with snow cover.

During the case studies with snow on the ground, temperatures dropped between 8 and 18K from the warmest surface temperature of the day to the lowest. But, in looking at only the spring cases with snow cover, the temperature dropped 18K one day and 16K for two of the other nights. Thus, closer examination of this set suggests the 8K surface change represented an outlier. This case occurred in late November, when the sun rose only 5˚ above the horizon, and the temperature profile always indicated a well-defined surface-based inversion. The comparatively small 8K drop in the late November case study may be considered relative to the incoming radiation of only 23 Wm^{-2}.

The comparable case study from the spring was February 24th. This case study exhibited a temperature drop of 16K. An examination of the case studies on April 5th and 7th indicate a temperature drop of comparable magnitude, despite receiving almost twice the incoming radiation as the February 24th case study. This suggests that the presence of a snow cover limits warming that would otherwise have resulted from absorption of solar radiation. This is contrasted with May 1st where the lack of snow cover resulted in a greater temperature drop of 22K. The November 21st case study represents the extreme end of the snow cover/low radiation combination, exhibiting a surface temperature drop of only 8K. In figure 4.1, the Nov. 21st case (black dots) shows the lack of change in surface temperature due to little incoming solar radiation.

During the cases without snow on the ground, temperatures dropped between 8K and 15K from maximum surface temperature to minimum surface temperature. Though the October 13th and

15th launches had a much warmer atmospheric profile than the February case (likely due to snow cover), there was not a large difference in surface cooling (16K on February 24th and 12K-15K on October 13th and 15th, respectively). A noticeable difference between the February and October launches as mentioned earlier was that the October launches have a steep, surface based inversion which increases with height over time, but does not change as drastically as the February case – where the SBI deepens substantially with time. According to Estournal and Guedalia's (1985) model results, we would expect the inversion to deepen all night, which is the case for all of the case studies, yet it is curious to note that the cases in which snow cover exists, inversion tops increase more rapidly as the surface temperature cools. This was expected because of the effect of snow on the radiative fluxes between the surface and the air immediately above it. With the "no snow" cases, the data suggest a more drastic cooling of the surface before the profile shows cooling with height, as shown in Figure 4.1.

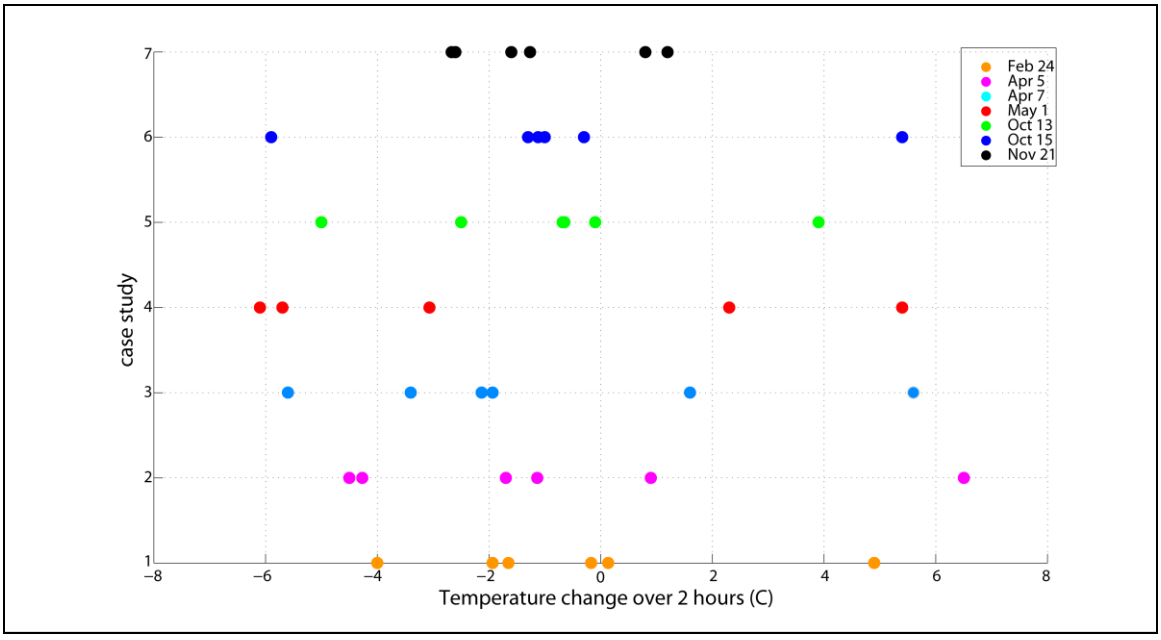

Figure 4.1: Standardized 2-hour surface temperature changes between balloon launches for all case studies. The dots indicate the degrees Celsius in which the surface temperature dropped between radiosonde launches standardized to two hours. This indicates the rate of cooling at the surface

throughout the night. Y-axis indicates a unique number for each case study, ranging from 1-7 in sequential calendar order. Cases with snow on the ground are Feb. 24, Apr. 5, Apr. 7, Nov. 21 and cases without snow on the ground are May 1, Oct. 13, Oct. 15.

Minimum temperature

On three case studies (Feb. 24th, Oct. 13th and 15th) it was observed that the temperature did not continue to decrease through the night, and instead appeared to settle on a specific temperature. Figure 4.1 above identifies these three launches by the data markers near the zero x-axis (Feb. 24th -yellow dots, Oct. 13th -green dots, Oct. 15th -blue dots. Two possible explanations for this can be suggested: 1) a balance could have been reached between the IR fluxes between the ground and the atmospheric layers just above; that is, the atmospheric layers are emitting enough IR to offset the cooling at the surface, or 2) vertical mixing introduces enough warmer air from higher levels to offset the surface-based radiative cooling.

In practice it is difficult to conclusively pin down because each case study presented a slightly different aspect about minimum temperature convergence idea, a result of the number of variables involved. According to the February 24th case study, it is evident that the minimum surface temperature bottomed out at -20C around 1100 UTC, but that cooling continued over the next six hours vertically up to about 650m, where the temperature converged at about -7C.

On April 5th, the surface temperature dropped 6C in two hours from 0600 UTC to 0800 UTC - 3 hours after sunset. Similar to April 5th, on April 7th, the surface temperature dropped the most between 0400 and 0600 UTC, about an hour after sunset. The April 5th profiles do not show a deepening of the SBI with time, and neither does the April 7th profiles. This could be due to the

length of night being too short to reach a well-defined minimum temperature at the surface. If the surface had a longer time to cool before incoming shortwave radiation warmed up the surface in the morning, then the surface may have shown more cooling than the April case studies show.

Both October 13 and 15th show that the first profile which exhibits surface warming (1900 UTC) from incoming solar radiation only mixed approximately 65m of the atmosphere. This could suggest that the worst air pollution in Fairbanks during this time of year would occur during this time period when the inversion is at such a low height. Tying this data together with air quality data would provide further information on this phenomenon just as the ground begins to heat in the solar morning.

Unlike all other case studies which indicated maximum rates of cooling just after sunset was the May 1st case study, in which observations show a nearly constant temporal cooling at the surface as the vertical profile cools with time. The development of the inversion on May 1st is unique due to the large fluctuation in the surface temperature as well as what looked like an oscillation of cooling vertically between launches, all the way up to about 600m ASL during the last launches of the case.

Wind

The final factor to discuss is the potential effects of wind on the vertical profile due to mechanical mixing. Though case study dates were carefully chosen to occur on days with little to no forecasted surface wind, the level of temporal and vertical detail at which these observations are being conducted exceeds that of any model or forecast analysis. There will

always be some sort of atmospheric motion over a 24 hour period in the lowest 2000m of the atmosphere. A wind, even if located above a surface-based inversion, can still exert a discernible impact on the development of the inversion. Winds can change the inversion height, advect warm or cool air horizontally, and break an inversion completely. It is expected that some light winds will exist, since temperature changes create a gradient in temperature. In the case of cold surface temperatures, gravity-induced density flows can be established which can act to perform mechanical mixing near the surface.

The occurrence of winds during the case studies was observed to affect the vertical profile by warming or cooling a given layer or slowing the development of an inversion as the warmer air above the inversion is driven down into the near-surface layers. The occurrence of strong winds aloft, such as a small jet above a cold layer of air, was not always able, however, to affect the inversion because typically the night time profile of the atmosphere shows a decoupled statically stable layer at the surface which inhibits vertical mixing, as distinct from the remainder of the profile. In general, however, given the sensitivity of the vertical profile to even small wind perturbations, it was found to be very difficult to parse out particulars about how winds were affecting the inversion.

Two episodes during which weak surface winds developed were during the February 24th case study. The wind appears to affect the inversion, the wind maximum heightening over time throughout the night. The 3kt of wind at the surface on April 5th does not seem to mitigate the 6.4K drop from the three hours previous. There was a broken cloud layer at 0400 UTC during the first launch on April 5th, which may have hindered the inversion from developing faster for the 0600 UTC launch. On April 7th, where winds were very minimal, the inversion developed

faster just after sunset than the April 5th launches, likely indicative of the cloud cover present on April 5th at sunset. The April 7th case shows a faster cooling than the April 5th case, which is likely due to the cloud cover which blocked incoming radiation before the balloon launches on April 5th. This observation shows that the greater the number of consecutive clear and calm days, the faster the surface temperature drops off after sunset due to the larger amount of surface warming during the day and emittance from the surface of long wave radiation at night. The vertical profile for April 7th is overall about 5K warmer than the profile for April 5th.

Neither May 1st nor October 13th show any particular example of wind involvement in the SBI development. On October 15th however, the evening begins with a defined wind above the surface at about 1000-1600 m ASL – which could identify a level at which the atmosphere is decoupled from the surface profile November 21st also shows a wind maximum between 1000 and 1500m ASL and slightly chaotic between launches above that level. What is noticeable though is that the warmer the profile, the higher the winds, and vice versa. This is expected since winds provide mixing and inhibit air to become stagnant and cool.

Final thoughts and future work

This dataset represents the first detailed consideration of the temporal evolution of the surface-based radiation inversion in Fairbanks, AK during the spring and autumn seasons. We have learned that only after the surface temperature converges on a minimum temperature does the inversion begin to develop upward. When snow cover is present, the vertical propagation of cool temperatures will happen more rapidly assuming the inversion has enough shortwave radiation to break the inversion during the day.

This purely observational study has suggested a variety of directions in which future work involving microphysics and modeling studies based on these data could proceed. Operationally, there is the potential to develop a sort of user interface for forecasters to figure out how cold the temperature can get if conditions are favorable for a strong SBI. This would be very useful to forecasters, who are currently using experience and persistence to forecast minimum temperatures for inversion cases.

A modeling perspective would be useful to isolate wind effects. For example, a radiative convective model could be implemented to investigate the influence of winds on the inversion in Fairbanks, taking into account local ground emissivity, atmospheric mediums, and surface fluxes.

A tethered balloon (tethersonde) had been discussed as a part of this project, but current federal aviation rules and time constraints did not allow the implementation into this particular experiment. A tethersonde would be useful in looking at the microphysics of the inversion, but could give insight into more specifics of the temperature inversion in specific case studies. One of the microphysical processes which could be measured is whether the IR radiative flux is divergent and the divergence decreases as the surface temperature approaches a minimum. If so, the radiative equilibrium would be working and a minimum surface temperature may be able to be resolved in clear and calm nights. Creating a meteorological tower, during wintertime inversions would allow a much larger dataset, though only at fixed heights in the atmosphere.

References

André, J. C., and L. Mahrt, 1981: The Nocturnal Surface Inversion and Influence of Clear-Air Radiative Cooling. *Journal of the Atmospheric Sciences*, **39**, 864-878.

Ball, F. K., 1956: The theory of strong katabatic winds. *Aust. J Physics*, 9, 373-386.

Bridgman, H. A., R. C. Schnell, J. D. Kahl, G. A. Herbert and E. Joranger, 1989: A major haze event near Point Barrow, Alaska: Analysis of probably source regions and transport pathways. *Atmos. Environment*, 23, 2537-2549.

Bohren, C. and Clothiaux, E. 2006. Fundamentals of Atmospheric Radiation: An Introduction with 400 Problems. Weinheim: Wiley-VCH GmbH & Co. KGaA, pp. 12-37, 327-335.

Bourne, Stefanie M. *A Climate Perspective of Observed and Modeled Surface-based Temperature Inversions in Alaska*. MS Thesis, University of Alaska Fairbanks, Fairbanks, 2008.

Bourne, S.M., U.S. Bhatt, J. Zhang, R. Thoman, 2010: Surface-based temperature inversions in Alaska from a climate perspective. Atmos. Res., doi:10.1016/j.atmosres.2009.09.013

Bowling, S. A., T. Ohtake, C.S. Benson, 1968: Winter Pressure Systems and Ice Fog in Fairbanks, Alaska. *Journal of Applied Meteorology*, 7, 961-968.

Bradley, R. S., F. T. Keimeg, and H. F. Diaz, 1992: Climatology of Surface-Based Inversions in the North American Arctic. *Journal of Geophysical Research*, 97, 15699-15712.

Estournel, C. and D. Guedalia, 1985: Influence of Geostrophic Wind on Atmospheric Nocturnal Cooling. *J. Atmos. Sci.*, 42(23), 2695-2698.

Fairbanks Department of Environmental Conservation (DEC)
http://www.dec.state.ak.us/air/anpms/pm/pm2-5_fbks.htmFisch, G., R,B, da Silveira, L.A.T.

Machado, 1999: Intercomparisons Between Sondes RS80 Vaisala and MKII Sippican Used in Brazil. TECO-2006 - World Meteorological Organization Technical Conference on Meteorological and Environmental Instruments and Methods of Observation. Geneva, Switzerland, 4-6 December 2006.

Hartmann B., Wendler G., 2005: Climatology of the Winter Surface Temperature Inversion in Fairbanks, Alaska. 85th AMS Annual Meeting, San Diego, CA, 1-7.

Hogan, A., and M. Ferrick, 1996: Winter Morning Air Temperature. *Journal of Applied Meteorology*, 36, 52-69.

Kadygrov, E. N., A. S. Viazankin, E. R. Westwater, and K. B. Widener, 1999: Characteristics of the Low-Level Temperature Inversion at North Slope of Alaska on the Base of Microwave Remote Sensing Data. *Ninth ARM Science Team Meeting Proceedings, San Antonio, Texas*, March 22-26, 1999.

Kahl, J. D., M. C. Serreze, R. C. Schnell, 1992: Tropospheric Low-Level Temperature Inversions in the Canadian Arctic. *Atmosphere-Ocean*, 30 (4), 511-529.

Kakanala, Pavan Kumar Reddy. *Doppler Sodar Observations of the Winds and Structure in the Lower Atmosphere Over Fairbanks, Alaska*. MS Thesis, University of Alaska Fairbanks, Fairbanks, 2007.

Molders and Kramm, 2009: A case study on wintertime inversions in Interior Alaska with WRF. Atmos. Res., doi: 10.1016/j.atmosres.2009.06.002

Morton, D., "Comparison of ARSCwrf Surface Variables with Observations" *The Alaska Weather Symposium*, Fairbanks, AK, 10-12 March 2009.

Pepin, N.C., M.K. Schaefer, L.D. Riddy, 2009: Quantification of the cold-air pool in Kevo Valley, Finnish Lapland. *Weather*, 64(3), 60-67.

Salby, M., 1996. Fundamentals of Atmospheric Physics, Vol. 61. San Diego: Elsevier, pp. 10-35.

Stevens, E., 2009: An investigation of the relationship between surface temperatures and the establishment of snowpack during October..., *Atmospheric Research*, doi:10.1016/j.atmosres.2009.04.009

Tilley, J. S., and C. Weatherby, 2001: On the sensitivity of simulated subarctic wintertime inversions to PBL parameterization. Preprints, 11th PSU/NCAR Mesoscale Model Users' Workshop, 25-27 June, Boulder, CO, 106-109.

Vaisala, Technical specification for RS-80 radiosonde. Ref. A571en 1997-08. http://www.hobeco.net/pdf/RS80_radiosondes.pdf

VIZ Meteorological Systems Group of Sippican, Inc., Technical specifications for Mark II Microsonde. http://www.sippican.com/stuff/contentmgr/files/3e8052902595d3629c7b01ca9f4201b0/sheet/mark2.pdf

Wallace and Hobbs, 2006. Atmospheric Science: An Introductory Survey. Burlington: Elsevier, pp. 6-19.

Walsh. J.E., W.H. Jasperson, B. Ross, 1985:Influences of Snow Cover and Soil Moisture on Monthly Air Temperature. *Mon. Wea. Rev.,* 113, 756-768.

Webmet.com, 2010. Radiosonde Sounding System: http://www.webmet.com/met_monitoring/912.html

Wendler, G., and K. O. L. F. Jayaweera, 1972: Some Measurements on the Development of the Surface Inversion in Central Alaska During Winter. *Pure and Applied Geophysics*, 92, 209-221.

Wendler, G., and P. Nicpon, 1974: Low-Level Temperature Inversions in Fairbanks, Central Alaska. *Mon. Wea. Rev*., 103, 34-44.

Wexler, H., 1936: Cooling in the Lower Atmosphere and the Structure of Polar Continental Air. *Mon. Wea. Rev.*, 122-136

Appendix 1: Upper air charts.

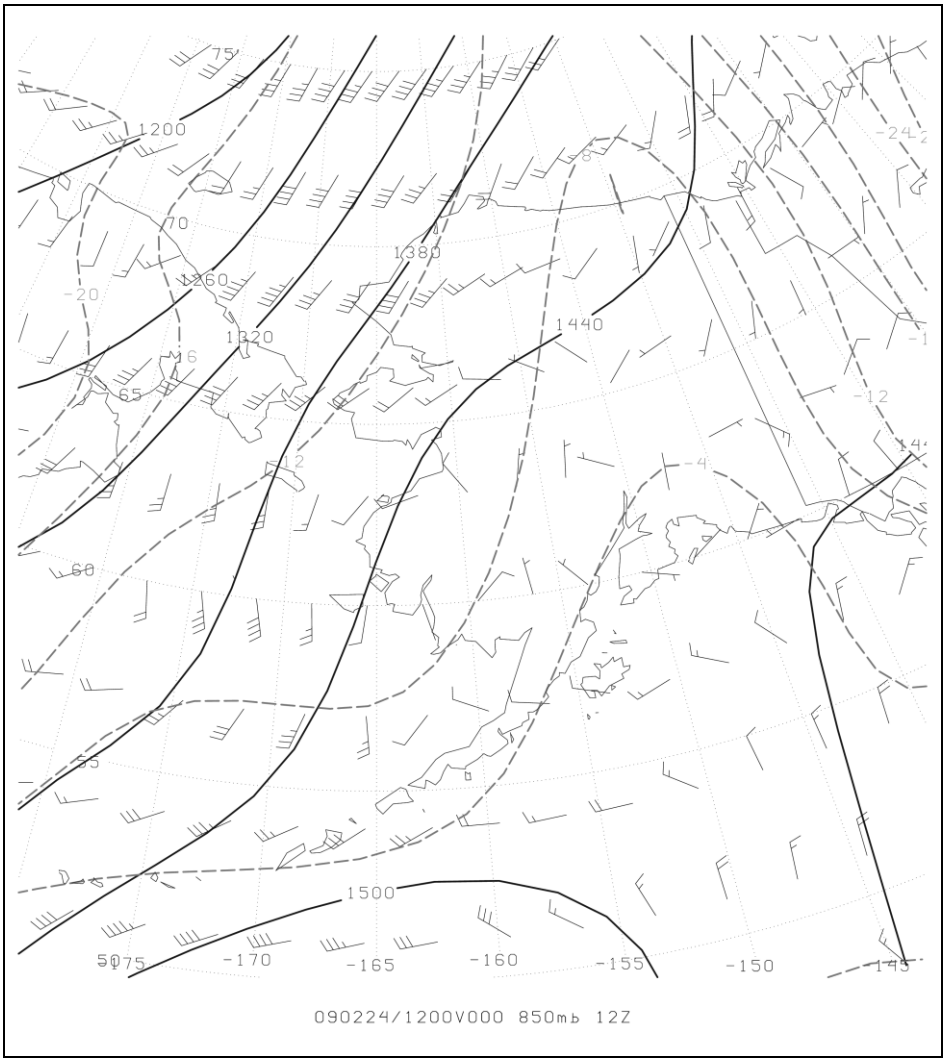

Figure A.1: 850 hPa upper air chart for 12 UTC February 24, 2009. Geopotential height (solid line), temperature (dashed line), and wind barbs as derived from NOAA Global Forecast System model initialization.

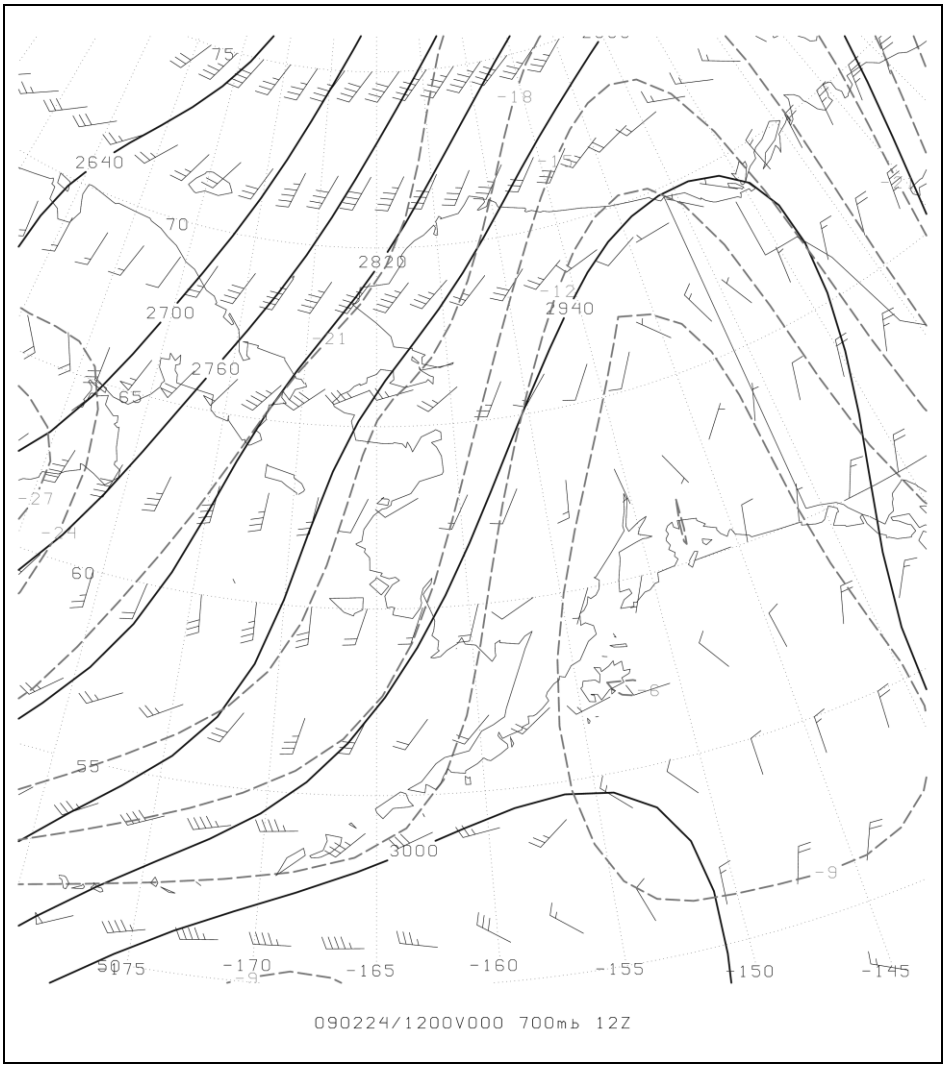

Figure A.2: 700 hPa upper air chart for 12 UTC February 24, 2009. Geopotential height (solid line), temperature (dashed line), and wind barbs as derived from NOAA Global Forecast System model initialization.

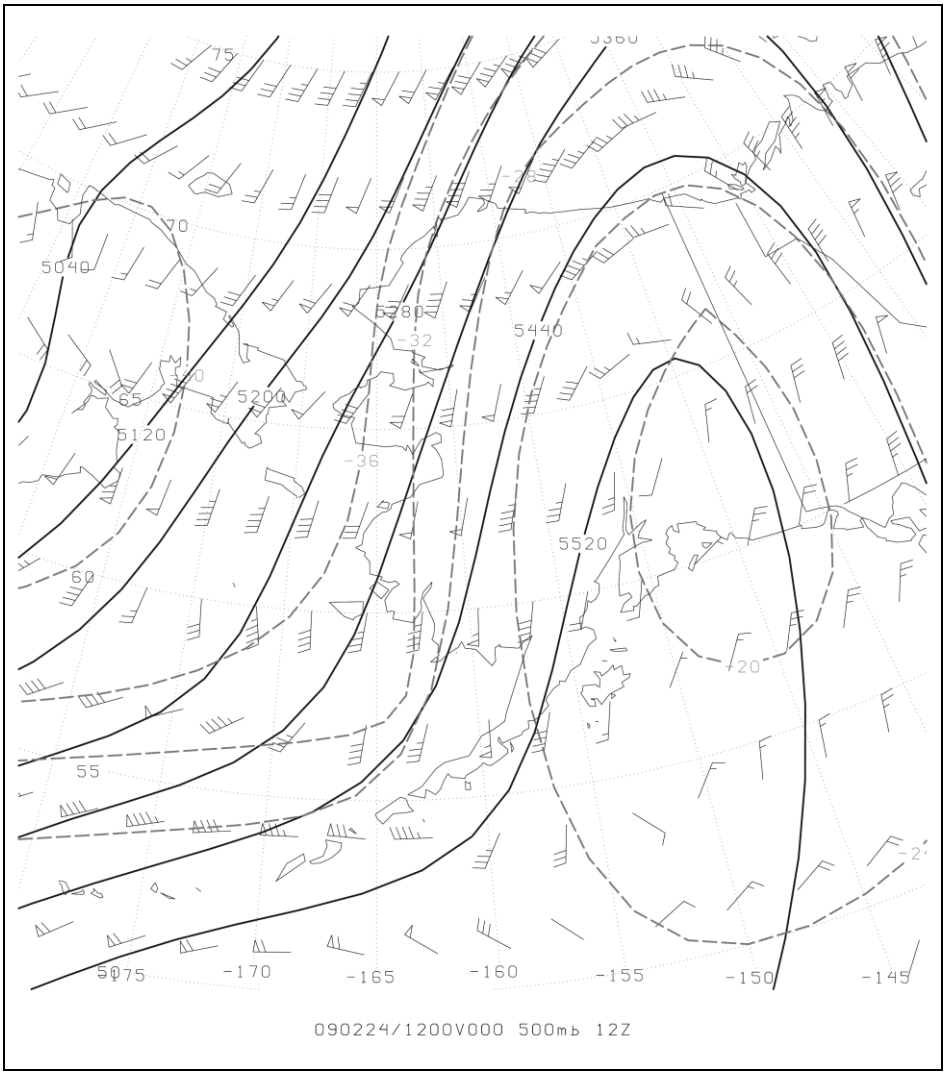

Figure A.3: 500 hPa upper air chart for 12 UTC February 24, 2009. Geopotential height (solid line), temperature (dashed line), and wind barbs as derived from NOAA Global Forecast System model initialization.

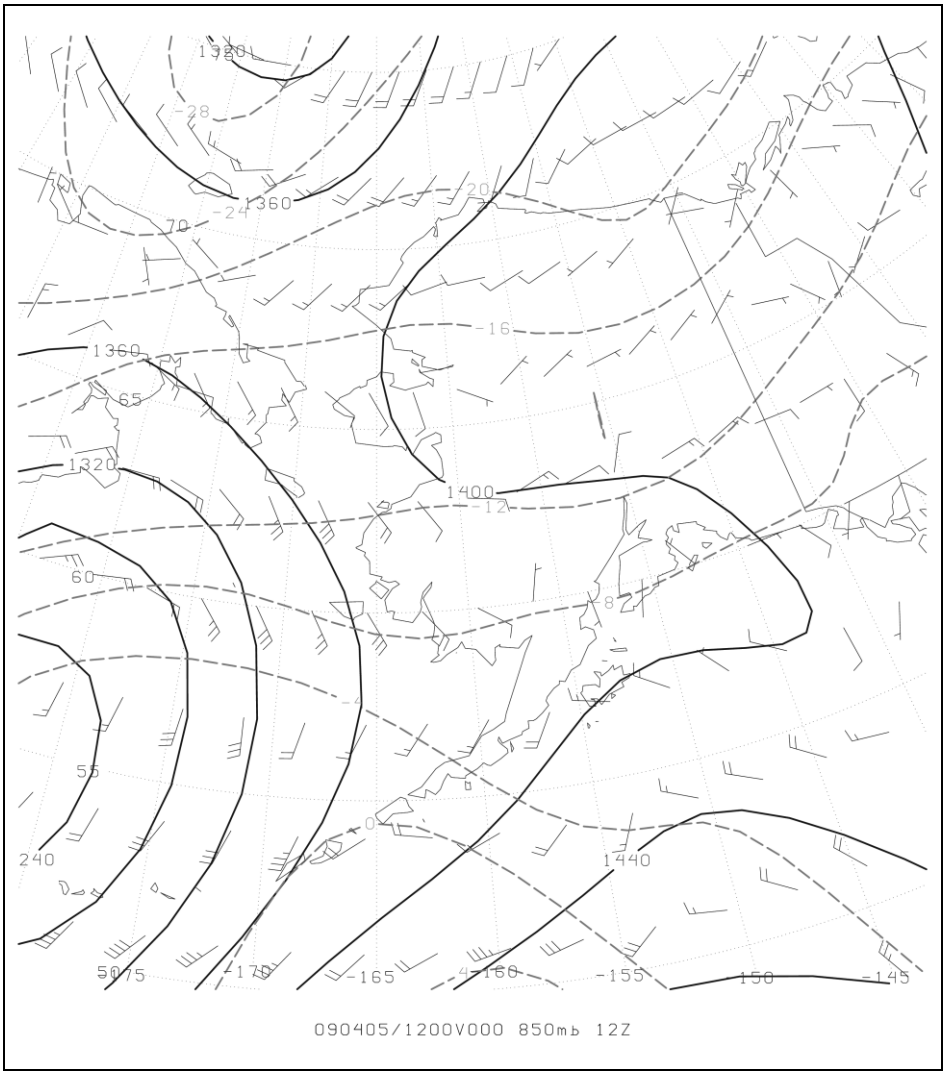

Figure A.4: 850 hPa upper air chart for 12 UTC April 5, 2009. Geopotential height (solid line), temperature (dashed line), and wind barbs as derived from NOAA Global Forecast System model initialization.

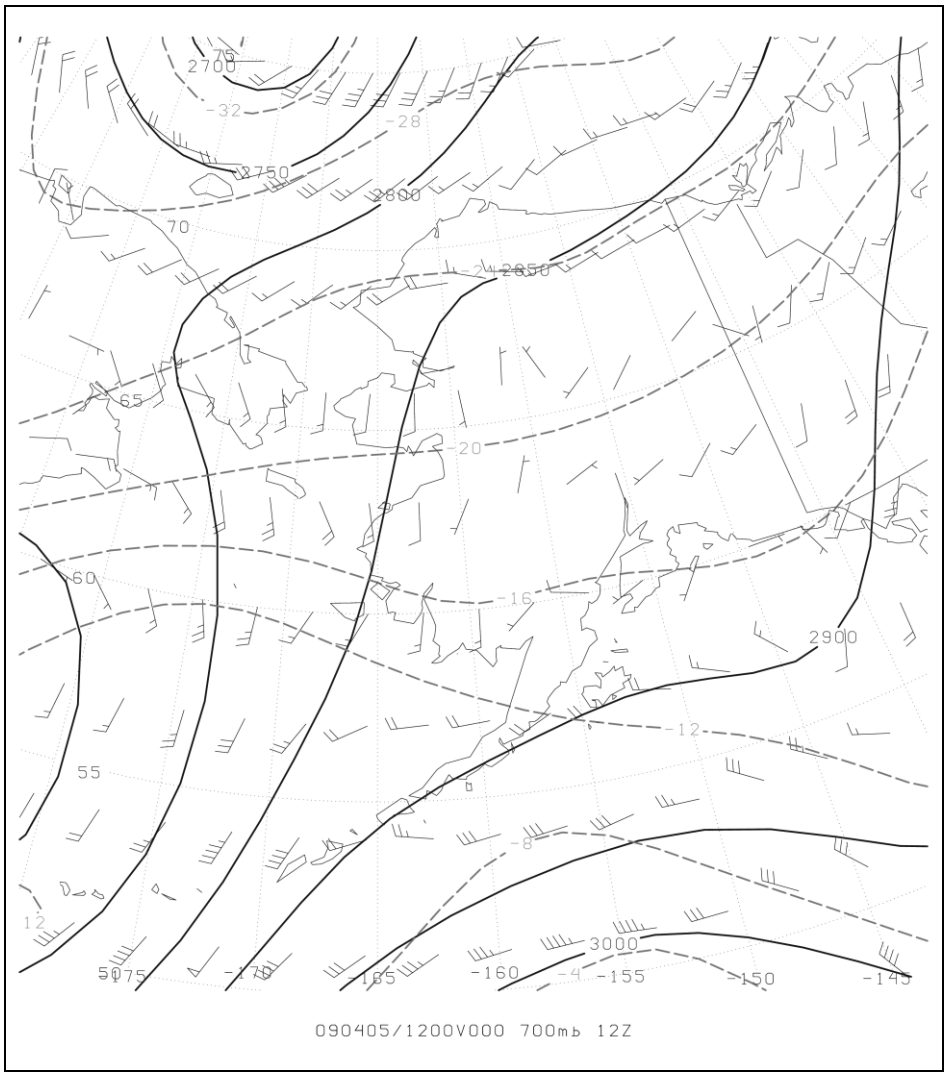

Figure A.5: 700 hPa upper air chart for 12 UTC April 5, 2009. Geopotential height (solid line), temperature (dashed line), and wind barbs as derived from NOAA Global Forecast System model initialization.

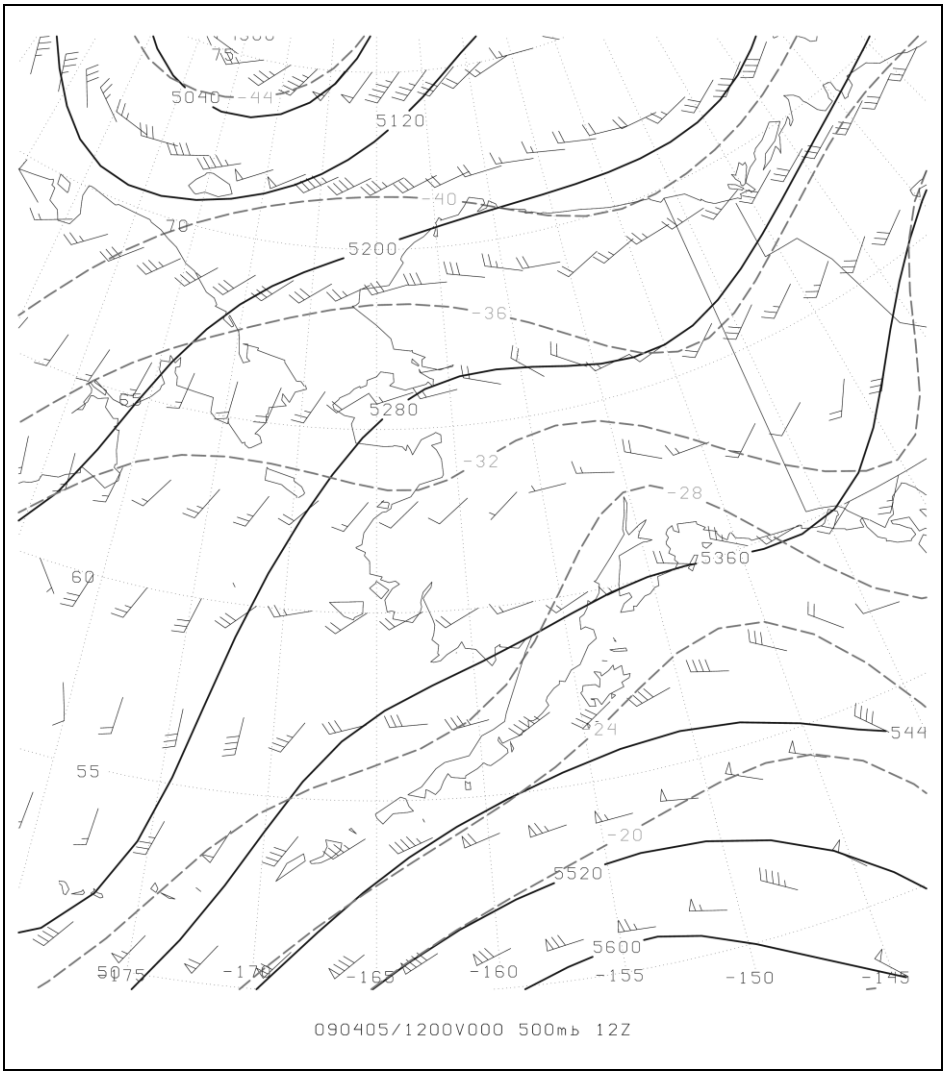

Figure A.6: 500 hPa upper air chart for 12 UTC April 5, 2009. Geopotential height (solid line), temperature (dashed line), and wind barbs as derived from NOAA Global Forecast System model initialization.

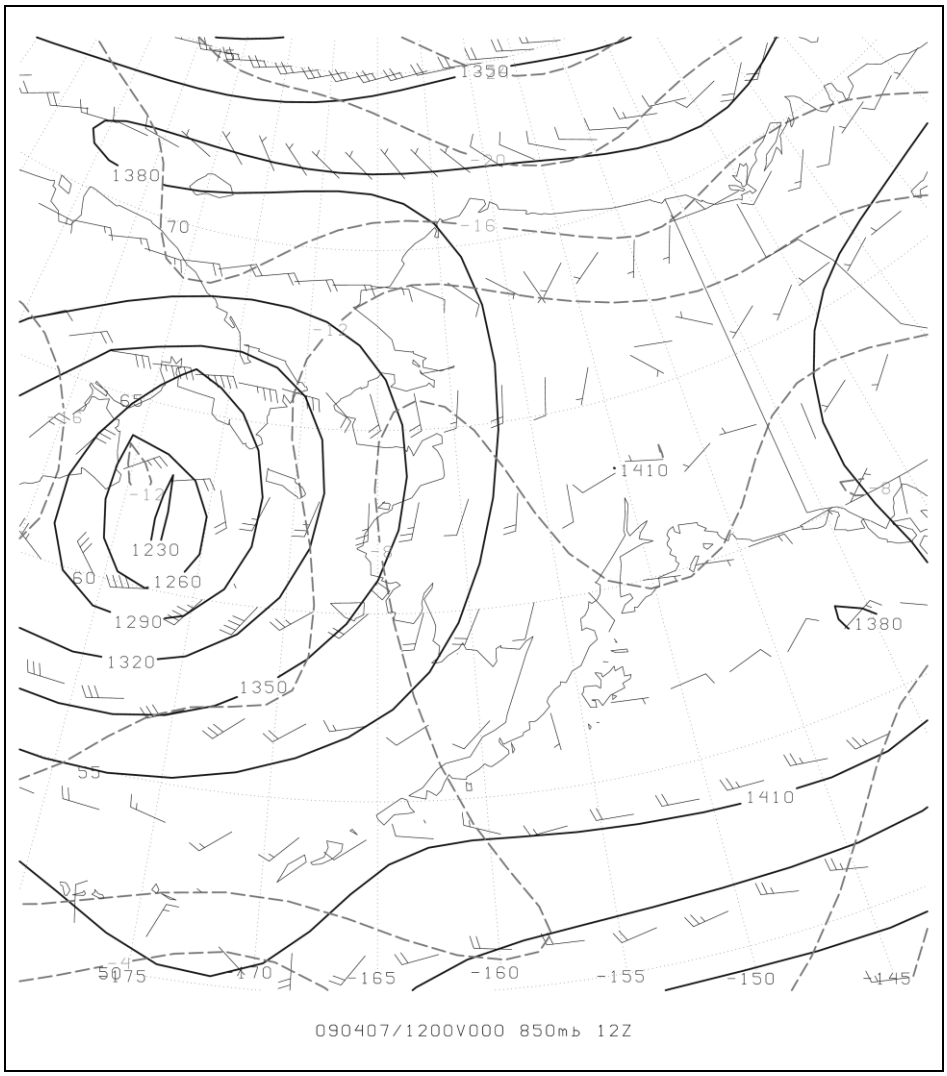

Figure A.7: 850 hPa upper air chart for 12 UTC April 7, 2009. Geopotential height (solid line), temperature (dashed line), and wind barbs as derived from NOAA Global Forecast System model initialization.

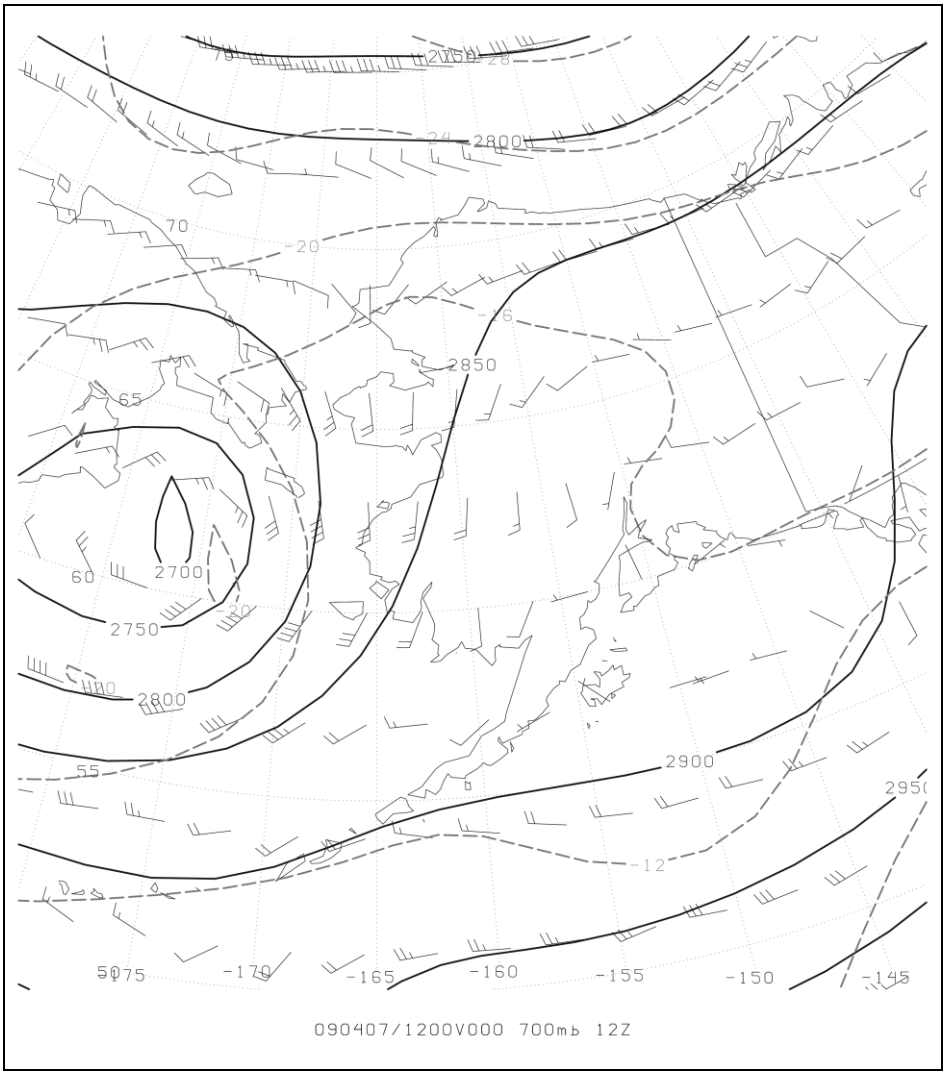

Figure A.8: 700 hPa upper air chart for 12 UTC April 7, 2009. Geopotential height (solid line), temperature (dashed line), and wind barbs as derived from NOAA Global Forecast System model initialization.

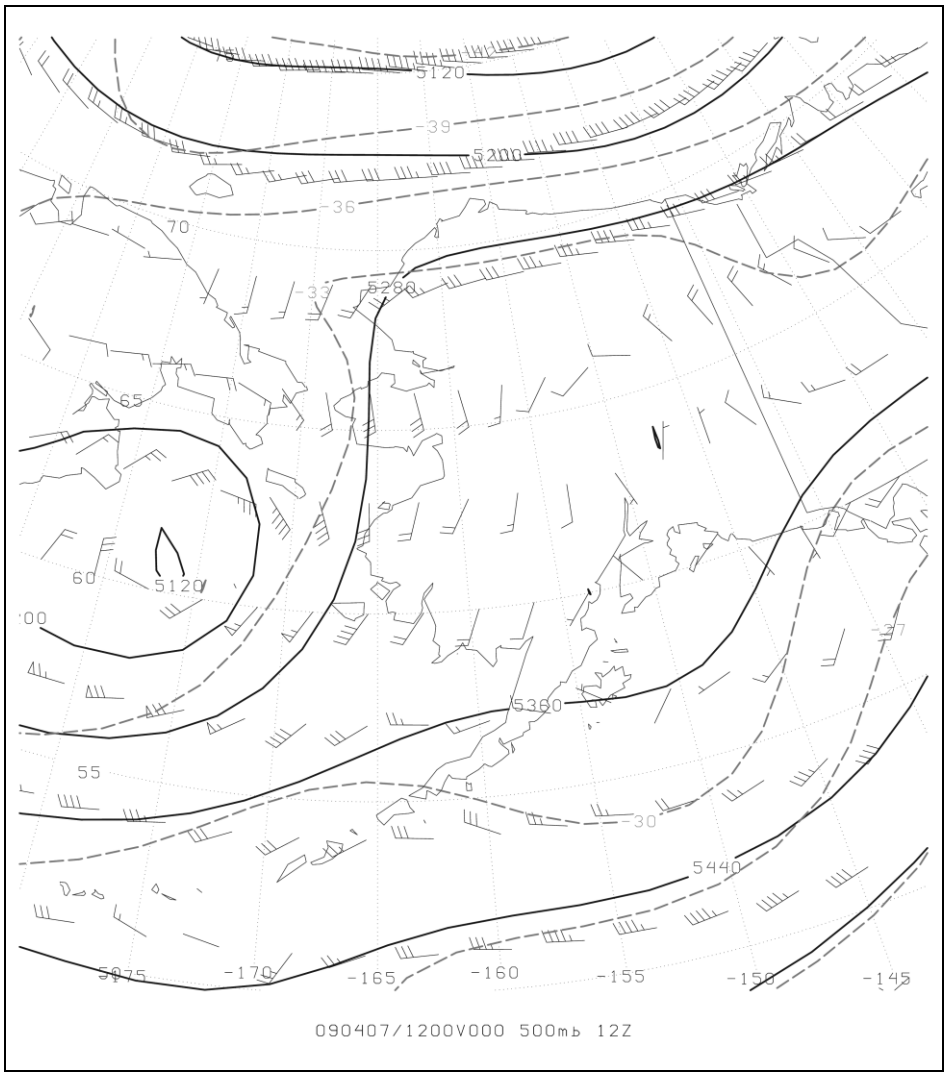

Figure A.9: 500 hPa upper air chart for 12 UTC April 7, 2009. Geopotential height (solid line), temperature (dashed line), and wind barbs as derived from NOAA Global Forecast System model initialization.

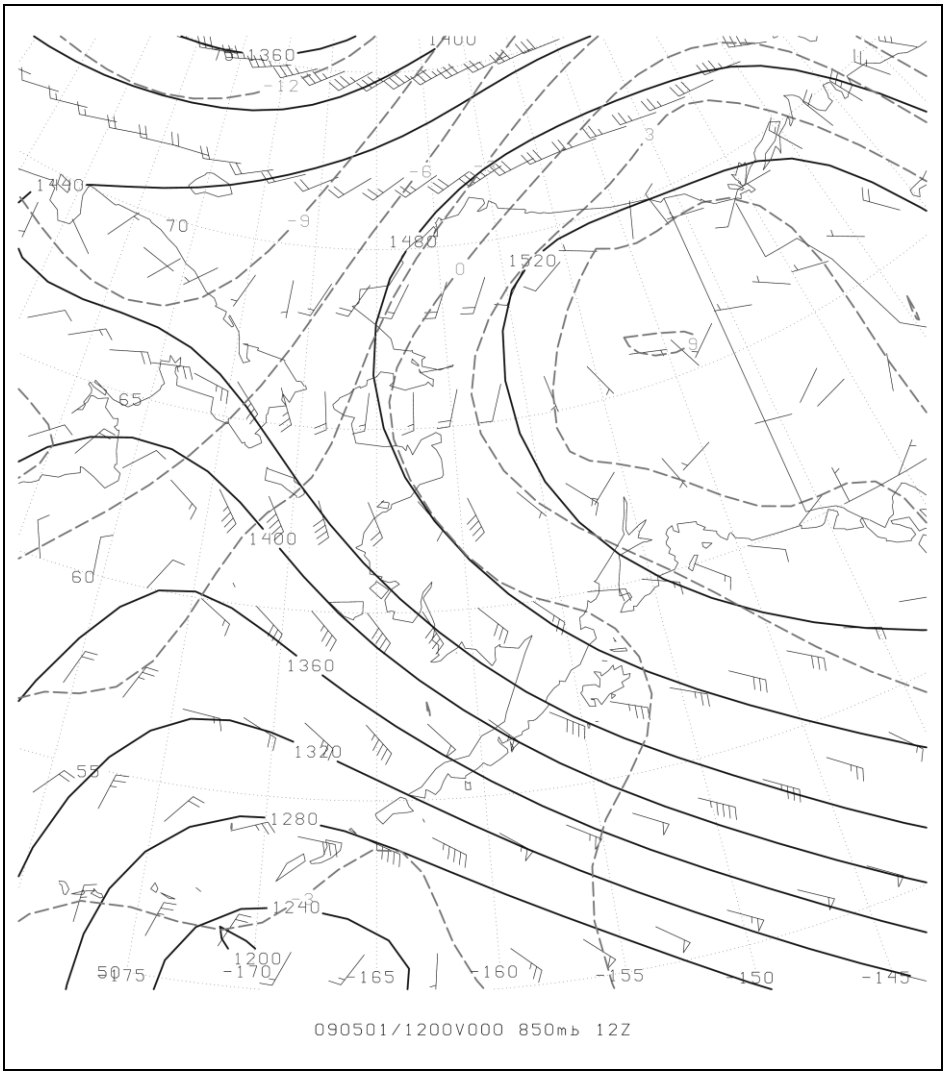

Figure A.10: 850 hPa upper air chart for 12 UTC May 1, 2009. Geopotential height (solid line), temperature (dashed line), and wind barbs as derived from NOAA Global Forecast System model initialization.

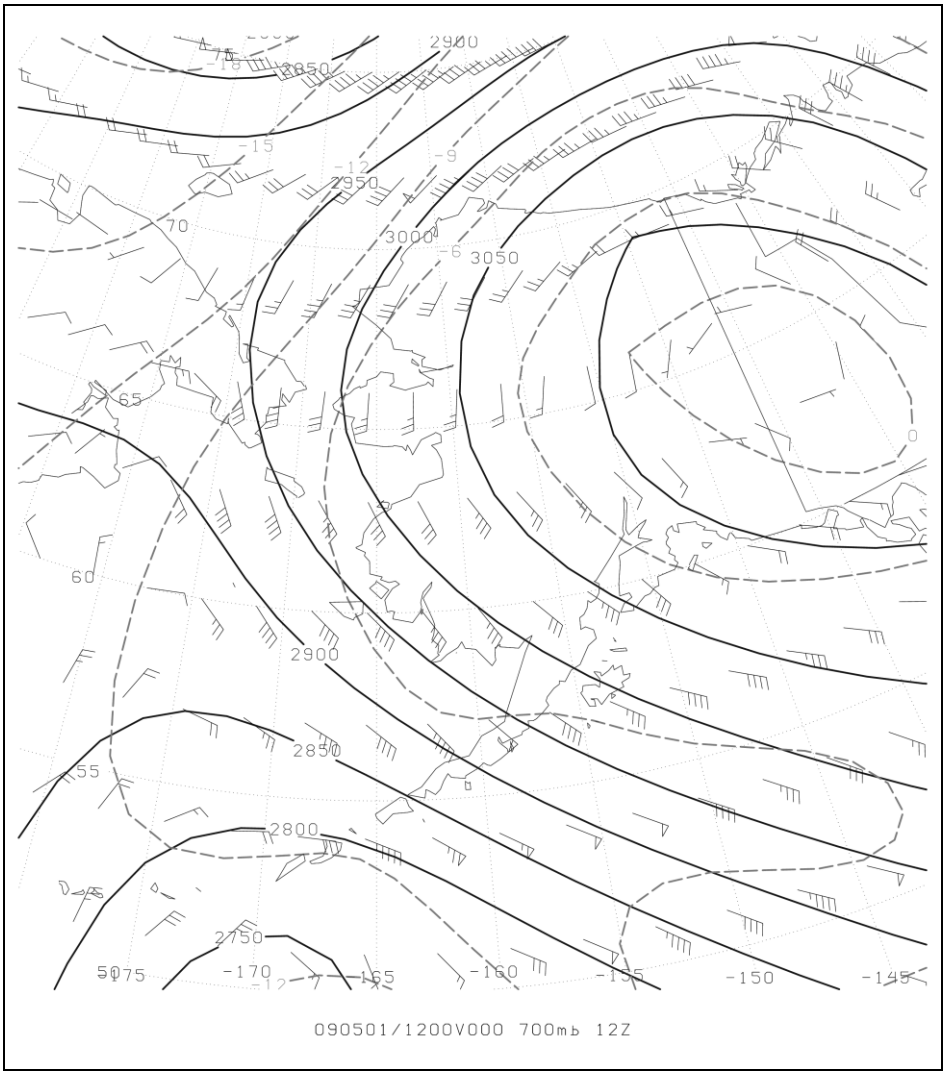

Figure A.11: 700 hPa upper air chart for 12 UTC May 1, 2009. Geopotential height (solid line), temperature (dashed line), and wind barbs as derived from NOAA Global Forecast System model initialization.

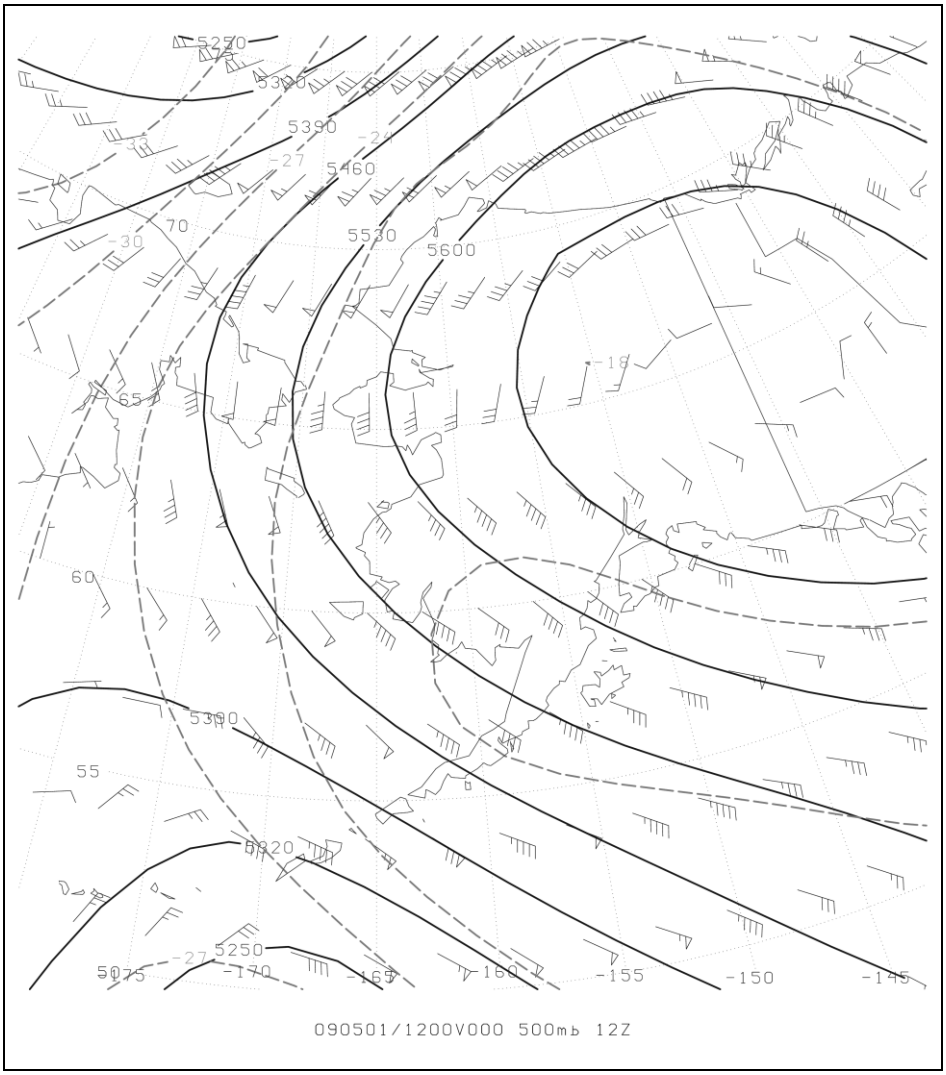

Figure A.12: 500 hPa upper air chart for 12 UTC May 1, 2009. Geopotential height (solid line), temperature (dashed line), and wind barbs as derived from NOAA Global Forecast System model initialization.

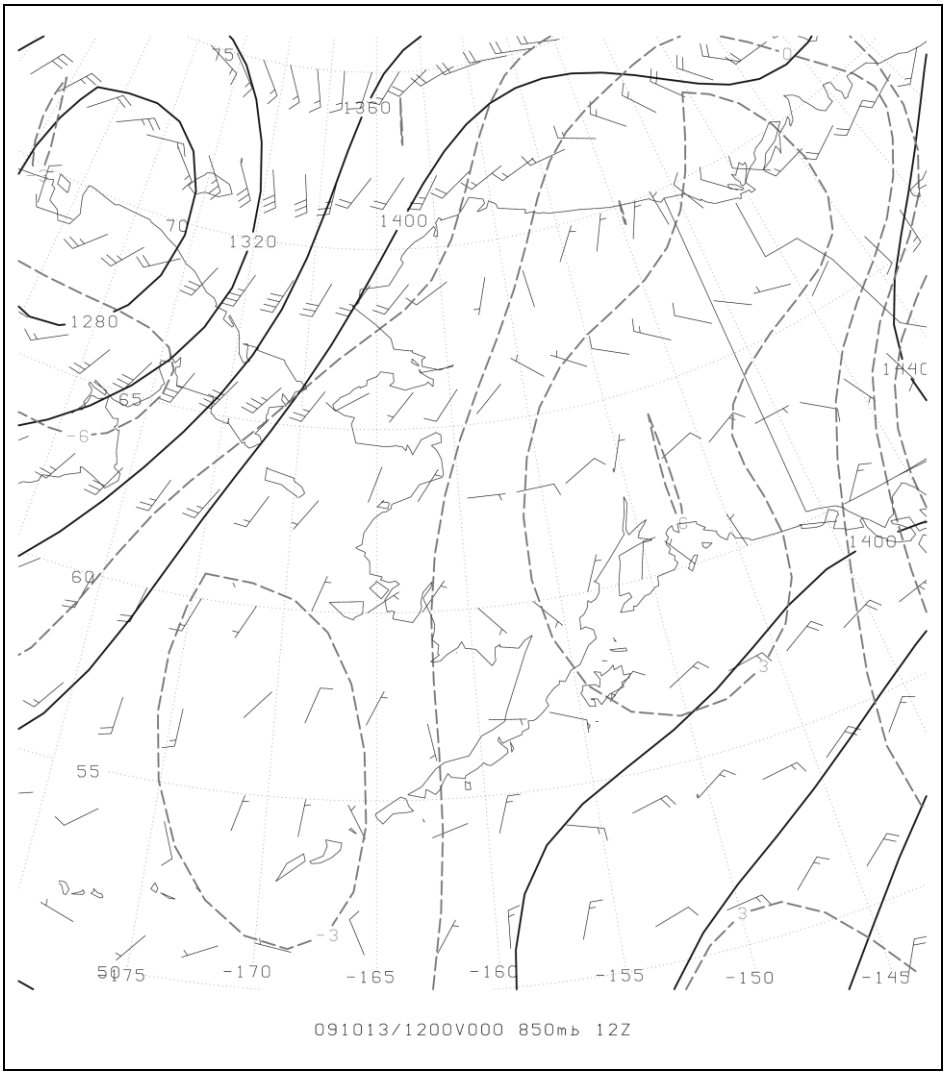

Figure A.13: 850 hPa upper air chart for 12 UTC October 13, 2009. Geopotential height (solid line), temperature (dashed line), and wind barbs as derived from NOAA Global Forecast System model initialization.

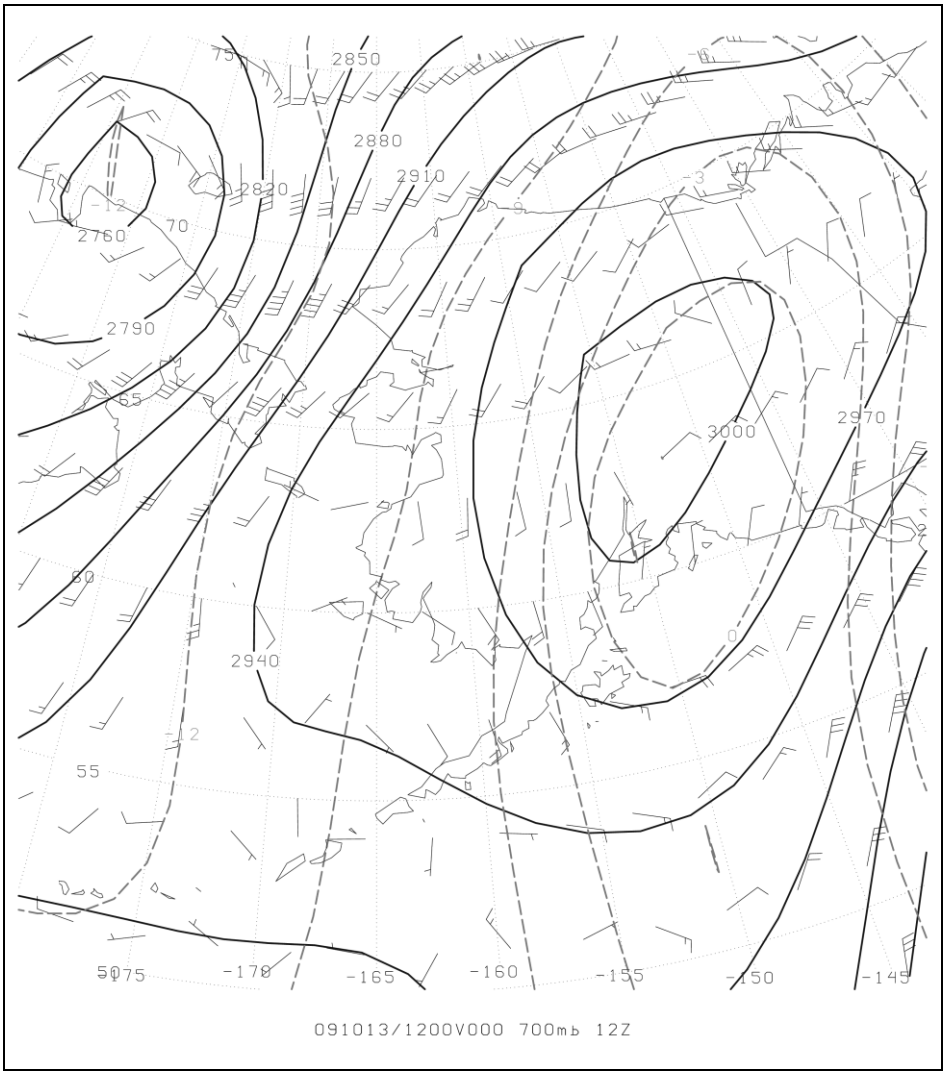

Figure A.14: 700 hPa upper air chart for 12 UTC October 13, 2009. Geopotential height (solid line), temperature (dashed line), and wind barbs as derived from NOAA Global Forecast System model initialization.

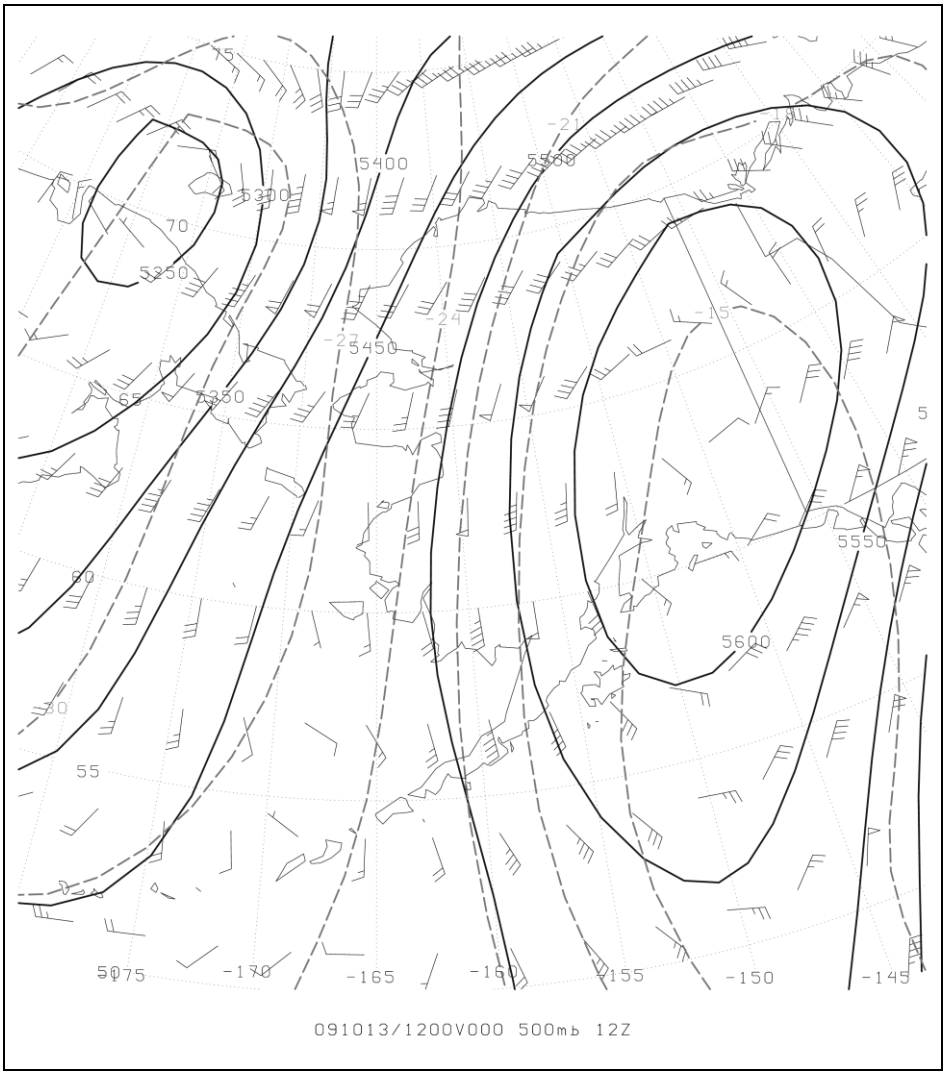

Figure A.15: 500 hPa upper air chart for 12 UTC October 13, 2009. Geopotential height (solid line), temperature (dashed line), and wind barbs as derived from NOAA Global Forecast System model initialization.

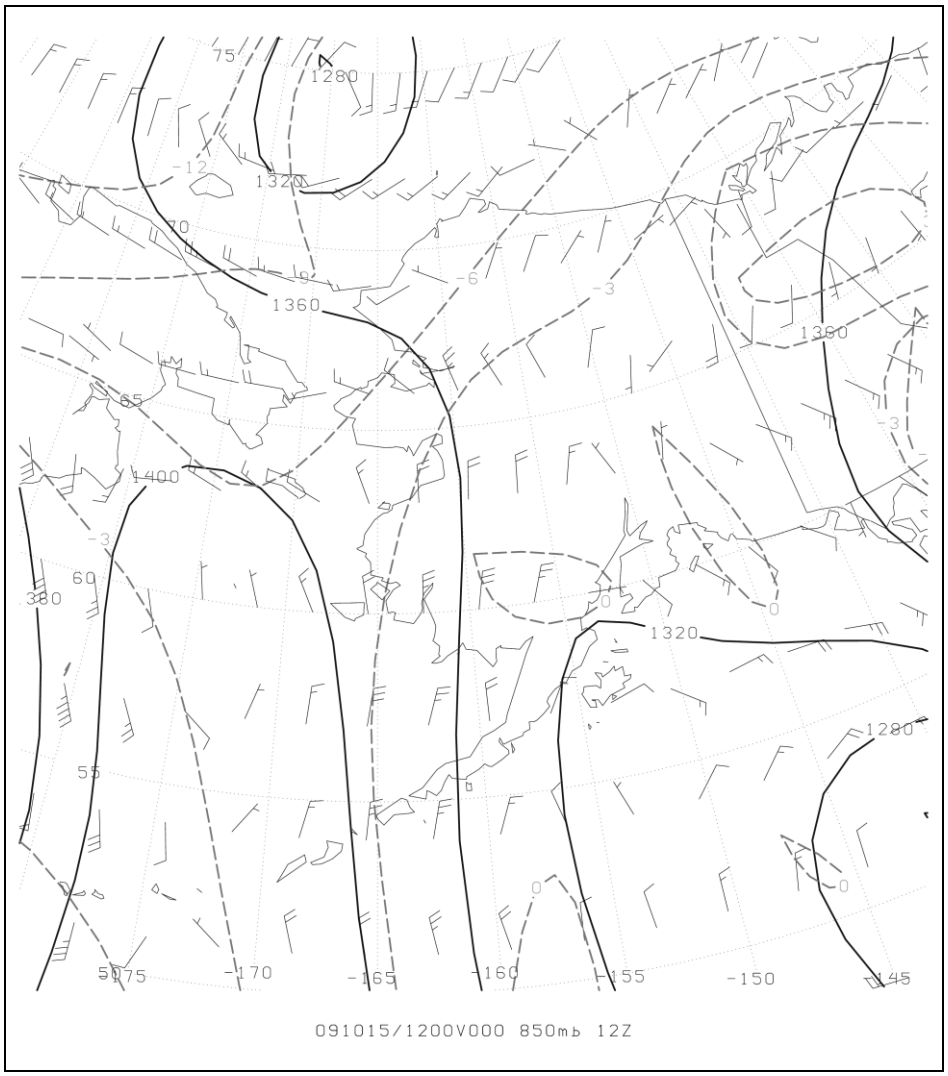

Figure A.16: 850 hPa upper air chart for 12 UTC October 15, 2009. Geopotential height (solid line), temperature (dashed line), and wind barbs as derived from NOAA Global Forecast System model initialization.

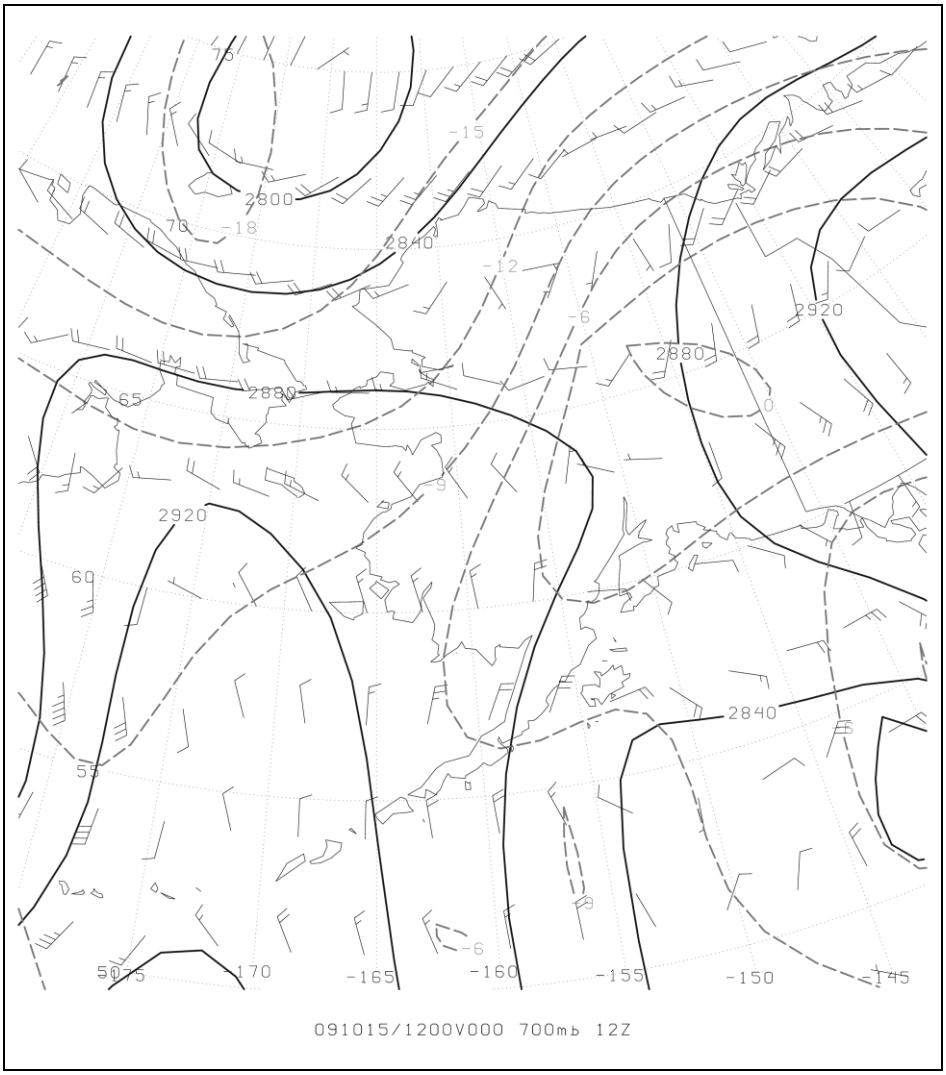

Figure A.17: 700 hPa upper air chart for 12 UTC October 15, 2009. Geopotential height (solid line), temperature (dashed line), and wind barbs as derived from NOAA Global Forecast System model initialization.

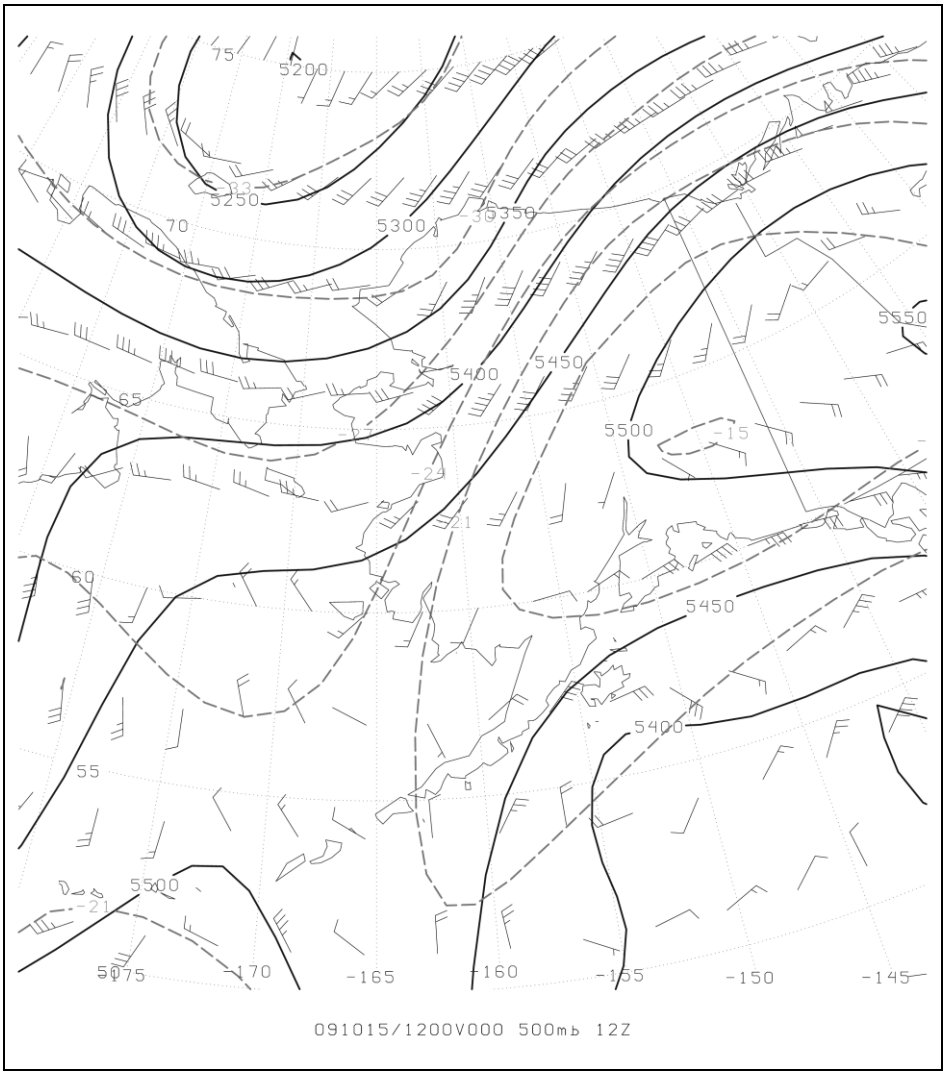

Figure A.18: 500 hPa upper air chart for 12 UTC October 15, 2009. Geopotential height (solid line), temperature (dashed line), and wind barbs as derived from NOAA Global Forecast System model initialization.

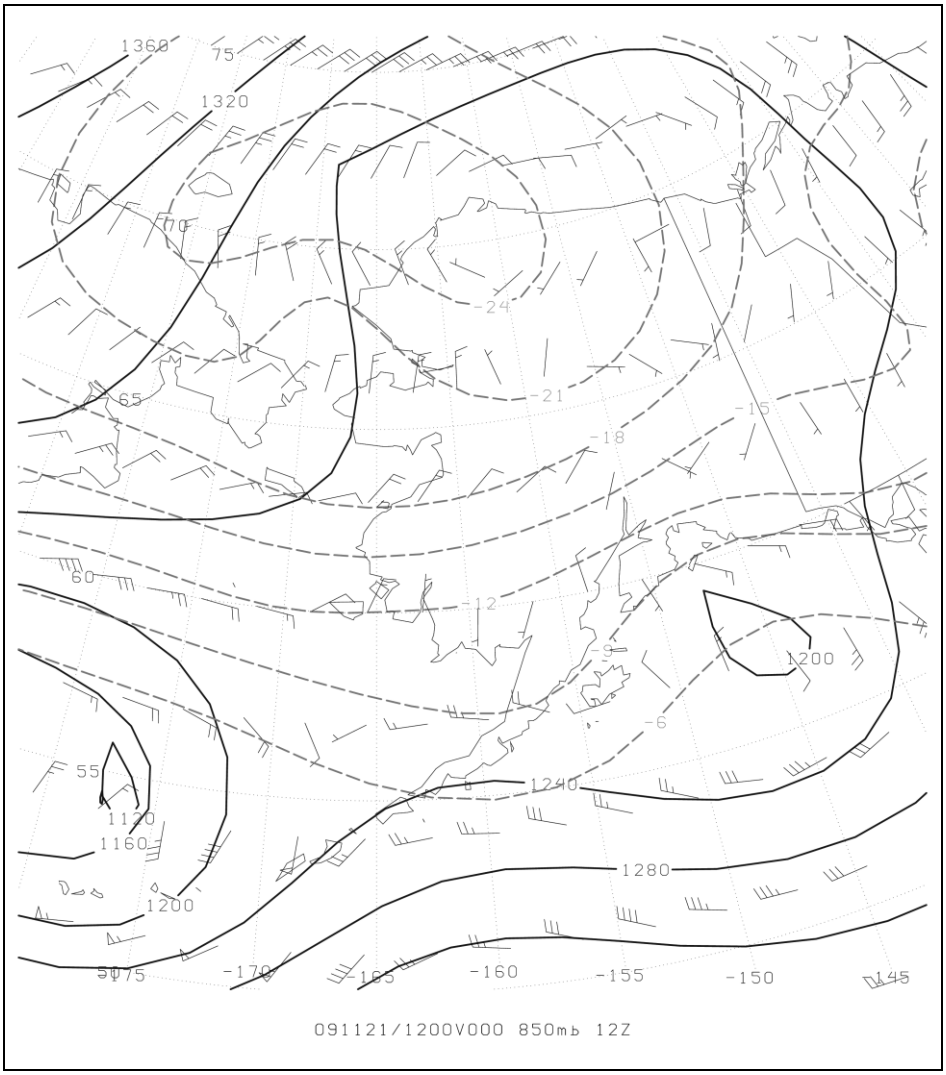

Figure A.19: 850 hPa upper air chart for 12 UTC November 21, 2009. Geopotential height (solid line), temperature (dashed line), and wind barbs as derived from NOAA Global Forecast System model initialization.

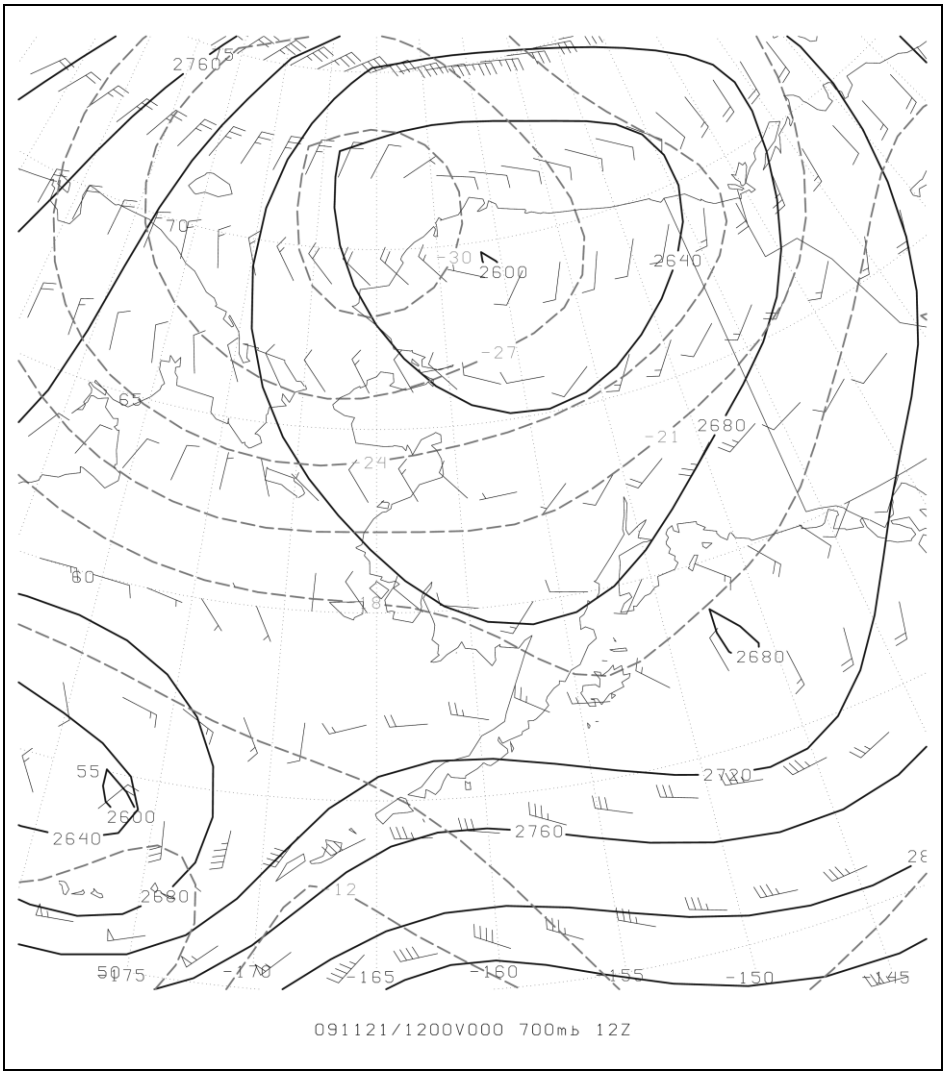

Figure A.20: 700 hPa upper air chart for 12 UTC November 21, 2009. Geopotential height (solid line), temperature (dashed line), and wind barbs as derived from NOAA Global Forecast System model initialization.

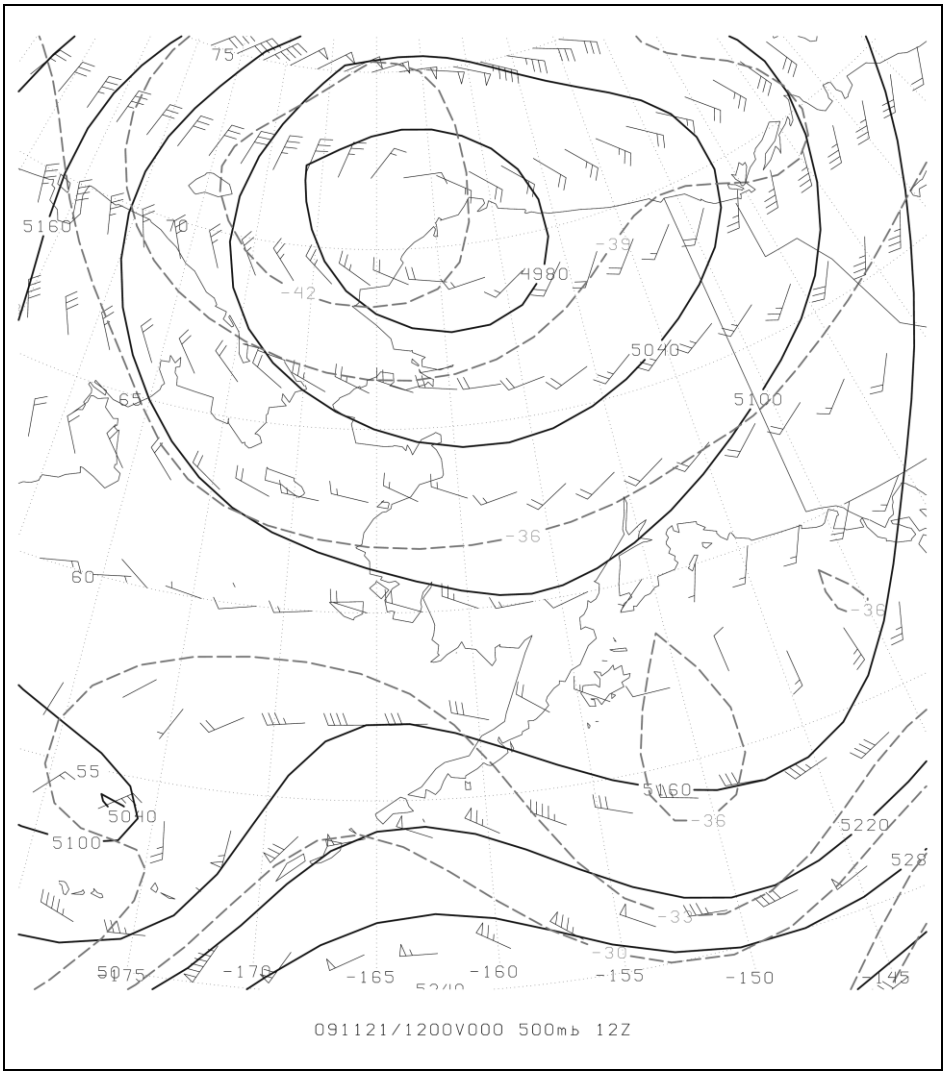

Figure A.21: 500 hPa upper air chart for 12 UTC November 21, 2009. Geopotential height (solid line), temperature (dashed line), and wind barbs as derived from NOAA Global Forecast System model initialization.